METHODOLOGY TO ANALYZE THE SENSITIVITY OF BUILDING ENERGY CONSUMPTION TO HVAC SYSTEM SENSOR ERROR

A Thesis

by

LIANG MA

Submitted to the Office of Graduate Studies of
Texas A&M University
in partial fulfillment of the requirements for the degree of

MASTER OF SCIENCE

December 2011

Major Subject: Mechanical Engineering

METHODOLOGY TO ANALYZE THE SENSITIVITY OF BUILDING ENERGY CONSUMPTION TO HVAC SYSTEM SENSOR ERROR

A Thesis

by

LIANG MA

Submitted to the Office of Graduate Studies of
Texas A&M University
in partial fulfillment of the requirements for the degree of

MASTER OF SCIENCE

Approved by:

Chair of Committee,	David E. Claridge
Committee Members,	Dennis L. O'Neal
	Charles H. Culp
Head of Department,	Jerald A. Caton

December 2011

Major Subject: Mechanical Engineering

ABSTRACT

Methodology to Analyze the Sensitivity of Building Energy Consumption to HVAC System Sensor Error. (December 2011)

Liang Ma, B.En., Harbin Institute of Technology

Chair of Advisory Committee: Dr. David E. Claridge

This thesis proposes a methodology for determining sensitivity of building energy consumption of HVAC systems to sensor error. It is based on a series of simulations of a generic building, the model for which is based on several typical input parameters.

There are a total of eight scenarios considered in this simulation. The simulation tool was developed based on Excel. The control parameters examined include room temperature, cold deck temperature, hot deck temperature, pump pressure, and fan pressure. All of the parameters considered are varied in order to analyze the sensitivity of building energy consumption to their variation. In this tool, different operation schedules for equipment, occupancy, and lighting are considered. By changing each control parameter, the sensitivity of energy use to sensor error is simulated, a regression model is generated, and the energy consumption change is expressed as a function of sensor error and outside air percentage.

Two applications of this methodology are presented in this thesis. One is a SDVAV system and the other is a DDVAV system. The outside air percentage changes the trend of the sensor error curve.

After the sensitivity study is discussed, some recommendations regarding the calibration intervals of the sensors are given.

To my beloved parents

ACKNOWLEDGEMENTS

Foremost, I would like to express my gratitude to my advisor, David E. Claridge. Without his patience and guidance, I could not have finished this thesis. Dr. Claridge has always been patient when guiding me through this thesis work. His insightful and encouraging words were the inspirational light I followed on my sometimes dark way.

I would also like to thank the rest of my thesis committee: Dr. Charles H. Culp and Dr. Dennis L. O'Neal for their encouragement, insightful comments, and willingness to always ask the hard questions.

I must thank my family, and especially my parents. Thank you for your support during this difficult time in my life. Also, I must express my thanks to my lab mates: Zhiqin Zhang, Jing Ji, Juan Zhao, Lei Wang, Guanjing Lin, Xiaoli Li, and Nanxi Li. Thanks for your warm and encouraging words during the completion of my thesis. I could never make it without your encouragement and help.

NOMENCLATURE

DDVAV	Dual Duct Variable Air Volume
Eff_{pump}	Pump Efficiency
HVAC	Heating Ventilating and Air Conditioning
q_{cl}	Cooling Coil Latent Load
q_{cs}	Cooling Coil Sensible Load
$q_{e,rh}$	Exterior Zone Reheat
$q_{e,s}$	Exterior Zone - Sensible Loads
q_{er}	Exterior Zone Return Pipe Heat Gain
q_{h}	Heating Coil Load
$q_{i,rh}$	Interior Zone Reheat
$q_{i,s}$	Interior Zone - Sensible Loads
q_{ir}	Interior Zone Return Pipe Heat Gain
SDVAV	Single Duct Variable Air Volume
T_{ce}	Cooling Coil Entering Temperature
T_{er}	Exterior Zone Return Air Temperature
T_{es}	Exterior Zone Supply Temperature
T_{he}	Heating Coil Entering Temperature
T_{hl}	Heating Coil Leaving Temperature
T_{ir}	Interior Zone Return Air Temperature
T_{is}	Interior Zone Supply Temperature

T_{ma}	Mixed Air Temperature
T_{oa}	Outside air Temperature
T_{ph}	Preheat Coil Temperature
T_r	Return Air Temperature
T_{sf}	Temperature Rise from Supply Fan
V_c	Total Air Flow through Cooling Coil
V_e	Exterior Zone supply volume
$V_{e,c}$	Exterior zone cold deck flow – VAV
$V_{e,h}$	Exterior zone hot deck flow – VAV
V_{ec}	Exterior Zone Air Flow from Cooling Coil
V_{eh}	Exterior Zone Air Flow from Heating Coil
V_h	Total Air Flow through Heating Coil
V_i	Interior Zone Supply volume
$V_{i,c}$	Interior zone cold deck flow – VAV
$V_{i,h}$	Interior zone hot deck flow – VAV
V_{ic}	Interior Zone Air Flow from Cooling Coil
V_{ih}	Interior Zone Air Flow from Heating Coil
W_{fan}	Fan Power Consumption
W_{fluid}	Fluid Power Consumption
W_{pump}	Pump Power Consumption
W_r	Actual Return Air Humidity Ratio
$W_{r'}$	Return Air Humidity Ratio - Wet Coil

$W_{r''}$	Return Air Humidity Ratio - Dry Coil
X_{oa}	Outside air Ratio
$\Delta P_{elevation}$	Pressure Difference Caused by Elevation
$\Delta P_{friction}$	Pressure Difference Caused by Friction
ΔP_{static}	Static Pressure Difference
ΔP_{total}	Total Pressure Difference
$\Delta P_{velocity}$	Pressure Difference Caused by Velocity

TABLE OF CONTENTS

Page

ABSTRACT iii

DEDICATION v

ACKNOWLEDGEMENTS vi

NOMENCLATURE vii

TABLE OF CONTENTS x

LIST OF FIGURES xii

LIST OF TABLES xiv

1. INTRODUCTION 1

1.1 Research Motivation 1

1.2 Research Objective 2

2. LITERATURE REVIEW 3

2.1 Temperature Sensors 3

2.1.1 Thermocouples 3

2.1.2 Thermistors 3

2.1.3 RTDs (Resistive temperature devices) 4

2.2 Pressure Sensors 4

2.2.1 Piezoresistive Pressure Sensor 4

2.3 CO2 Sensors 5

2.3.1 NDIR CO2 Sensor 5

2.3.2 Chemical CO2 Sensor 5

2.4 RH Sensors 6

2.4.1 Capacitive Humidity Sensors 6

2.4.2 Resistive Humidity Sensors 7

2.4.3 Thermal Conductivity Humidity Sensors 8

2.5 Manufacturers' Calibration Frequency Recommendations for HVAC Sensors 9

2.5.1 Temperature Sensors 9

Page

2.5.2 Pressure Sensors 10
2.5.3 CO2 Sensors 11
2.5.4 Relative Humidity Sensors 11
2.6 Sensor Drift 13
2.7 Sensor Failure Modes 15
2.8 Review of Related Studies 16
3. METHODOLOGY 19
3.1 Simulation Input Parameters and Baseline 21
3.2 Air Side Model 23
3.2.1 Dual Duct Various Air Volume System 24
3.2.2 Single Duct Various Air Volume System 26
3.3 Pump and Fan Model 28
3.3.1 Pump model 28
3.3.2 Fan model 29
3.4 Sensor Error Function 30
3.4.1 SDVAV System Interior Zone 31
3.4.2 SD VAV System Exterior and Interior Zone 35
3.4.3 DDVAV System Interior Zone 40
3.4.4 DDVAV System Exterior and Interior Zone 45
4. APPLICATIONS 50
4.1 Eller Oceanography and Meteorology Building 50
4.2 Veterinary Research Building 52
5. SUMMARY 55
REFERENCES 58
APPENDIX A 63
VITA 88

LIST OF FIGURES

Page

Figure 1. Relationship of impedance change to humidity (Denes, 2001) 8

Figure 2. Thermal conductivity (or absolute) humidity sensors (Roveti,2001). 9

Figure 3. Humidity sensor calibration intervals (Bruce) 13

Figure 4. Input parameters for simulation 21

Figure 5. SDVAV Interior Zone Room Temperature Error vs Energy Consumption under 0% Minimum Flow 32

Figure 6. SDVAV Interior Zone Cold Deck Temperature Error vs Energy Consumption under 0% Minimum Flow 33

Figure 7. SDVAV Interior Zone Room Temperature Error vs Energy Consumption under 50% Minimum Flow 34

Figure 8. SDVAV Interior Zone Cold Deck Temperature Error vs Energy Consumption under 50% Minimum Flow 35

Figure 9. SDVAV Exterior and Interior Zone Room Temperature Error vs Energy Consumption under 0% Minimum Flow 36

Figure 10. SDVAV Exterior and Interior Zone Cold Deck Temperature Error vs Energy Consumption under 0% Minimum Flow 38

Figure 11. SDVAV Exterior and Interior Zone Room Temperature Error vs Energy Consumption under 50% Minimum Flow 39

Figure 12. SDVAV Exterior and Interior Zone Cold Temperature Error vs Energy Consumption under 50% Minimum Flow 40

Figure 13. DDVAV Interior Zone Room Temperature Error vs Energy Consumption under 0% Minimum Flow 41

Figure 14. DDVAV Interior Zone Cold Deck Temperature Error vs Energy Consumption under 0% Minimum Flow 42

Figure 15. DDVAV Interior Zone Room Temperature Error vs Energy Consumption under 50% Minimum Flow 43

Page

Figure 16. DDVAV Interior Zone Cold Temperature Error vs Energy Consumption under 50% Minimum Flow 44

Figure 17. DDVAV Exterior and Interior Zone Room Temperature Error vs Energy Consumption under 0% Minimum Flow 46

Figure 18. DDVAV Exterior and Interior Zone Cold Temperature Error vs Energy Consumption under 0% Minimum Flow 47

Figure 19. DDVAV Exterior and Interior Zone Room Temperature Error vs Energy Consumption under 50% Minimum Flow 48

Figure 20. DDVAV Exterior and Interior Zone Cold Deck Temperature Error vs Energy Consumption under 50% Minimum Flow 49

Figure 21. Eller O&M Building 50

Figure 22. Building location 50

Figure 23. Eller Building Simulation vs Error Function Room Temperature 51

Figure 24. Eller Building Simulation vs Error Function Cold Deck Temperature 52

Figure 25. VMA Building Simulation vs Error Function Room Temperature 53

Figure 26. VMA Building Simulation vs Error Function Cold Deck Temperature 54

LIST OF TABLES

Page

Table 1. Recommended Calibration Intervals for Temperature Sensors from Two Manufacturers 10

Table 2. Pressure Sensor Recommended Calibration Interval from Calibrator Manufacturers 10

Table 3. Recommended Calibration Interval for NDIR CO_2 Sensors from Eight Manufacturers 11

Table 4. Recommended Calibration Intervals for Capacitive Humidity Sensors from Four Manufacturers 12

Table 5. 10-month Drift (Measurement,2003) 14

Table 6. 100-month Drift (8 Years) Data (Measurement,2003) 14

Table 7. Normalized failure mode distributions for thermistors (NAVSEA, 2010) 16

Table 8. Room Temperature Sets 20

Table 9. Pressure Sensor Sets 20

Table 10. Simulation Scenarios 20

Table 11. Weekday occupancy, equipment, and lighting schedules 22

Table 12. Weekend occupancy, equipment, and lighting schedules 23

Table 13. Eller Building Simulation Baseline Inputs 51

Table 14. VMA Building Simulation Baseline Inputs 53

1. INTRODUCTION

1.1 Research Motivation

Heating, ventilating, and air conditioning systems maintain and control temperature and humidity levels in order to provide a comfortable indoor environment for building occupants. The cost of HVAC system operation can be significant. It is estimated that the energy used to operate HVAC systems can represent approximately 50% of the total electrical energy used in a typical commercial building(Krarti,2000).

Sensors play an important role in HVAC system operation. They are used to control the cooling and heating provided by coils, to maintain static pressure or differential pressure by controlling the fan and pump speeds in variable speed systems, and to control outside air intake through CO2 sensors in demand-based control systems (Di Giacomo,1999). Sensors drifting away from their set points can not only result in complaints, but may also increase the energy consumption of the building. Building owners can improve their efficiency and reduce their costs by calibrating the sensors at a proper time interval. But this begs the question, how often do a building's sensors need to be recalibrated? The immediate objective of a calibration interval analysis system is the establishment of a set of calibration intervals that will ensure that appropriate measurement reliability targets are met (Castrup,1994). In this thesis, sensitivity of energy use to temperature sensor and pressure sensor errors is studied. Based on a particular sensor's impact on building energy performance, building operators should be

---

This thesis follows the style of *ASHRAE Journal.*

able to determine which sensors are of paramount importance, and which need to be calibrated more often than the others.

1.2 Research Objective

The goal of this thesis is to develop a methodology for determining sensor calibration interval with applications for two types of AHU systems. Manufacturers don't give a specific calibration interval for different sensor applications in HVAC systems. With the information about the sensor drift rate and the cost of sensor error on HVAC system operating cost, the optimal sensor calibration interval can be determined by interpolating the two factors. Extra energy consumption caused by sensor-error in HVAC systems can be estimated by simulating a building's operation. After taking several runs, the extra energy consumption caused by sensor error on HVAC systems can be determined. Using the sensor drift rate and the extra cost caused by sensor error, the optimized calibration interval can be calculated.

Two building applications will also be introduced in the thesis to illustrate how this methodology can be applied.

2. LITERATURE REVIEW

Studies examining the different types of sensors used in HVAC systems are introduced first to aid the engineer in selecting the right sensors for a particular job. This section is followed by the recommended calibration intervals provided by the manufacturers. Studies of sensor failure modes and the concept of drift are then presented.

2.1 Temperature Sensors

2.1.1 Thermocouples

A thermal couple consists of two different metals which are connected to form a circuit including two junctions. When the two different junctions of a thermal couple are exposed to different temperatures, there will be current in the circuit. One of the two junctions in the thermocouple circuit is called the “hot” junction and the other is called the “cold” junction. The “hot” junction will be exposed to the environment whose temperature will be measured. The “cold” junction can be either a reference temperature that is maintained at 0°C or at an electronically compensated meter interface (Williams,2002)

2.1.2 Thermistors

Thermistors are devices that change their electrical resistance when their temperature changes. There are two types of thermistors: positive temperature coefficient (PTC) and negative temperature coefficient (NTC). If the resistance increases

with increasing temperature, the device is called PTC, while if the resistance decreases with increasing temperature, the device is called NTC. Thermistors consist of two or three metal oxides that are sintered in a ceramic base material and have wires soldered to a semiconductor wafer. (Wilson,2005)

2.1.3 RTDs (Resistive temperature devices)

RTDs, like thermistors, employ a change in electrical resistance to measure or control temperature. Thermistors differ from resistance temperature detectors (RTD) in that the material used in a thermistor is generally a ceramic or polymer, while RTDs use pure metals. The temperature response is also different; RTDs are used over larger temperature ranges, while thermistors typically achieve a higher precision within a limited temperature range (Kimball,2003).

2.2 Pressure Sensors

2.2.1 Piezoresistive Pressure Sensor

There are various types of pressure sensors or pressure transducers. A widely used pressure sensor is the piezoresistive pressure sensor (Nadvi,2010).

Piezoresistive pressure sensors contain a sensing element made up of a silicon chip. The resistors are buried in the surface of the silicon. The resistor values change with the amount of pressure applied to the diaphragm outside of the resistor. Therefore, a change in pressure is converted to a change in resistance (electrical output).

2.3 CO2 Sensors

The major CO2 sensors can be divided into two types. One is using the NDIR (Non-Dispersive Infrared) method; the other uses a chemical method. The NDIR method is the one that has been used widely since chemical CO2 sensors have many limitations for application in certain fields.

2.3.1 NDIR CO2 Sensor

NDIR sensors use the absorption rate of IR radiation by CO2 to measure the level of CO2 present. An NDIR sensor is composed of an infrared source, a light tube, an interference filter and an infrared detector (Miller,2001). The gas mixture which includes CO2 is pumped into the light tube and then the absorption of the characteristic wavelength of light is measured. According to the Lambert-Beer law, the mole concentration can be calculated (Wong,1995).

2.3.2 Chemical CO2 Sensor

Chemical CO_2 gas sensors with sensitive layers based on polymer- or hetero polysiloxane have the principal advantage of very low energy consumption and can be reduced in size to fit into microelectronic-based systems (Sashida,2002).

For air conditioning applications these kinds of sensors can be used to monitor the quality of air and the tailored need of fresh air, respectively. For air conditioning applications these kinds of sensors can be used to monitor the quality of air and the tailored need of fresh air, respectively. These sensors are found to be extremely reliable

for the detection of CO2 below about 70 ºC. At higher temperatures, they are not suitable due to the hetero-polysiloxane structure (Stegmeier,2009).

2.4 RH Sensors

2.4.1 Capacitive Humidity Sensors

Capacitive relative humidity sensors are widely used in industrial, commercial, and weather telemetry applications (Wilson,2005).

Capacitive relative humidity sensors are based on the theory that the dielectric constant of a medium will change due to the absorption or adsorption of water vapor (Lacote,2003). The sensor based on this principle consists of two conductive electrodes between which a substrate is placed. The substrate could be glass, ceramic or silicon. The incremental change in the dielectric constant is proportional to the relative humidity of the surrounding environment. Typical change in capacitance is 0.2-0.5 pF for 1% RH change. Bulk capacitance is between 100 and 500 pF at 50% PH at 25 °C. These sensors have a low temperature coefficient and can function at temperatures up to 200°C. They are able to fully recover from condensation and resist chemical vapors. Response time ranges from 30 to 60 seconds for a 63% RH step change (Laville,2002). The typical uncertainty of capacitive sensors is ±2% RH from 5% to 95% RH with two-point calibration (Wilson,2005).

2.4.2 Resistive Humidity Sensors

Resistive humidity sensors are based on the principle that the impedance change has an inverse exponential relationship to humidity which is shown in Figure 1. The typical mediums used in this type of sensors are conductive polymer, salt, or treated substrate. These sensors use noble metal electrodes or wire-wound electrodes. A substrate coated with a salt or conductive polymer is also a part of it. The whole sensor is protected in a plastic housing. The response time for most resistive sensors ranges from 10 to 30 s for a 63% step change. The impedance range of typical resistive elements varies from 1 kΩ to 100 MΩ. Resistive humidity sensors can be calibrated without humidity calibration standards since the interchangeability is usually within ±2% RH, which allows the calibration to be done by a resistor at a fixed RH point. The resistive humidity sensors are field replaceable. Nominal operating temperature of resistive sensors ranges from –40°C to 100°C (Johari,2003).

In residential and commercial environments, the life expectancy of these sensors is >>5 yr., but exposure to chemical vapors and other contaminants such as oil mist may lead to premature failure. Another drawback of some resistive sensors is their tendency to shift values when exposed to condensation if a water-soluble coating is used. Resistive humidity sensors have significant temperature dependencies when installed in an environment with large (>10°F) temperature fluctuations (Roveti,2001).

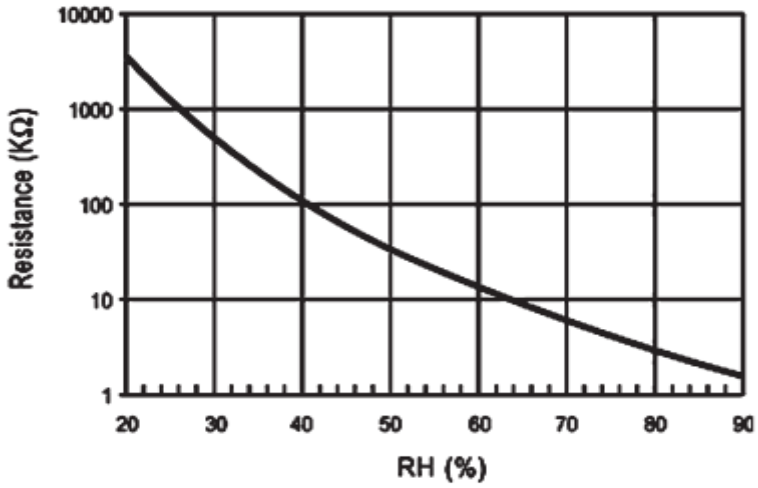

Figure 1. Relationship of impedance change to humidity (Denes, 2001)

2.4.3 Thermal Conductivity Humidity Sensors

Thermal conductivity humidity sensors are known as absolute humidity sensors. They are constructed with two negative temperature coefficient thermistors in a circuit. One is sealed with dry nitrogen and another is exposed to the environment. The circuit is shown in Figure 2. When the current is passing through the thermistors, the resistance of the thermistors transfers heat to their surroundings. Since dry air has lower heat capacity than the moist air, the temperatures around the two thermistors are different which results in different resistances. This difference is proportional to the absolute humidity. The sensor can be calibrated by exposing it in dry air and adjusting the results to zero. Absolute humidity sensors are very durable, operate at temperatures up to 575°F(300°C) and are resistant to chemical vapors by virtue of the inert materials used for their construction. Absolute humidity sensors have higher resolution at temperatures larger than 200 °F and can be applied in many occasions where capacitive and resistive sensors

do not survive. The typical accuracy of an absolute humidity sensor is +3 g/m^3, which converts to about ±5% RH at 40°C and ±0.05% RH at 100°C (Johari,2003).

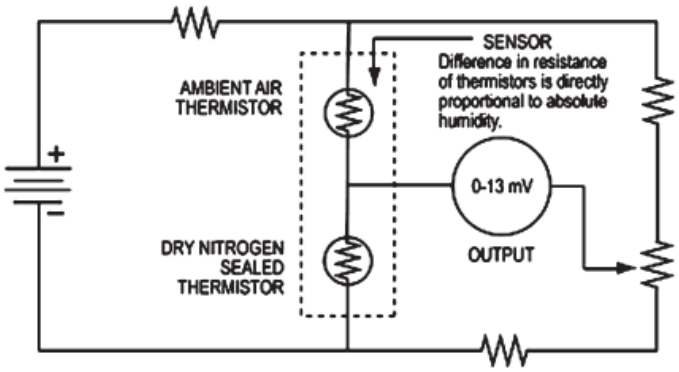

Figure 2. Thermal conductivity (or absolute) humidity sensors (Roveti,2001).

2.5 Manufacturers' Calibration Frequency Recommendations for HVAC Sensors

According to the manufacturers included in this survey, sensor calibration intervals are dependent on the location, the applications, and the frequency that the sensor has been used. In the sensor specifications from these manufacturers, a default calibration interval is one year for most sensors but the interval will vary according to their specific application conditions. The best calibration interval should be determined according to the customer's need, since calibration intervals will vary with the sensor's location and operation conditions. Below are some common recommendations offered by different manufacturers.

2.5.1 Temperature Sensors

Based on the review of manufacturers' specification literature, the most commonly used temperature sensors in HVAC systems are thermistors. The

recommended calibration interval for these temperature sensors is one year to maintain their specified accuracy. Table 1 shows the recommended calibration intervals from two manufacturers.

Table 1. Recommended Calibration Intervals for Temperature Sensors from Two Manufacturers

Company Name	Sensor Name	Recommended Calibration Interval
Siemens	TR 200/300	1 yr. (Siemens)
GE Sensing	Telaire 7000	1 yr.(GE-B,2011)

2.5.2 Pressure Sensors

Based on the review of the manufacturers' specification literature, the most commonly used pressure sensors in HVAC systems are piezoresistive pressure sensors. No official pressure recalibration intervals were recommended by the manufacturers in the literature surveyed. However, GE Sensing, who manufactures pressure calibrators recommends one year as the calibration interval for pressure sensors. Table 2 shows the recommended calibration intervals from two pressure calibrators manufactured by GE Sensing.

Table 2. Pressure Sensor Recommended Calibration Interval from Calibrator Manufacturers

Company Name	Calibrator Name	Recommended Calibration Interval
GE Sensing	7250 sys	1 yr. (GE-C,2011)
GE Sensing	7251 LP	1 yr.(GE-D,2011)

2.5.3 CO2 Sensors

Based on the manufacturers specification literature review (see Table 3), the most commonly used CO2 sensor for HVAC systems is the NDIR (Non-Dispersive infrared) CO2 sensor. The recommended calibration interval for this type of sensor is five years, in order to maintain their initial accuracy as shown in Table 3. These sensors are typically used for metering installed in the HVAC system. For CO2 measurement equipment used for spot measurements, the calibration interval varies. Table 3 shows the recommended calibration intervals from eight manufacturers for nine different installed CO2 monitors and in-hand meters.

Table 3. Recommended Calibration Interval for NDIR CO_2 Sensors from Eight Manufacturers

Company Name	Sensor Name	Recommend Calibration Interval
Vaisala	CARBOCAP	5 yr.(VAISALA-A,2011)
Trane	CO2 DCV Duct Sensor	5 yr.(Trane-A,2011)
Trane	CO2 Duct Sensor and CO2 Wall Sensor	5 yr.(Trane-B,2011)
Honey Well	CO2 Sensor	5 yr.(Honeywell)
Innovia		5 yr.(Innovair)
Greystone	CO2 Detectors	5 yr.(Greystone)
TSI		1 month(TSI)
GE	T5000 Airestat CO2 & Temperature Transmitter	12 month(GE-A.,2011)
Fluke		1 yr.(Fluke)

2.5.4 Relative Humidity Sensors

The most commonly used relative humidity sensor is a capacitive-type sensor. The commonly recommended calibration interval is one year (Clay,2011). Since the

humidity sensor's accuracy is influenced significantly by the operation conditions, the calibration interval should be changed according to the customer's needs. If the environment is a humid, pollution-heavy, or a dusty area, the sensor may need to be calibrated twice or more per year. Table 4 shows the recommended calibration intervals from four manufacturers. Figure 6 shows the recommended humidity sensor calibration intervals from VAISALA for maintaining two different accuracy levels under broad ranges of operating conditions.

Table 4. Recommended Calibration Intervals for Capacitive Humidity Sensors from Four Manufacturers

Company Name	Sensor Name	Sensor Type	Recommend Calibration Interval
Vaisala	HUMICAP	Capacitive	1 yr.(VAISALA-B,2011)
APT system			1 yr.(Conservatory, 2011)
Veriteq	Validatable Relative Humidity & Temperature Data Loggers	Capacitive	1 yr.(VERITEQ, 2011)
Ohmic	Instruction Manual for Relative Humidity & Temperature Meter DM-509		1 yr.(OHMICO, 2011)

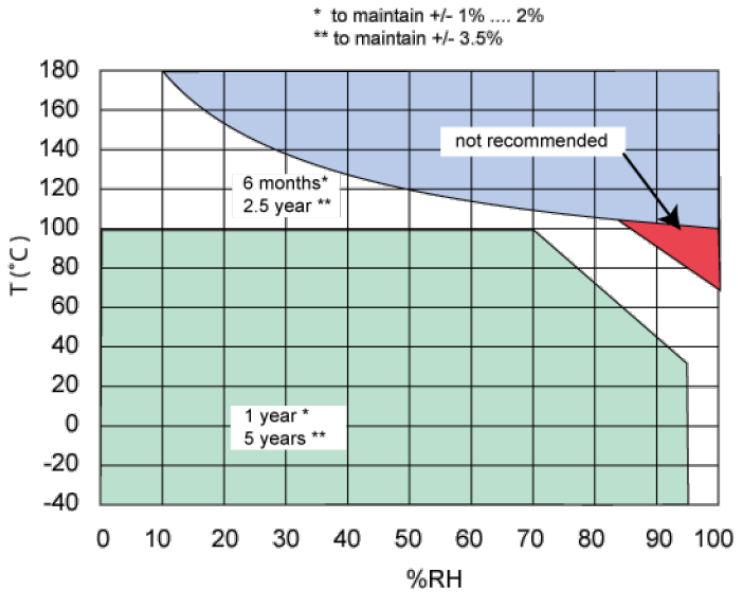

Figure 3. Humidity sensor calibration intervals (Bruce)

2.6 Sensor Drift

Figure 4 (Measurement, 2003) below shows the 10 month drift data for thermistors of different coating types. From this table, we can see that coating types do not affect sensor accuracy until the operation temperature grows higher than 70°C. From this point, we can see that the operation temperature has a significant impact on the sensor drift rate. For operation above 100°C, glass-coated Super-Stable thermistors are most accurate, as compared to expoxy-coated and glass-coated thermistors. The type of coating will affect accuracy when the operation temperature is higher than 100°C.

Table 5. 10-month Drift (Measurement,2003)

Operating Temperature	Epoxy-Coated	Glass-Coated	Glass-Coated Super-Stable
0˚C	<0.01˚C	<0.01˚C	<0.01˚C
25˚C	<0.01˚C	<0.01˚C	<0.01˚C
70˚C	not available	not available	<0.01˚C
100˚C	0.20˚C	0.12˚C	0.02˚C
150˚C	1.50˚C	0.15˚C	0.05˚C
200˚C	not applicable	0.20˚C	0.22˚C

Table 5 (Measurement, 2003) shows the 100-month data for thermistors of different coating types. From this table, we can conclude that the operation temperature is of great importance to the sensor's accuracy.

Table 6. 100-month Drift (8 Years) Data (Measurement,2003)

Operating Temperature	Epoxy-Coated	Glass-Coated	Glass-Coated Super-Stable
0˚C	<0.01˚C	not available	<0.01˚C
25˚C	<0.02˚C	not available	<0.01˚C
70˚C	not available	not available	<0.01˚C
100˚C	0.32˚C	not available	0.03˚C
150˚C	not recommended	not available	0.08˚C
200˚C	not applicable	not available	0.60˚C

The data for 100 months continuous use indicates that the drift is no more than three times the 10 month drift. This reflects the flattening of drift rates over time (Measurement, 2003).

2.7 Sensor Failure Modes

Failure mode is defined as the consequence of the mechanism through which the failure occurs (MIL-HDBK-338B, 2008). The report entitled "Failure Mode/Mechanism Distribution 1997" offers abundant failure mode data defined alternatively for equipment, actuators, etc. In this report, short, open and drift are all considered failure modes of sensors. In this report, actuator failure modes are also classified and quantified (RIAC,1997).

In 1974, Gaw also mentioned two common failure modes, open sensor and shorted sensor, for thermistors and thermocouples. Gaw stated that an open sensor can occur as a result of mechanical abuse, friction or vibration, and a shorted sensor is caused either by abrasion or vibration (Gaw, 1974). A thermistor report from Naval Sea Systems Command (NAVSEA, 2010) mentioned three failure modes for thermistors. These three references indicate that the open circuit is the most common failure mode of a thermistor. The second most common failure mode is drift in resistance value as the thermistor ages; this is also called parameter change, as shown in Table 7 (NAVSEA, 2010). The least common failure mode is the shorted circuit, which comprises 15% of thermistor failures. The Electronic Reliability Design Handbook (MIL-HDBK-338B, 2008) uses a different classification system for thermistor failure modes classifying them as: out of tolerance, false response, open and shorted circuit. I have chosen to use the

classification system of Williams, Gaw and NAVSEA as open curcuit, short curcuit and parameter change.

Table 7. Normalized failure mode distributions for thermistors (NAVSEA, 2010)

Failure Mode	Relative Probability
Open	63%
Parameter change	22%
Short	15%

2.8 Review of Related Studies

Fisk has conducted a study to assess the accuracy of 44 CO_2 sensors located in 9 buildings in California. The results showed that the accuracy of CO_2 sensors in commercial buildings is less than needed to measure the CO_2 concentration differences with less than a 20% error. The authors conclude that there is a need for more accurate CO_2 sensors and better maintenance and calibration (Fisk,2006; Fisk,2008)

Iowa Energy Center has carried out a study to evaluate the performance of Non-dispersive Infrared wall-mounted CO2 transmitters used in typical building HVAC applications. They adopted the NDIR transmitters from different manufacturers and tested the different models. The results have shown a different aging effect among CO2 transmitter models (Shrestha,2010).

Iowa Energy Center has tested and evaluated the performance of resistive and capacitive duct-mounted relative humidity transmitters used in typical building HVAC applications. The humidity transmitters used in the test are from six leading

manufacturers. The results show that few of the commercial humidity sensors met the manufacturers claimed accuracy (NBCIP,2004; NBCIP,2005)

Taylor has built a DOE-2.2 model of a typical office building to test the impact on energy use of various high limit control options including sensor error. In this test, different sensor errors including temperature and humidity sensors are compared under different high limit control strategies. Different climates are also compared in this test (Steven,2010).

In this literature review, the recommended calibration intervals for different types of sensors have been studied and sensor drift rates and failure modes and the related studies have been reviewed. A sensor's preferred recalibration interval will be affected by many factors such as sensor drift rate, operation range, application, and installed location. From the literature reviewed we can see that CO2 sensors and humidity sensors seldom have met the manufacturers claimed accuracy. The study from Taylor has shown the sensor errors impact different outside air control strategies but no study has stated how the specific application will affect the energy consumption. This thesis will focus on the effect of different applications on the energy consumption for temperature sensors and pressure sensors. For example, cold deck temperature sensors and room temperature sensors are two different applications in a HVAC system. How will the two different applications affect the calibration interval even if the same type of temperature sensor is used? A sensitivity study will be carried out to determine the energy impact of sensor error in different applications and assist in the determination of calibration intervals. The study will make several simulations to compare the annual energy consumption under

different sensor error levels in various applications. Using the results of this sensitivity study, a methodology for determining the calibration interval based on specific applications will be developed.

3. METHODOLOGY

The study of the sensitivity of building energy consumption and its relation to sensor error is divided into two stages. The simulation model is a Microsoft® Excel-based implementation of the ASHRAE Simplified Energy Analysis Procedure (Knebel,1983) developed by Wei which has been modified for this sensor error sensitivity analysis (Wei,1998). This is a quick and easy simulation tool which only requires a few easily-obtained inputs. The first stage is to simulate the HVAC system under different sensor error values. During this stage, different scales of room temperature sensor errors, cold deck temperature sensor errors, hot deck temperature sensor errors, fan differential pressure errors and pump differential pressure sensor errors are simulated within the this tool. The second stage is to determine the energy consumption change and sensor error function to be applied when certain building operations and building load characteristics are met.

The simulation was carried on the Excel spreadsheet. There were six control parameters considered in this series simulation: room temperature, cold deck temperature, hot deck temperature (considered in DDVAV systems), HHW pump differential pressure, CHW pump differential pressure, and fan differential pressure. By changing each control parameter in each run, the energy consumption was different. Once there was a sensor error, the actual building operation changed. The simulations were used to analyze the energy consumption under different sensor error scales. There were ten additional runs for each control parameter, beyond that of the baseline run. For the pressure control parameters, the values were changed by 1% of the baseline value for

each additional run. For the temperature control parameters, the values were changed by 1 degree of the baseline value for each additional run. Table 8 and Table 9 show the parameters changed in the simulations. Table 8 shows10 additional runs besides the baseline for room temperature run sets. Table 9 shows a series of pressure sensor run sets.

Table 8. Room Temperature Sets

Run 1	Run 2	Run 3	Run 4	Run 5	Baseline	Run 6	Run 7	Run 8	Run 9	Run 10
68°F	69°F	70°F	71°F	72°F	73°F	74°F	75°F	76°F	77°F	78°F

Table 9. Pressure Sensor Sets

Run 1	Run 2	Run 3	Run 4	Run 5	Baseline	Run 6	Run 7	Run 8	Run 9	Run 10
-5%	-4%	-3%	-2%	-1%	0%	1%	2%	3%	4%	5%

The simulation results are shown in terms of energy consumption, which can be found in Appendix A. There are eight total simulation scenarios considered in

Table 10. For each scenario, there are three baseline simulations with the outside air of 10%, 20% and 30%.

Table 10. Simulation Scenarios

System	Zone	Minimum Flow
SDVAV	Interior	0%
SDVAV	Interior	50%
SDVAV	Exterior & Interior	0%
SDVAV	Exterior & Interior	50%
DDVAV	Interior	0%
DDVAV	Interior	50%
DDVAV	Exterior & Interior	0%
DDVAV	Exterior & Interior	50%

3.1 Simulation Input Parameters and Baseline

The simulation is a generic building which has an area of 100,000 square feet, and a people density of 100 square feet per person. The input parameters included people sensible load, people latent load, equipment load, lighting load, etc. The baseline inputs of both the interior zone and the exterior zone load and a 10% (this number could be different for different baselines) outside air pressure level are given in the input screen shown as Figure 4.

People Sensible Load	250	Btu/hr.person
People Latent Load	105	Btu/hr.person
Equipment Load	2.1	W/ft2
Light Load	1.5	W/ft2
Total Floor Area	100,000	ft2
Exterior Zone Fraction	25%	
People Density	100	ft2/person
Building UA/ft2	0.33	Btu/hr-F-ft^2
Exterior Zone T	73	°F
Design Supply Air Flow Rate =	1	cfm/SF
Ventilation Air (Outside Air) % of Total =	10%	%OA
Design Fan Power, Pfan =	200	HP
Minimum supply air flow (Fraction of des. flow)=	0.3	
Cold Deck Temperature=	55	
qir =	170,650	Btu/hr
qer =	85,325	Btu/hr

Figure 4. Input parameters for simulation

Another set of inputs are the occupancy schedules, equipment schedules and lighting schedules for both weekdays and weekends. The input screens for these variables are shown in the Table 11 and Table 12 (Claridge,2004).

Table 11. Weekday occupancy, equipment, and lighting schedules

Hour	Occupancy Schedule	Equipment Schedule	Light Schedule
0	0.5	0.63	0.37
1	0.5	0.61	0.33
2	0.5	0.60	0.30
3	0.5	0.58	0.29
4	0.5	0.58	0.29
5	0.5	0.59	0.37
6	0.5	0.65	0.61
7	0.5	0.76	0.70
8	1	0.86	0.78
9	1	0.88	0.80
10	1	0.89	0.79
11	1	0.88	0.79
12	1	0.89	0.80
13	1	0.88	0.80
14	1	0.88	0.80
15	1	0.85	0.80
16	1	0.78	0.77
17	1	0.71	0.63
18	0.5	0.68	0.51
19	0.5	0.67	0.48
20	0.5	0.66	0.45
21	0.5	0.65	0.43
22	0.5	0.65	0.42
23	0.5	0.64	0.40

Table 12. Weekend occupancy, equipment, and lighting schedules

Hour	Occupancy Schedule	Equipment Schedule	Light Schedule
0	0.5	0.59	0.33
1	0.5	0.59	0.33
2	0.5	0.58	0.33
3	0.5	0.57	0.32
4	0.5	0.57	0.32
5	0.5	0.57	0.33
6	0.5	0.58	0.33
7	0.5	0.58	0.34
8	0.5	0.58	0.38
9	0.5	0.59	0.43
10	0.5	0.59	0.43
11	0.5	0.60	0.48
12	0.5	0.59	0.54
13	0.5	0.59	0.55
14	0.5	0.59	0.54
15	0.5	0.59	0.53
16	0.5	0.59	0.52
17	0.5	0.59	0.37
18	0.5	0.60	0.36
19	0.5	0.60	0.36
20	0.5	0.61	0.36
21	0.5	0.61	0.36
22	0.5	0.60	0.36
23	0.5	0.59	0.34

The baseline settings for this building are room temperature 73°F, cold deck temperature 55°F, hot deck temperature 110°F, and design flow 1cfm /ft^2.

3.2 Air Side Model

The algorithms used in the air side models for DDVAV and SDVAV are presented in the following subsections.

3.2.1 Dual Duct Various Air Volume System

After the load calculation was achieved from the previous descriptions, the cold deck flow of the exterior zone and interior zone can both be determined.

$$V_{e,c}=q_{e,s}/(1.08*(T_r-T_{cl})) \text{ when } q_{e,s}>0 \quad \textbf{(1)}$$

$$V_{e,h}=q_{e,s}/(1.08*(T_r-T_{hl})) \text{ when } q_{e,s}<0 \quad \textbf{(2)}$$

$$V_{i,c}=q_{i,s}/(1.08*(T_r-T_{cl})) \text{ when } q_{i,s}>0 \quad \textbf{(3)}$$

$$V_{i,h}=q_{i,s}/(1.08*(T_r-T_{hl})) \text{ when } q_{i,s}<0 \quad \textbf{(4)}$$

$$V_e=max\ (V_{e,c}+V_{e,h},V_{e,min}) \quad \textbf{(5)}$$

$$V_i=max(V_{i,c}+V_{i,h},V_{i,min}) \quad \textbf{(6)}$$

The supply temperature then can be determined by the following equations:

$$T_{es}=T_r-q_{e,s}/1.08/V_e \quad \textbf{(7)}$$

$$T_{is}=T_r-q_{i,s}/1.08/V_i \quad \textbf{(8)}$$

The return air temperature is calculated by the following equations, which consider the return duct heat gain:

$$T_{ir}=T_i + q_{ir}/(1.08V_i) \quad \textbf{(9)}$$

$$T_{er}=T_e + q_{er}/(1.08V_e) \quad \textbf{(10)}$$

$$T_r=(V_i*T_{ir} + V_e*T_{er})/(V_i + V_e) \quad \textbf{(11)}$$

When the return air temperature is calculated, the mixed air temperature can be determined.

$$T_{ma}=T_r + X_{oa}(T_{oa} - T_r) \quad \textbf{(12)}$$

Temperature entering the coil is calculated by taking the temperature after the preheat coil and adding it to the temperature rise across the fan.

$$T_{ce}=T_{he} =T_{ph} + T_{sf} \quad \textbf{(13)}$$

The hot deck temperature is determined according to the hot deck temperature schedule.

$$T_{hl} =IF(T_{oa}>T_{oa1},IF(T_{oa}>T_{oa2},T_{L2},T_{L1}+(T_{oa}-T_{oa1}) \quad \textbf{(14)}$$

Air flow from the coil side is calculated by the following equations:

$$V_{ih} =V_i*(T_{is} - T_{cl})/(T_{hl} - T_{cl}) \quad \textbf{(15)}$$

$$V_{ic} =V_i - V_{ih} \quad \textbf{(16)}$$

$$V_{eh} =V_e*(T_{es} - T_{cl})/(T_{hl} - T_{cl}) \quad \textbf{(17)}$$

$$V_{ec} =V_e - V_{eh} \quad \textbf{(18)}$$

$$V_h =V_{ih} + V_{eh} \quad \textbf{(19)}$$

$$V_c =V_{ic} + V_{ec} \quad \textbf{(20)}$$

Return air humidity is the minimum value of the wet-coil humidity, $W_{r'}$, and the dry-coil humidity, $W_{r''}$.

$$W_r = min(W_{r'}:W_{r''}) \quad \textbf{(21)}$$

Sensible heat is calculated by the following equation:

$$q_{cs} =1.08*V_c*(T_{ce} - T_{cl}) \quad \textbf{(22)}$$

Latent heat is calculated by:

$$q_{cl} = IF(W_r > W_{cl},\ 4840*V_c*(W_r - W_{cl}),\ 0) \quad \textbf{(23)}$$

Heating is calculated by:

$$q_h = IF(T_{hl} > T_{he},\ 1.08*V_h*(T_{hl} - T_{he}),\ 0) \quad \textbf{(24)}$$

3.2.2 Single Duct Various Air Volume System

For an SDVAV system, after the load calculation is achieved according to the previous equations, the cold deck flow of the exterior zone and the interior zone can be determined as follows:

$$V_e = max(q_{e,s}/(1.08*(T_r - T_{cl}),\ V_{min}) \text{ when } q_{e,s} > 0 \quad \textbf{(25)}$$

$$V_e = max(q_{e,s}/(1.08*(T_r - T_{hl}),\ V_{min}) \text{ when } q_{e,s} < 0 \quad \textbf{(26)}$$

$$V_i = max(q_{e,s}/(1.08*(T_r - T_{cl}),\ V_{min}) \text{ when } q_{i,s} > 0 \quad \textbf{(27)}$$

$$V_i = max(q_{e,s}/(1.08*(T_r - T_{hl}),\ V_{min}) \text{ when } q_{i,s} < 0 \quad \textbf{(28)}$$

The supply temperature can then be determined by the following equations:

$$T_{es} = T_r - q_{e,s}/1.08/V_e \quad \textbf{(29)}$$

$$T_{is} = T_r - q_{i,s}/1.08/V_i \quad \textbf{(30)}$$

The return air temperature is calculated by the following equations, which consider the return duct heat gain:

$$T_{ir} = T_i + q_{ir}/(1.08V_i) \quad \textbf{(31)}$$

$$T_{er} = T_e + q_{er}/(1.08V_e) \quad \textbf{(32)}$$

$$T_r=(V_i*T_{ir} + V_e*T_{er})/(V_i + V_e) \quad \textbf{(33)}$$

When the return air temperature is calculated, the mixed air temperature can then be determined:

$$T_{ma}=T_r + X_{oa}(T_{oa} - T_r) \quad \textbf{(34)}$$

Temperature entering the coil is calculated by the temperature taken from the preheat coil plus the temperature rise across the fan:

$$T_{ce}=T_{he} =T_{ph} + T_{sf} \quad \textbf{(35)}$$

SDVAV systems use reheat to control the temperature in a room. The reheat of both the interior zone and the exterior zone can be determined by the equations listed below:

$$q_{e,rh}=(T_{es}- T_{cl})*1.08*V_e \quad \textbf{(36)}$$

$$q_{i,rh}=(T_{is}-T_{cl})*1.08*V_i \quad \textbf{(37)}$$

Return air humidity is the minimum value of the wet-coil humidity, $W_{r'}$, and dry-coil humidity, $W_{r''}$.

$$W_r = min(W_{r'}:W_{r''}) \quad \textbf{(38)}$$

The sensible cooling load from the coil side is calculated by:

$$q_{cs} =1.08*V*(T_{ce} - T_{cl}) \quad \textbf{(39)}$$

Latent heat is calculated by:

$$q_{cl} =IF(W_r > W_{cl}, 4840*V*(W_r - W_{cl}), 0) \quad \textbf{(40)}$$

3.3 Pump and Fan Model

3.3.1 Pump model

The power used for carrying the fluid is determined by the flow rate multiplied by the pressure drop across the piping system.

$$W_{fluid} = V^* \Delta P_{total} \quad \textbf{(41)}$$

The power consumed by the pump is determined by the equation below, which equals the power carrying the fluid divided by the pump efficiency.

$$W_{pump} = W_{fluid} / Eff_{pump} \quad \textbf{(42)}$$

$$W_{pump}(hp) = V(gal/min)\ \Delta P_{total}(ft\text{-}H2O) / (3960(gal\text{-}ft/min\text{-}hp)^* Eff_{pump}) \quad \textbf{(43)}$$

The total pressure drop through the piping system includes the difference in static pressure of the inlet and outlet, the velocity loss, the elevation difference of the inlet and outlet, and the friction loss across the pipes.

$$\Delta P_{total} = (\Delta P_{static} + \Delta P_{velocity} + \Delta P_{elevation})_{inlet\text{-}outlet} + \Delta P_{friction} \quad \textbf{(44)}$$

Here in the Excel simulation, a simplified pump and fan model is used. It is assumed that the static pressure, the velocity of the fluid, and the fluid elevation of the inlet and outlet are the same.

Next, the model is simplified into a function that only includes friction loss.

$$\Delta P_{total} = \Delta P_{friction} = C^* V^2 \quad \textbf{(45)}$$

Here C stands for the constant coefficient of the curve. This is an ideal pump curve.

3.3.2 Fan model

The power used for carrying the fluid is determined by the flow rate times the pressure drop across the piping system.

$$W_{fluid} = V^* \Delta P_{total} \quad \textbf{(46)}$$

The power consumed by the fan is determined by the equation below, which equals the power carrying the fluid divided by the fan efficiency.

$$W_{fan} = W_{fluid} / Eff_{fan} \quad \textbf{(47)}$$

$$W_{fan}(hp) = V(gal/min)\ \Delta P_{total}(ft\text{-}H2O) / (3960(gal\text{-}ft/min\text{-}hp)^* Eff_{pump}) \quad \textbf{(48)}$$

The total pressure drop across the piping system includes the difference in static pressure of the inlet and outlet, the velocity loss, the elevation difference of the inlet and outlet, and the friction loss across the pipes.

$$\Delta P_{total} = (\Delta P_{static} + \Delta P_{velocity} + \Delta P_{elevation})_{inlet\text{-}outlet} + \Delta P_{friction} \quad \textbf{(49)}$$

Here in the Excel simulation, a simplified model pump and fan were used. It was assumed that the static pressure, the velocity of the fluid, and the fluid elevation of the inlet and outlet were the same.

Then the model was simplified into a function that only included friction loss.

$$\Delta P_{total} = \Delta P_{friction} = C^* V^2 \quad \textbf{(50)}$$

Here C stands for the constant coefficient of the curve. This is an ideal fan curve.

3.4 Sensor Error Function

By analyzing the results presented in Appendix A, it was found that the energy consumption change corresponding to the sensor error demonstrates a relationship between sensor error, the outside air ratio, minimum air flow ratio, zone load, and system type as shown in Equation 1.

$$EnergyConsumption = f(SystemType, Load, MinimumAirFlowRatio, Error, OutsideAirRatio) \quad \textbf{(51)}$$

When the zone load, zone minimum supply flow and systems type are fixed, it was found that the room temperature sensor and the cold deck temperature sensor have greater influence on the energy use than the hot deck temperature sensors and pressure sensors.

Here in this thesis, all charts' horizontal axes are expressed by the actual operation point changes relative to the baseline operation points. When the sensors shift positively, the actual system operation point is lower than the baseline. As a result, the value on the axis is negative. The vertical axis is the relative energy consumption change as compared to the baseline. There are four series represented in each figure: 10% outside air, 20% outside air, 30% outside air, and a regression model built based on the series simulation data.

3.4.1 SDVAV System Interior Zone

For an SDVAV system that serves the interior zone and has a minimum flow of 0% of the design flow, it can be concluded from Figure 5 and Figure 6 that the room temperature sensors affect the system's energy consumption more than the cold deck temperature sensor, when they both change to the same degree.

From Figure 5 we can see that when room temperature changes; building energy consumption change has a relationship with the outside air ratio and the room temperature sensor error. The relative energy consumption change can be expressed as a function of the outside air ratio and sensor error. The equation is shown in Equation 2.

$$REC = -0.00647E^2 * OA + 0.231OA^2 * E + 3.767OA * E + 0.00169E^2 - 0.114OA^2 + 0.4755OA - 0.01636E - 0.00431 \quad \textbf{(52)}$$

REC = Relative Energy Consumption

E = Error

OA = Outside Air Ratio

When the sensor shifts positively, the final operation point temperature will be lower than the actual operation point. From Figure 5, we can tell that when the sensor shifts positively, energy consumption will increase, and when the sensor shifts negatively, the energy consumption will decrease. For an SDVAV system that serves an interior zone, energy consumption will change more per degree when the sensor shifts positively than when the sensor shifts negatively.

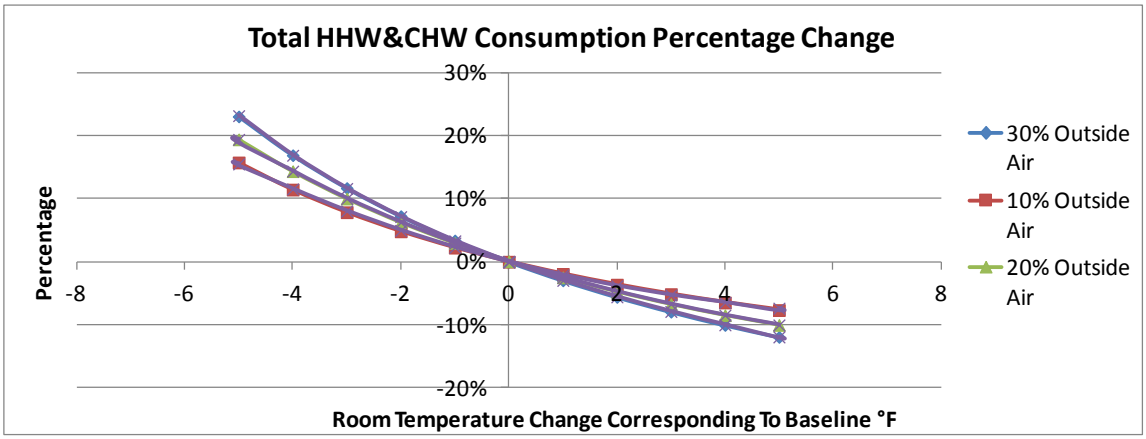

Figure 5. SDVAV Interior Zone Room Temperature Error vs Energy Consumption under 0% Minimum Flow

The reason why the chart follows this pattern is that for a single duct VAV system, the higher the room temperature set point the less energy the building consumed. From the chart above, when the sensor shifts positively, the final room temperature will be lower so that is why when the sensor shifts positively, the energy consumption will increase.

Figure 6 shows that a building's energy consumption change has a relationship with the cold deck sensor error and outside air ratio. But the outside air ratio's impact is so small that it can be neglected. This can also be applied for the following scenarios. In this way, energy consumption that changes with cold deck temperature will be a function of sensor error only. The energy consumption can be expressed as a function of cold deck sensor error.

$$REC = 8.37 * 10^{-5} E^3 + 0.001163 E^2 + 0.01382 * E - 0.0004 \qquad \textbf{(53)}$$

From Figure 6 we can see that the energy consumption increases when the actual operation point values increase; this is caused by the temperature rise considered in the simulation model. According to the equation $V_e=q_{e,s}/(1.08*(T_r-T_{cl})$, the higher the cold deck temperature, the larger the supply flow, and the more the energy consumption across the fan, the greater the total energy consumption.

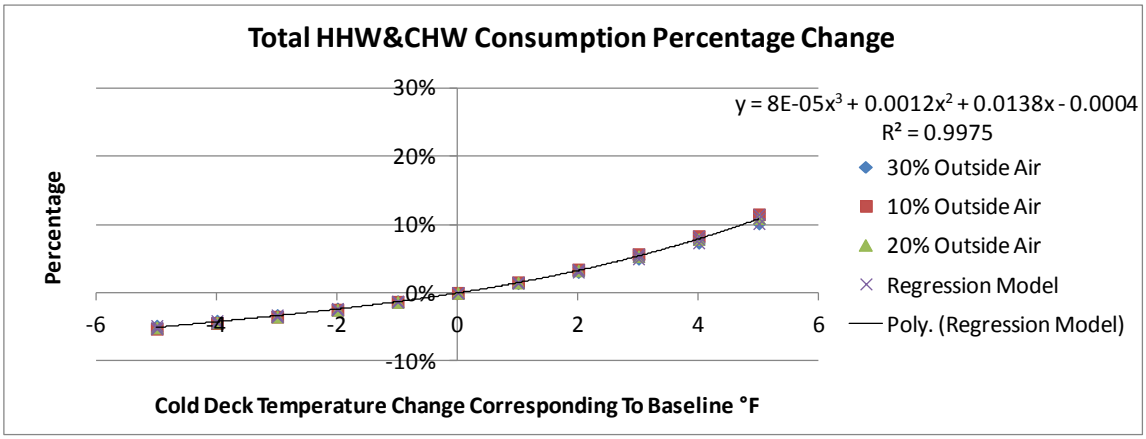

Figure 6. SDVAV Interior Zone Cold Deck Temperature Error vs Energy Consumption under 0% Minimum Flow

For an SDVAV system that serves the interior zone and has a minimum flow of 50% of the design flow, it can be seen from Figure 7 and Figure 8 that the room temperature sensor and the cold deck temperature sensor have almost the same impact when they both change to the same degree.

From Figure 7 we can see that when the room temperature changes, the building energy consumption change has a relationship to the outside air ratio and the room temperature sensor error. The energy consumption is expressed as a function of the outside air ratio and sensor error. The equation is shown below:

$$REC = -0.0004E^3 + 0.007E^2 * OA - 0.1506OA^2 * E - 0.9792OA * E + 0.0039E^2 - 0.0088OA^2 + 0.0024OA + 0.02E - 0.0004 \quad \textbf{(54)}$$

From Figure 7, we can tell that when the sensor shifts positively, energy consumption will increase, but when the sensor shifts negatively, energy consumption will also increase. For an SDVAV system that serves an interior zone and also has a minimum flow larger than that required by most operational flow, the energy consumption will change to the same scale when the sensor shifts either positively or negatively. From the charts we can see that in this situation, we should worry both when the sensor shifts negatively and when it shifts positively.

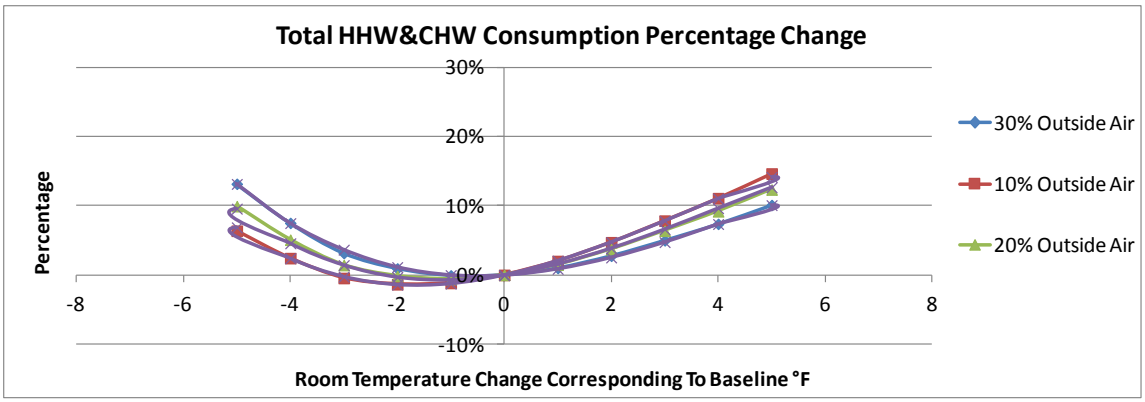

Figure 7. SDVAV Interior Zone Room Temperature Error vs Energy Consumption under 50% Minimum Flow

For a SDVAV system that has a 50% minimum air flow, the energy consumption change with the room temperature sensor will be affected by both the actual cooling required and the reheat required. When the sensor shifts positively, the actual cooling required increase and also the air flow required will increase. But when the sensor shifts negatively, the actual operation of the building becomes more like a constant volume

system in this way, although less cooling is required but the reheat increases with the room temperature increases thus the cooling increase.

Figure 8 shows that any energy consumption change with the cold deck temperature will be a function only of sensor error. The energy consumption can be expressed as a function of the cold deck sensor error. The equation is shown below:

$$REC = 0.000297E^3 + 0.003933E^2 - 0.02311E - 4.58*10^5 \qquad \textbf{(55)}$$

From Figure 8 we can see that the energy consumption increases when the sensor shifts positively. The energy consumption change will be greater when the sensor shifts positively, rather than when it shifts negatively.

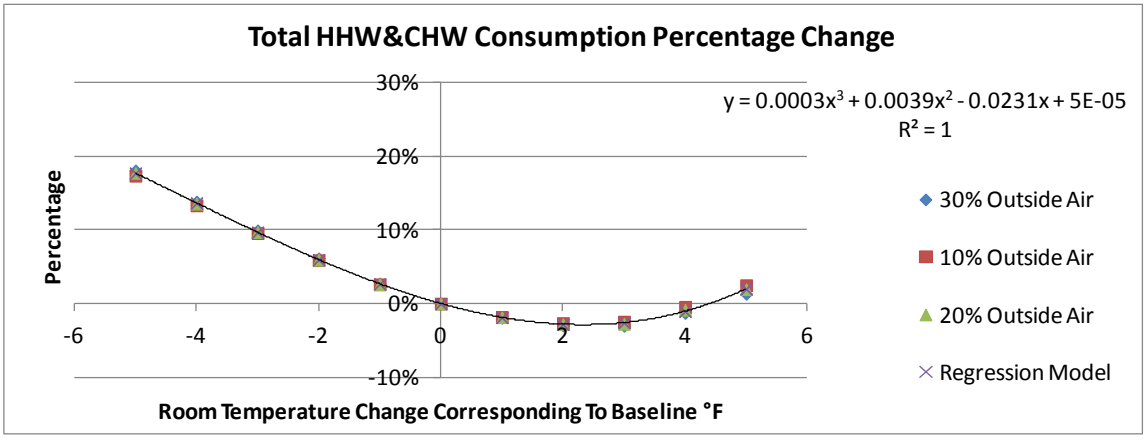

Figure 8. SDVAV Interior Zone Cold Deck Temperature Error vs Energy Consumption under 50% Minimum Flow

3.4.2 SD VAV System Exterior and Interior Zone

For a SDVAV system that serves the interior zone and has a minimum flow 0% of the design flow, it can be concluded from Figure 9 and Figure 10 that that the room

temperature sensors affect the system's energy consumption more than the cold deck temperature sensor, when they both change to the same degree.

From Figure 9 we can see that when room temperature changes; building energy consumption change has a relationship with the outside air ratio and the room temperature sensor error. The energy consumption change can be expressed as a function of the outside air ratio and sensor error. The equation is shown below:

$$REC = -0.0155E^2 * OA + 0.2805OA^2 * E + 4.5842OA * E + 0.00329E^2 - 0.15715OA^2 + 0.0664OA - 0.013E - 0.00598 \quad \textbf{(56)}$$

From Figure 9, we can tell that when the sensor shifts positively, energy consumption will increase, and when the sensor shifts negatively, the energy consumption will decrease. For an SDVAV system that serves both exterior and interior zones, energy consumption will change more per degree when the sensor shifts positively than when the sensor shifts negatively.

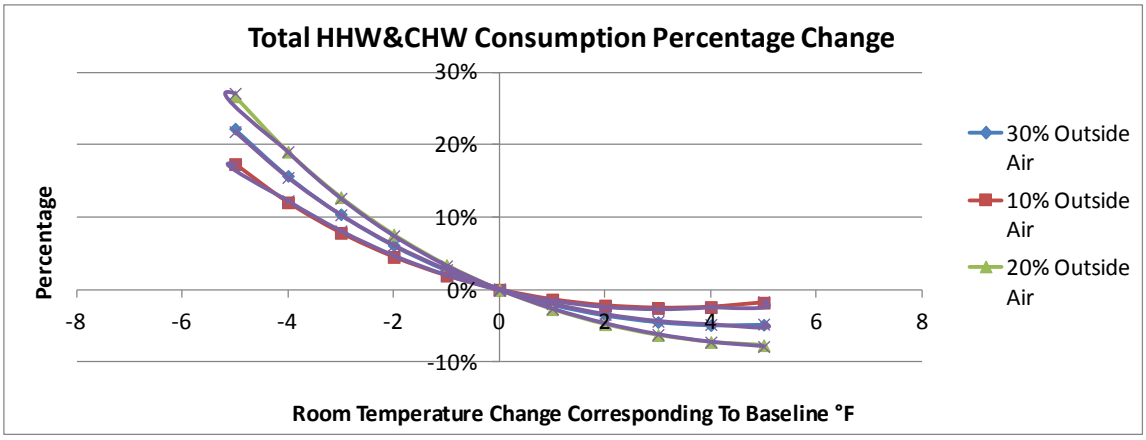

Figure 9. SDVAV Exterior and Interior Zone Room Temperature Error vs Energy Consumption under 0% Minimum Flow

The reason why the chart follows this pattern is that for a single duct VAV system, the higher the room temperature set point the less energy the building consumed. From the chart above, when the sensor shifts positively, the final room temperature will be lower so that is why when the sensor shifts positively, the energy consumption will increase.

Figure 10 shows the energy consumption change with the cold deck temperature will be a function of sensor error only. The energy consumption can be expressed as a function of cold deck sensor error. The equation is shown below:

$$REC = 7.75 * 10^{-5} E^3 + 0.00112 E^2 - 0.01E - 0.00035 \qquad \textbf{(57)}$$

Figure 10 indicates that the energy consumption increases when the actual operation point value increases, this is caused by the temperature rise considered in this simulation model. According to the equation, $V_e=q_{e,s}/(1.08*(T_r-T_{cl})$, the higher the cold deck temperature, the larger the supply flow, the more the energy consumption across the fan, the more the total energy consumption. If the temperature rise across the fan is not big or is not considered then the cold deck sensor has almost no impact on the energy consumption if the minimum flow of the system is 0%.

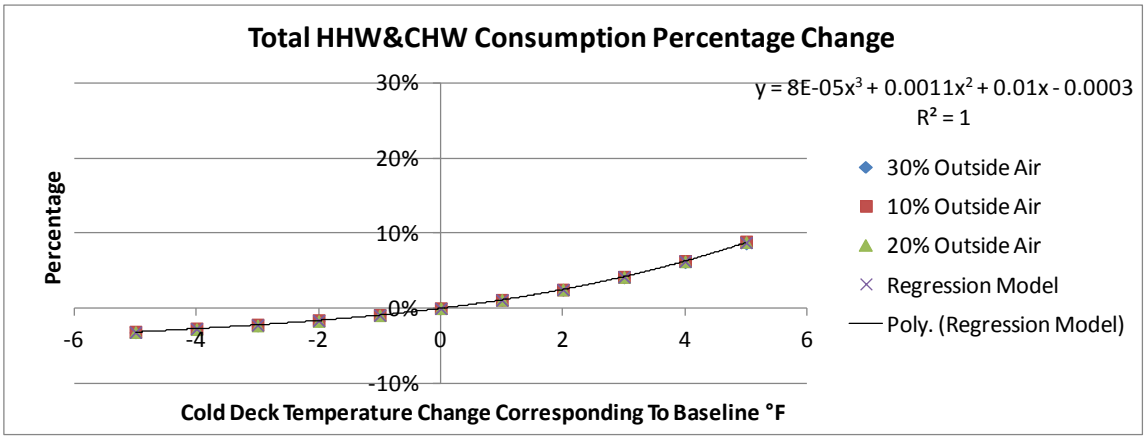

Figure 10. SDVAV Exterior and Interior Zone Cold Deck Temperature Error vs Energy Consumption under 0% Minimum Flow

For a SDVAV system that serves both the exterior zone and interior zone and has a minimum flow 50% of the design flow, Figure 11 and Figure 12 indicate that room temperature sensors affect systems energy consumption more than cold deck temperature sensors when they both change to the same degree.

From Figure 11 we can see that when the room temperature changes, the building energy consumption change has a relationship to the outside air ratio and the room temperature sensor error. The energy consumption can be expressed as a function of the outside air ratio and sensor error. The equation is shown below:

$$REC = -0.0002E^3 + 0.003E^2 * OA - 0.1731OA^2 * E - 0.0018OA * E + 0.0043E^2 - 0.0241OA^2 + 0.0089E - 0.0014 \quad \textbf{(58)}$$

From Figure 11, we can tell that when the sensor shifts positively, energy consumption will increase, but when the sensor shifts negatively, energy consumption will also increase. For an SDVAV system that serves both exterior and interior zones

and also has a minimum flow larger than that required by most operational flow, the energy consumption will change to the same scale when the sensor shifts either positively or negatively. From the charts we can see that in this situation, we should worry both when the sensor shifts negatively and when it shifts positively.

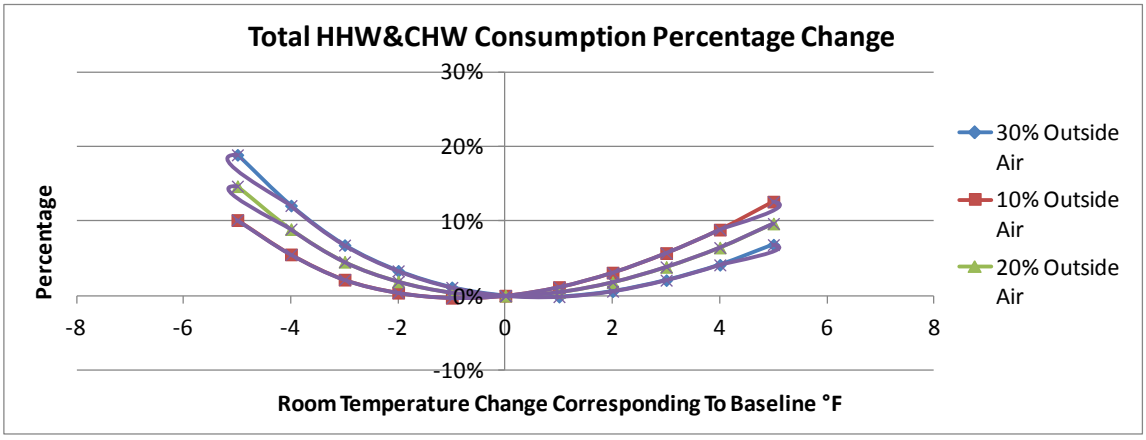

Figure 11. SDVAV Exterior and Interior Zone Room Temperature Error vs Energy Consumption under 50% Minimum Flow

For a SDVAV system that has a 50% minimum air flow, the energy consumption change with the room temperature sensor will be affected by both the actual cooling required and the reheat required. When the sensor shifts positively, the actual cooling required will increase and also the air flow required will increase. But when the sensor shifts negatively, the actual operation of the building becomes more like a constant volume system. Although less cooling is required, the reheat increases with the room temperature increase, causing the cooling required increasing.

Figure 12 shows that any energy consumption change with the cold deck temperature will be a function only of sensor error. The energy consumption can be expressed as a function of the cold deck sensor error. The equation is shown below:

$$REC = 0.000193E^3 + 0.002656E^2 - 0.01325E - 0.00011 \quad \textbf{(59)}$$

From Figure 6 we can see that the energy consumption increases when the sensor shifts positively. The energy consumption change will be greater when the sensor shifts positively, rather than when it shifts negatively.

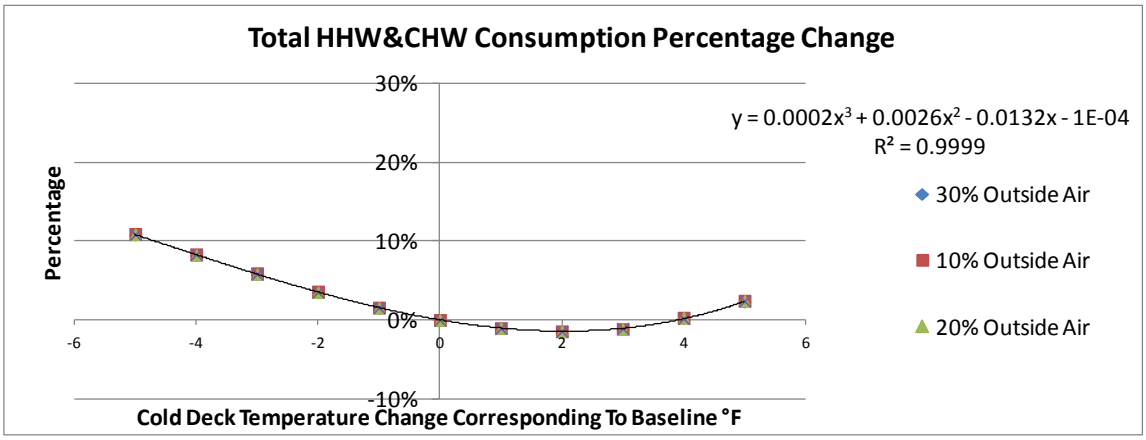

Figure 12. SDVAV Exterior and Interior Zone Cold Temperature Error vs Energy Consumption under 50% Minimum Flow

3.4.3 DDVAV System Interior Zone

For a DDVAV system that serves the interior zone and has a minimum flow of 0% of the design flow, it can be concluded from Figure 13 and Figure 14 that the room temperature sensors affect the system's energy consumption more than the cold deck temperature sensor, when they both change to the same degree, which is the same as an SDVAV system.

Figure 13 indicates a relationship between outside air ratio and the room temperature sensor error. The energy consumption change can be expressed as a function of the outside air ratio and sensor error. The equation is shown below:

$$REC = -0.0069E^2 * OA + 0.2556OA^2 * E + 4.9303OA * E + 0.0013E^2 - 0.1693OA^2 + 0.0697OA - 0.0101E - 0.006 \quad \textbf{(60)}$$

When the sensor shifts positively, the final operation point temperature will be lower than the actual operation point. From Figure 13, we can tell that when the sensor shifts positively, energy consumption will increase, and when the sensor shifts negatively, the energy consumption will decrease. For a DDVAV system that serves an interior zone, energy consumption will change more per degree when the sensor shifts positively than when the sensor shifts negatively.

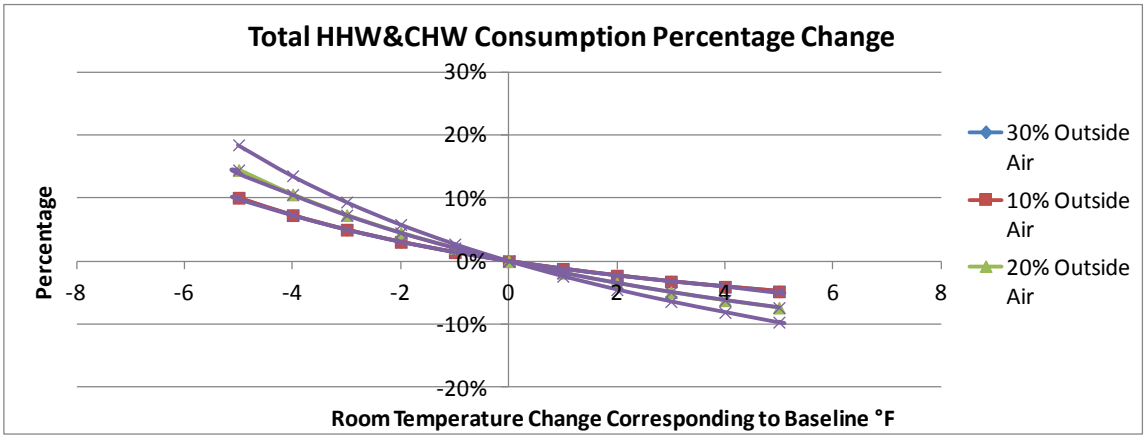

Figure 13. DDVAV Interior Zone Room Temperature Error vs Energy Consumption under 0% Minimum Flow

The reason why the chart follows this pattern is that for a dual duct VAV system, the higher the room temperature set point the less energy the building consumed. From the chart above, when the sensor shifts positively, the final room temperature will be lower so that is why when the sensor shifts positively, the energy consumption will increase.

Figure 14 indicates a polynomial function of the energy consumption change and cold deck temperature sensor error. The energy consumption can be expressed as a function of cold deck sensor error. The equation is shown below:

$$REC = 4.59 * 10^{-5} + 0.000591E^2 + 0.00513E - 0.00023 \qquad \textbf{(61)}$$

From Figure 14, the energy consumption increases when the actual operation point value increases. This is caused by the temperature rise considered in this simulation model. According to the equation, $V_e=q_{e,s}/(1.08*(T_r-T_{cl})$, the higher the cold deck temperature, the larger the supply flow, the more the energy consumption across the fan, the more the total energy consumption.

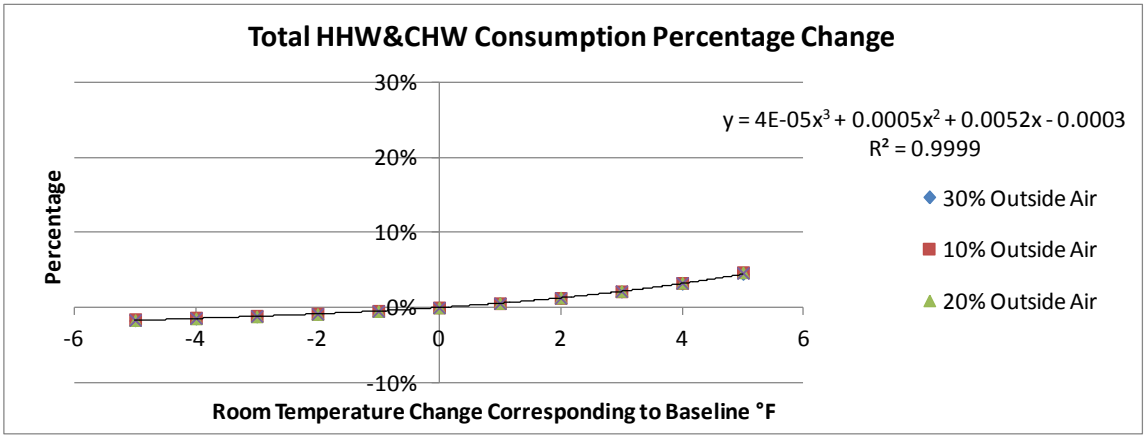

Figure 14. DDVAV Interior Zone Cold Deck Temperature Error vs Energy Consumption under 0% Minimum Flow

For a DDVAV system that serves the interior zone and has a minimum flow of 0% of the design flow, the cold deck temperature sensor affects the systems energy consumption more than the room temperature sensor when they both change by the same amount (Figure 15 and Figure 16).

From Figure 15 we can see that when the room temperature changes, the building energy consumption change has a relationship to the outside air ratio and the room temperature sensor error. The energy consumption can be expressed as a function of the outside air ratio and sensor error. The equation is shown below:

$$REC = 0.0033E^2 * OA + 0.0309OA^2 * E + 3.6184OA * E - 0.0009E^2 - 0.0984OA^2 + 0.0445OA - 0.0022E - 0.0047 \quad \textbf{(62)}$$

For a DDVAV system that serves an interior zone and has a minimum flow of 50%, it is different from the previous situation. From Figure 17, we can tell that when the sensor shifts positively, the energy consumption change is less than when the sensor shifts negatively. But on both sides, the energy consumption will change by almost the same amount.

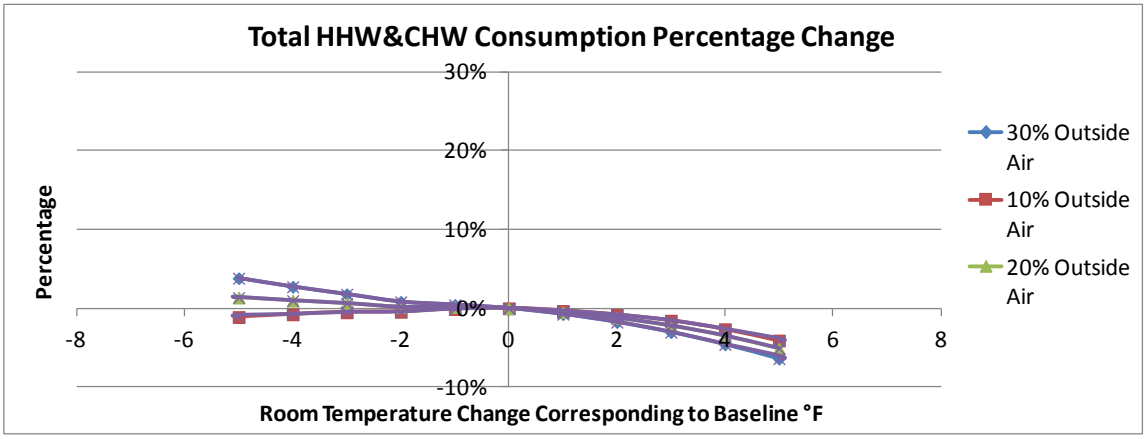

Figure 15. DDVAV Interior Zone Room Temperature Error vs Energy Consumption under 50% Minimum Flow

For a DDVAV system that has a 50% minimum air flow, the energy consumption change with the room temperature sensor will only be affected by the actual cooling required. When the sensor shifts positively, the actual cooling amount required increases. When the sensor shifts negatively, the cooling required will decrease because the room temperature is higher.

From Figure 18 we can see that when the room temperature changes, the building energy consumption change has a relationship to the outside air ratio and the room temperature sensor error. The energy consumption can be expressed as a function of the outside air ratio and sensor error. The equation is shown below:

$$REC = 0.000114E^3 + 0.000266E^2 - 0.02198E - 0.00098 \qquad \textbf{(63)}$$

Figure 16 indicates that the cold deck sensor will affect the energy consumption change in the same scale when it shifts either positively or negatively.

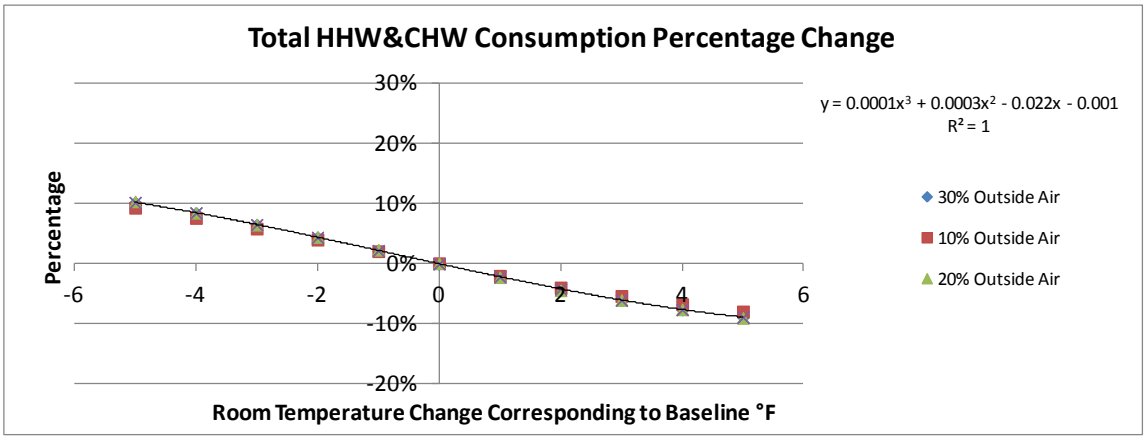

Figure 16. DDVAV Interior Zone Cold Temperature Error vs Energy Consumption under 50% Minimum Flow

3.4.4 DDVAV System Exterior and Interior Zone

For a DDVAV system that serves the interior zone and has a minimum flow 0% of the design flow, it can be concluded from Figure 17 and Figure 18 that the room temperature sensors affect the system's energy consumption more than the cold deck temperature sensor, when they both change to the same degree.

From Figure 17, we can see that when room temperature changes; building energy consumption change has a relationship with the outside air ratio and the room temperature sensor error. The energy consumption change can be expressed as a function of the outside air ratio and sensor error. The equation is shown below:

$$REC = -0.0035E^2 * OA + 0.1837OA^2 * E + 2.5574OA * E + 0.0019E^2 - 0.1915OA^2 + 0.0781OA - 0.0261E - 0.0071 \quad \textbf{(64)}$$

From Figure 17, we can tell that when the sensor shifts positively, energy consumption will increase, and when the sensor shifts negatively, the energy consumption will decrease. For an DDVAV system that serves an interior zone, energy consumption will change more per degree when the sensor shifts positively than when the sensor shifts negatively.

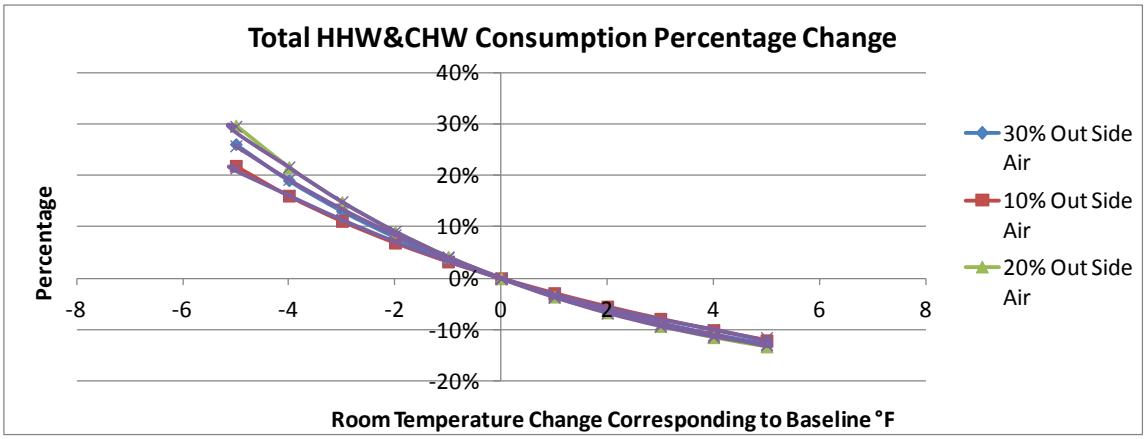

Figure 17. DDVAV Exterior and Interior Zone Room Temperature Error vs Energy Consumption under 0% Minimum Flow

The reason why the chart follows this pattern is that for a dual duct VAV system, the higher the room temperature set point the less energy the building consumes. From the chart above, when the sensor shifts positively, the final room temperature will be lower so that is why when the sensor shifts positively, the energy consumption will increase.

Figure 18 shows that the energy consumption change with the cold deck temperature will be a function of sensor error only. Energy consumption change can be expressed as a function of cold deck sensor error. The equation is shown below:

$$REC = 5.1*10^{-5} + 0.000733E^2 + 0.009447E - 0.00025 \qquad \textbf{(65)}$$

From Figure 18 we can see that the energy consumption increases when the actual operation point values increase; this is caused by the temperature rise considered in the simulation model. According to the equation $V_e=q_{e,s}/(1.08*(T_r-T_{cl})$, the higher the

cold deck temperature, the larger the supply flow, and the more the energy consumption across the fan, the greater the total energy consumption.

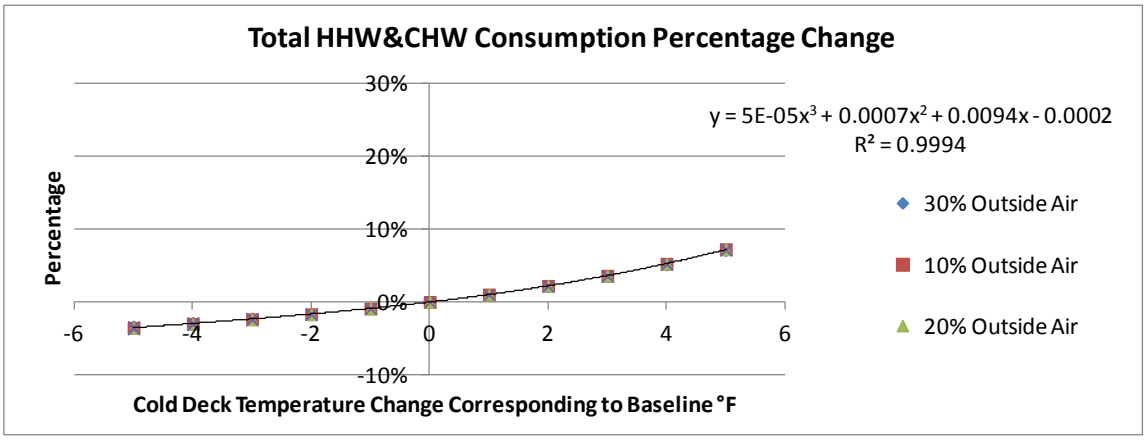

Figure 18. DDVAV Exterior and Interior Zone Cold Temperature Error vs Energy Consumption under 0% Minimum Flow

For a DDVAV system that serves the interior zone and has a minimum flow 50% of the design flow, it can be seen from Figure 19 and Figure 20 that that the room temperature sensor and the cold deck temperature sensor have almost the same impact when they both change to the same degree.

From Figure 19 we can see that when the room temperature changes, the building energy consumption change has a relationship to the outside air ratio and the room temperature sensor error. The energy consumption can be expressed as a function of the outside air ratio and sensor error. The equation is shown below:

$$REC = 0.0054E^2 * OA - 0.0793OA^2 * E - 0.0017OA * E + 0.0003E^2 - 0.0339OA^2 - 0.0234E - 0.0007 \quad \textbf{(66)}$$

From Figure 19, we can tell that when the sensor shifts positively, energy consumption will increase, when the sensor shifts negatively, the energy consumption will decrease. But under this situation, the outside air does not play a role as important as in the situations before. For a DDVAV system that serves an interior zone, the energy consumption will change more when the sensor shifts positively than the sensor shifts negatively.

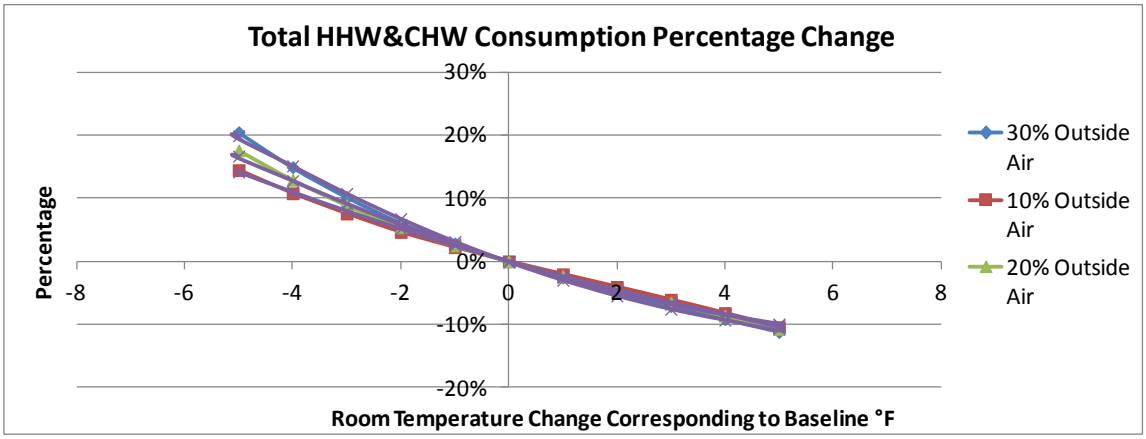

Figure 19. DDVAV Exterior and Interior Zone Room Temperature Error vs Energy Consumption under 50% Minimum Flow

The reason why the chart follows this pattern is that for a dual duct VAV system, the higher the room temperature set point the less energy the building consumes. From the chart above, when the sensor shifts positively, the final room temperature will be lower so that is why when the sensor shifts positively, the energy consumption will increase.

Figure 20 shows that any energy consumption change with the cold deck temperature will be a function only of sensor error. The energy consumption can be expressed as a function of the cold deck sensor error. The equation is shown below:

$$REC = 8.88 * 10^{-5} E^3 + 0.000528E^2 - 0.00728E - 0.00068 \quad \textbf{(67)}$$

From Figure 20 we can see that the energy consumption increases when the sensor shifts positively. The energy consumption change will be greater when the sensor shifts positively, rather than when it shifts negatively.

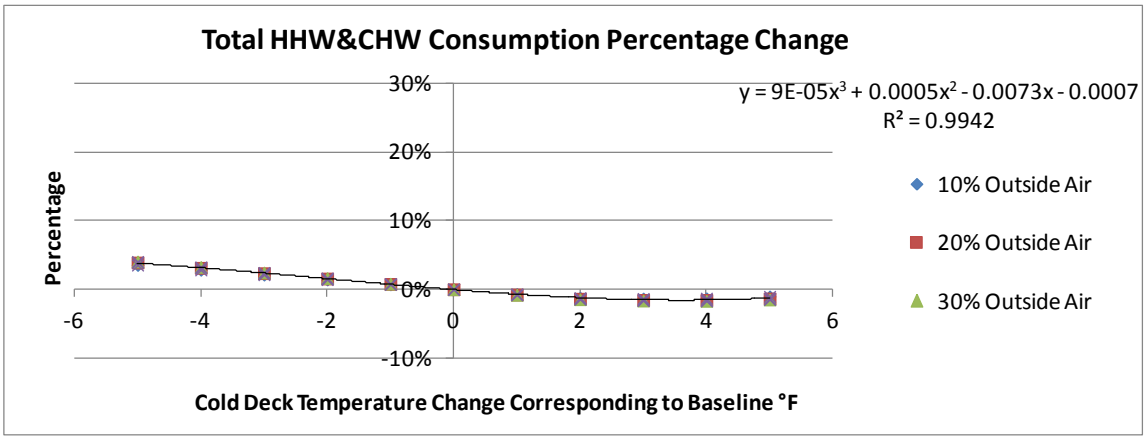

Figure 20. DDVAV Exterior and Interior Zone Cold Deck Temperature Error vs Energy Consumption under 50% Minimum Flow

4. APPLICATIONS

4.1 Eller Oceanography and Meteorology Building

Figure 21. Eller O&M Building

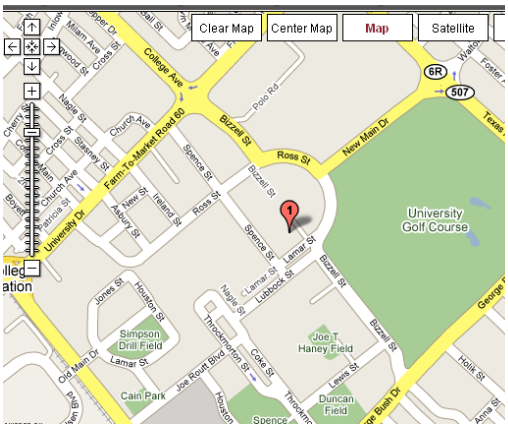

Figure 22. Building location

The Eller Oceanography and Meteorology (O&M) Building, pictured above in Figure 21 and Figure 22, was constructed in 1973 and is located on the main campus of Texas A&M University (see Figure 33 above). It houses the Dean's office of the College of Geosciences, the Department of Meteorology, and the Department of Ocean Engineering, and consists primarily of offices, laboratories, classrooms, and storage space. The building has sixteen floors (including the basement), for a total area of 180,316 square feet. It is generally occupied on weekdays from 8:00 AM to 5:00 PM, but it also has some occupancy later in the evenings and on weekends.

The two series in Figure 23 and Figure 24, one is from the real building simulation, and the other is the result of using the error function developed in equations 66 and 67. The baseline inputs for the simulation are shown in Table 13.

Table 13. Eller Building Simulation Baseline Inputs

Parameter	Number	Unit	Zone
Minimum Flow	0.8	cfm/ft^2	Exterior
Minimum Flow	0.5	cfm/ft^2	Interior
Design Flow	1.5	cfm/ft^2	Exterior
Design Flow	1.3	cfm/ft^2	Interior
OA	0.21	cfm/ft^2	Both
Exterior Zone Percentage	40%	%	
Room Temperature	70	Heating	Both
Room Temperature	72	Cooling	Both

According to this baseline, the outside air ratio is 15% and the minimum flow is 45%. Consequently, the DDVAV that serves both the interior zone and the exterior zone, and also has a minimum flow of 50% and an OA ratio of 15% can be used.

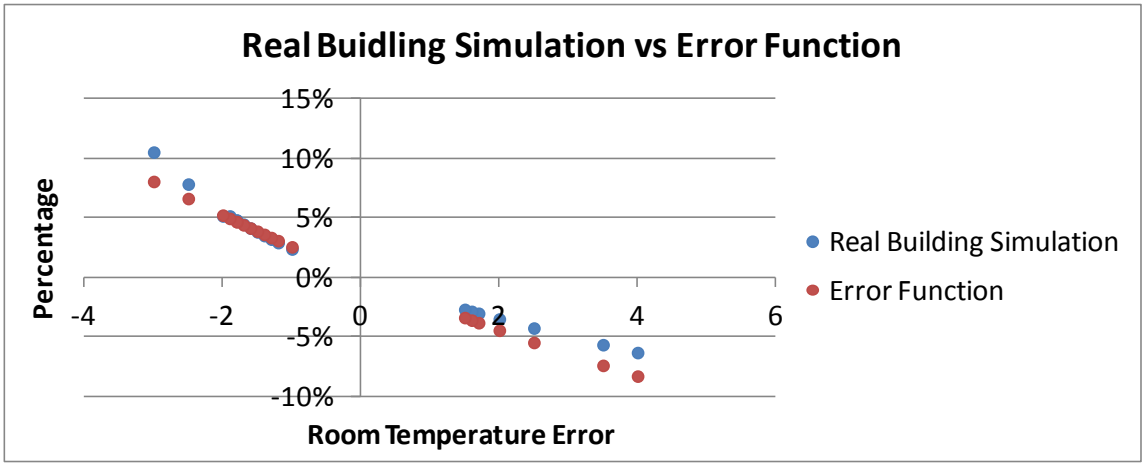

Figure 23. Eller Building Simulation vs Error Function Room Temperature

Figure 23 and Figure 24 indicate the small differences between these two series.

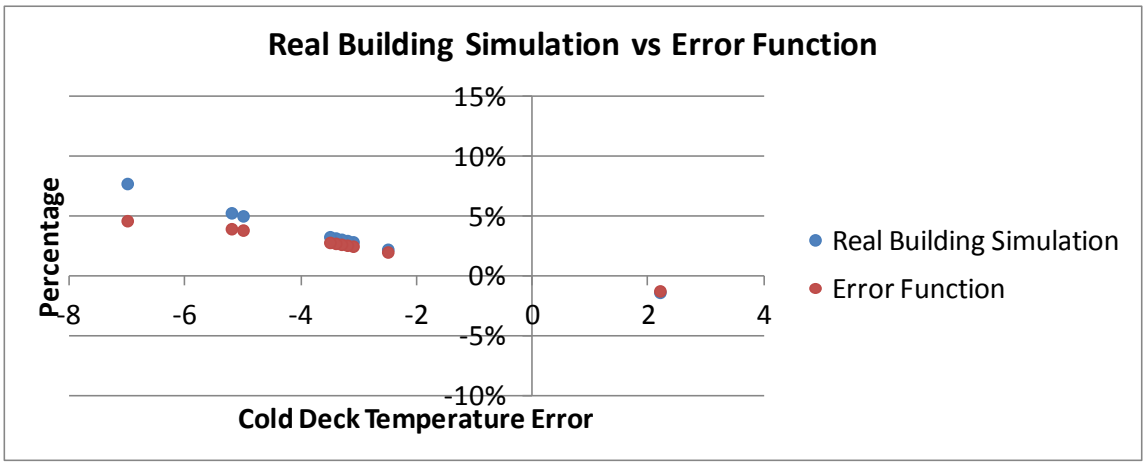

Figure 24. Eller Building Simulation vs Error Function Cold Deck Temperature

4.2 Veterinary Research Building

The Veterinary Research Building on the campus of Texas A&M University in College Station, TX, is a five story building with 115,000 square feet of conditioned space. The building is comprised primarily of laboratories, but also contains classrooms and offices. Thermal energy is supplied to the building by hot water and chilled water pumped from the central utility plant. The majority of the building is served by five SDVAV AHUs, four of which operate with 100% outside air.

Of the two series in Figure 25 and Figure 26, one is from the real building simulation and the other is from an error function developed in equation 58 and 59. The baseline inputs for the simulation are shown in Table 14.

Table 14. VMA Building Simulation Baseline Inputs

Parameter	Number	Unit
Minimum Flow	0.64	cfm/ft^2
Design Flow	1.15	cfm/ft^2
OA	0.7	cfm/ft^2
Exterior Zone Percentage	50	%
Room Temperature	70	Heating
Room Temperature	72	Cooling

According to this baseline, the outside air ratio is 50%, and the minimum flow is 55%. There is no exact error function for this situation. The nearest is the function that has a minimum flow of 50%, in which case an OA ratio of 30% can be used.

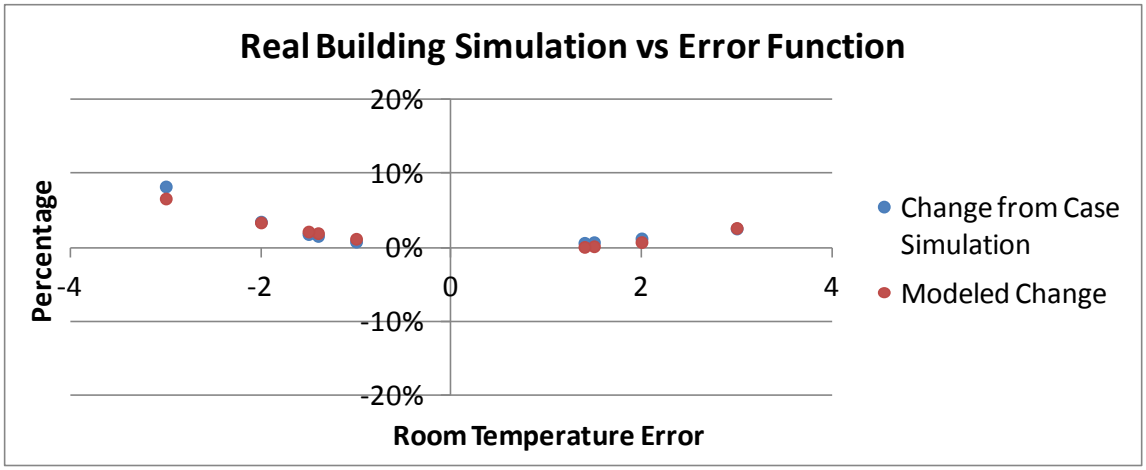

Figure 25. VMA Building Simulation vs Error Function Room Temperature

Figure 26indicates that indicate when the outside air ratio is too far from the provided situation, the error of the function may be very large, but the change trend will remain the same.

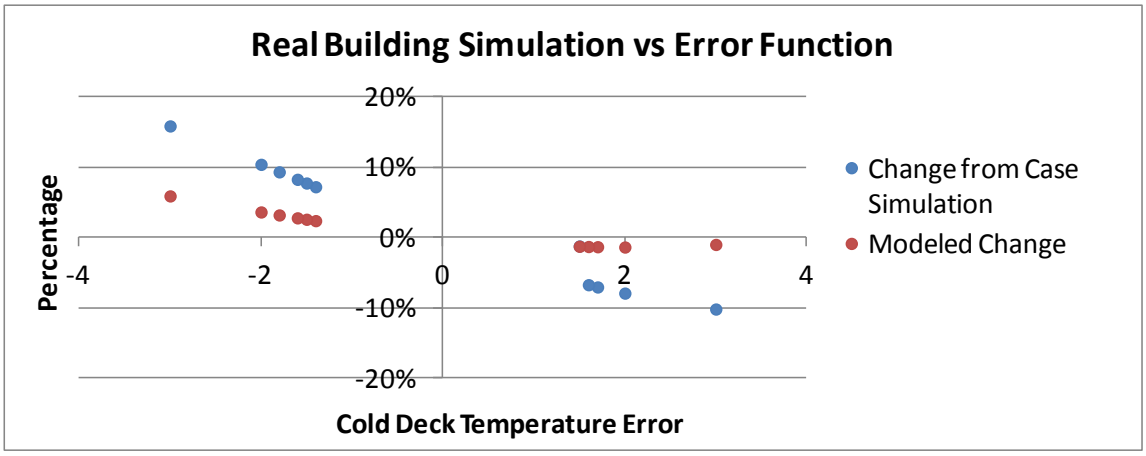

Figure 26. VMA Building Simulation vs Error Function Cold Deck Temperature

5. SUMMARY

From the above discussion, it can be concluded that room temperature sensors and cold deck temperature sensors play paramount roles in the operation of SDVAV systems and DDVAV systems.

In an SDVAV system, when the minimum flow is set to 0% or the minimum air flow set point is lower than the building common operation air flow volume, one should become concerned when the room temperature shifts positively. However, in a situation where the minimum flow is as high as 50% or the set point is larger than the building common operation air flow volume, a positive or negative shift in room temperature will cause almost the same change in energy consumption. Room temperature calibration really depends upon the minimum flow settings.

For an SDVAV system, when the minimum flow is 0% or lower than most operation times, cold deck temperature sensor errors will have no effect if the temperature rise across the fan is not significant. But when the minimum flow is as high as 50% or is larger than most operation times, the cold deck temperature sensors will greatly affect the energy consumption when it shifts positively.

It is recommended that for an SDVAV system that operates like an SDCAV system, both room temperature sensors and cold deck temperature sensors should be recalibrated (give a time – don't just say "short time"). However for the one that really operates as an SDVAV system, cold deck temperature sensor has little impact on energy use and calibration is not very important (as long as it doesn't cause comfort complaints).

For a DDVAV system, the situation is the same when the minimum flow is set to 0% or is lower than the building common operation air flow volume for the room temperature sensor. However, if the minimum flow is set as high as 50% or higher than the building common operation air flow volume, the results will be different according to the zone load applied to the building. If the system serves an interior zone, room temperature sensors will have the same effect whether they shift positively or negatively. If the system serves both exterior zones and interior zones, the energy consumption change will be larger when it shifts positively.

For a DDVAV system, when the minimum flow is 0% or lower than most operation times, the cold deck temperature sensor's impact will be the same as that of the SDVAV system.

It is recommended that a DDVAV system that operates like a DDCAV system should have a shorter recalibration time for both room temperature sensors and cold deck temperature sensors since Figure 15, Figure 16, Figure 19 and Figure 20have shown large change when the room temperature sensors and cold deck temperature sensors drift. However, for the system that truly operates as a DDVAV system, which is shown in Figure 14 and Figure 18, the cold deck temperature sensor is not very important (as long as it won't cause comfort complaints).

Room temperature sensors and cold deck temperature sensors have the greatest impact on building energy consumption. Their failure or error will affect thermal energy consumption and also pump and fan energy consumption (as shown in Appendix A).

Pressure sensor error will affect both the pump and the fan, but the results are not as significant as those produced by temperature sensors.

The tool and functions developed in this thesis can help predict sensor error impact on building energy consumption. It is an easy and convenient tool for analyzing sensor error sensitivity and for determining a building's current operation condition. This tool will also help predict the possible savings once sensors are properly calibrated.

REFERENCES

Bruce, M., and Yumi, S., 2010 "Humidity Sensor Technology." Retrieved 05/31, 2011, from http://www.vaisala.com/webinarrecordings/Humidity101_webinar2_SensorTechnology_2010.pdf.

Castrup, H. T., and Eicke, W.G., 1994. Metrology-Calibration and Measurement Processes Guidelines, NASA.

Claridge, D. E., Abushakra,B., and Haberl,J.S. 2004. Electricity Diversity Profiles for Energy Simulation of Office Buildings. *ASHRAE Transactions-Research* **110**(1): 365-377.

Clay, H., and Jeffrey, P., 2011. "Issues to Consider when Complying with ICH Guidelines Involving Temperature and Relative Humidity Conditions." Retrieved 05/31, 2011, from http://www.humiditycontrol.com/pgc-ich.

Conservatory, E., 2011 "APT System Specifications." Retrieved 05/31, 2011, from http://www.energyconservatory.com/products/products3.htm.

Di Giacomo, S. M., 1999. Differential CO2 Based Demand Control Ventilation (Maximum Energy Savings & Optimized IAQ) - History, Theory and Myths. *Energy Engineering* **96**(5): 58-+.

Fisk, W. J., Faulkner, D. and Sullivan, D.P., 2006. Accuracy of CO2 sensors in commercial buildings: a pilot study. Berkeley, CA.

Fisk, W. J., Faulkner, D. and Sullivan, D.P., 2008 A Pilot study of the accuracy of CO2 sensors in commercial buildings. *In IAQ 2007 Healthy and Sustainable Buildings*, *Baltimore, MD*, American Society of Heating, Refrigeratin and Air Conditioining Engineers, Inc., Atlanta, GA.

Fluke., 2011. "Gas Sensor Calibration Kit Instruction Sheet." Retrieved 05/31, 2011, from http://www.testequipmentdepot.com/fluke/pdf/975ck_instructions.pdf.

GE-A. 2011. "T5000 Airestat CO2 & Temperature Transmitter." Retrieved 05/31, 2011, from http://www.ge-mcs.com/en/co2/wall-mount/t5000-.html.

GE-B 2011. "Telaire® 7000 Series." Retrieved 05/31, 2011, from http://www.transcat.com/PDF/7000Series.pdf.

GE-C 2011. "7250 Sys Ruska Multi-Range Pressure Calibration System." Retrieved 05/31, 2011, from http://controlhouse.com/c/sites/default/files/7250_Sys.pdf.

GE-D 2011. "7250LP Ruska Low Pressure Digital Pressure Calibrator." Retrieved 05/31, 2011, from http://www.ex-calibra.pl/nowa/images/strony/File/PDF/KALIBRATORY%20STACJONARNE/RUSKA7250LP-precyzyjny-kontroler-niskiego-cisnienia.pdf.

Greystone., 2011 "Carbon Dioxide (CO2) Detectors." Retrieved 05/31, 2011, from https://www.hvacquick.com/catalog_files/Greystone_CDD_Catalog.pdf.

Honeywell., 2011 "The CO2 Sensor Family Expands." Retrieved 05/31, 2011, from http://www.wmitechnologies.com/pdfs/CO2%20Sensor.pdf.

Innovair., 2011 "CD100VC CO2 Ventilation Controller." Retrieved 05/31, 2011, from http://www.systemsensor.com/pdf/A05-1040.pdf.

Johari, H., 2003. Development of MEMS sensors for measurements of pressure, relative humidity, and temperature, Worcester Polytechnic Institute. **M.S. Thesis**.

Kimball, C. R., 2003. Integrated temperature measurement and control in polymer microfluidic systems University of Maryland, College Park. **Ph.D. Dissertation**.

Knebel, D. E., 1983. Simplified Energy Analysis Using The Modified Bin Method. Atlanta, GA, American Society of Heating, Refrigerating and Air-Conditioning Engineers, Inc.,.

Krarti, M., 2000. Energy Audit of Building Systems: An Engineering Approach. Boca Raton, FL, CRC Press.

Lacote, J., 2003 Capacitive Humidity Sensor Using a Polyimide Sensing Film. *DTIP*, *Cannes*.

Laville, C., and Pellet, C. 2002. Comparison of three humidity sensors for a pulmonary function diagnosis microsystem. *IEEE Sensors J.* **2**: 96-101.

Measurement 2003. "Temperature Sensors: Performance Characteristics." Retrieved 05/31, 2011, from http://www.meas-spec.com/downloads/Temperature_Sensor_Performance_Characteristics.pdf.

Miller, L. J. 2001. Principles of infrared technology: A Practical Guide to the State of the Art. *Springer*.

Nadvi, G., 2010. MEMS piezoresistive pressure sensor on flexible substrate using nichrome as piezoresistor and micro rressure sensorusing CNT/Polyimide nanocompositesas piesoresistive material, University of Texas at Arlington. M.S. Thesis.

NBCIP, 2004. Prodct Esting Report: Duct-Mounted Relative Humidity Transmitters, Iowa Energy Center.

NBCIP, 2005. Product Testing Report Supplement: Duct-Mounted Relative Humidity Transmitters, Iowa Energy Center.

OHMICO., 2011 "Instruction Manual for Relative Humidity & Temperature Meter DM-509." Retrieved 05/31, 2011, from http://www.ohmicinstruments.com/pdf/Manuals/DM-509man.pdf.

RIAC., 1997. Failure Mode/Mechanism Distribution, Reliability Information Analysis Center.

Roveti, D. 2001. "Choosing a Humidity Sensor: A review of Three Technologies.". Retrieved 05/31, 2011, from http://www.sensorsmag.com/sensors/humidity-moisture/choosing-a-humidity-sensor-a-review-three-technologies-840.

Sashida, T. S., T.; Egawa, M., 2002 Development of a carbon dioxide concentration meter using a solid electrolyte sensor. *SICE*, *Osaka*.

Shrestha, S. S. a. G. M. M., 2010. An experimental evaluation of HVAC-Grade carbon dioxide sensors-Part 4: Effects of Ageing on Sensor Performance. *Ashrae Transactions 2010* **116**(2): 412-423.

Siemens., 2011 "Functional Safety for SITRANS TR200/TR300." Retrieved 06/01, 2011, from https://www.automation.siemens.com/mdm/default.aspx?Language=en&GuiLanguage=en&DocVersionID=24259212811&TopicID=14010214795&Highlight=calibration interval&Query=calibration interval&cssearchengine=NEW.

Stegmeier, S., Fleischer, M., Tawil, A., and Hauptmann, P. 2009. Optimization of the work function response of CO2-sensing Polysiloxane layers by modification of the polymerization. *Sensor* **1-3**: 1664-1668.

Steven, T. T., Hwakong, C., 2010. Economizer high limit controls and why enthalpy economizers don't work. *ASHRAE Journal* **52**(11): 18.

Trane-A 2011., "CO2 Demand-Controlled Ventilation Duct-Sensor." Retrieved 05/31, 2011, from http://www.hvac.amickracing.com/RTU%20Training/Trane%20RTU%20info/CO2%20Sensors/CO2%20Duct%20sensor.pdf.

Trane-B 2011., "CO2 Duct Sensor and CO2 Wall Sensor." Retrieved 05/31, 2011, from http://www.trane.com/Commercial/Uploads/Pdf/1101/vav-slb008-en.pdf.

TSI., 2011. Retrieved 05/31, 2011, from http://www.tsi.com/FAQ.aspx?id=4458.

VAISALA-A., 2011. "Vaisala CARBOCAP® Sensor Technology for Stable Carbon Dioxide Measurement." Retrieved 05/31, 2011, from http://www.vaisala.com/Vaisala%20Documents/Technology%20Descriptions/CARBOCAP_TechnologyDescription.pdf.

VAISALA-B., 2011. "Vaisala HUMICAP® for Measuring Relative Humidity." Retrieved 05/31, 2011, from http://www.vaisala.com/Vaisala%20Documents/Technology%20Descriptions/HUMICAP%20Technology%20description%20EN%20lores.pdf.

VERITEQ., 2011 "Validatable Relative Humidity & Temperature Data Loggers - Specifications." Retrieved 05/31, 2011, from http://www.veriteq.com/validation-data-loggers/validation-humidity-specs.htm.

Wei, G., Liu, M., and Claridge, D. E., 1998 Signatures of Heating and Cooling Energy Consumption for Typical AHUs. *Proceedings of the Eleventh Symposium on Improving Building Systems in Hot and Humid Climates*, *Fort Worth, TX*.

Williams, S., 2002. Improvement in the measurement and control of glass melt temperature of high strength, continuous glass, University of South Carolina. M.S. Thesis.

Wilson, J., 2005. Sensor Technology Handbook, Newnes.

Wong, J. Y., 1995. NDIR gas sensor. US Patent No. 5,444,249.

APPENDIX A

On the figures in this Appendix, the horizontal axis represents the actual operation point change relative to the set point due to sensor error. When the sensors shift positively, the actual system operation point is lower than the baseline. As a result, the value on the axis is negative. The vertical axis is the relative energy consumption change as compared to the baseline. The figure title lists the energy quantity that is plotted. The series' names represent these sensors causing the change in energy use.

SDVAV Interior Zone Load with 0% Minimum Air Flow and 10% outside air

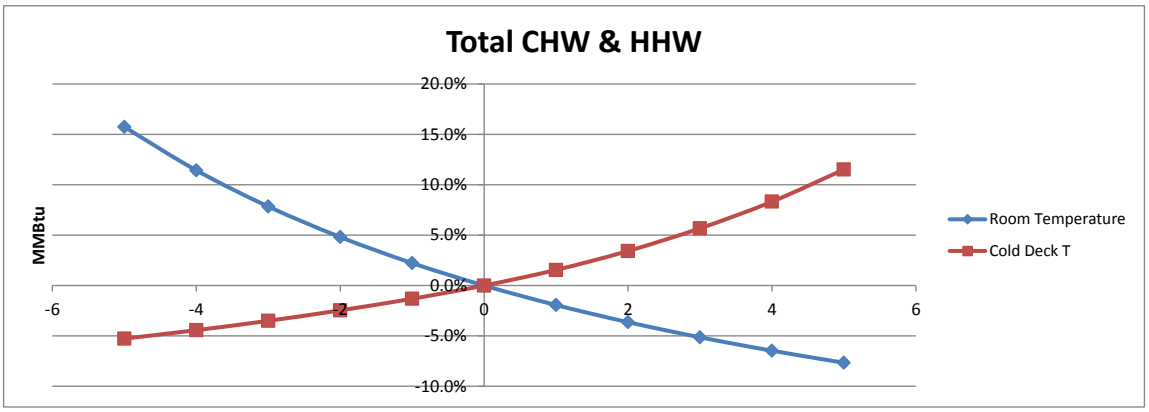

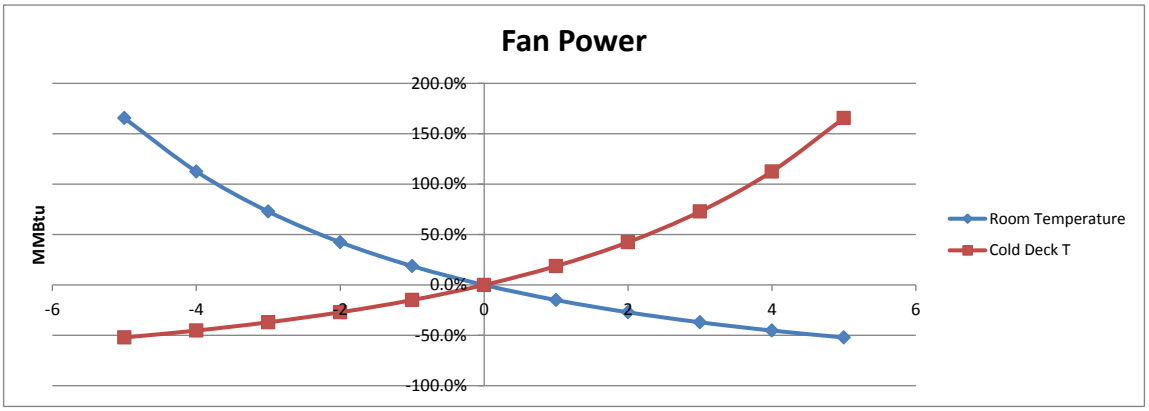

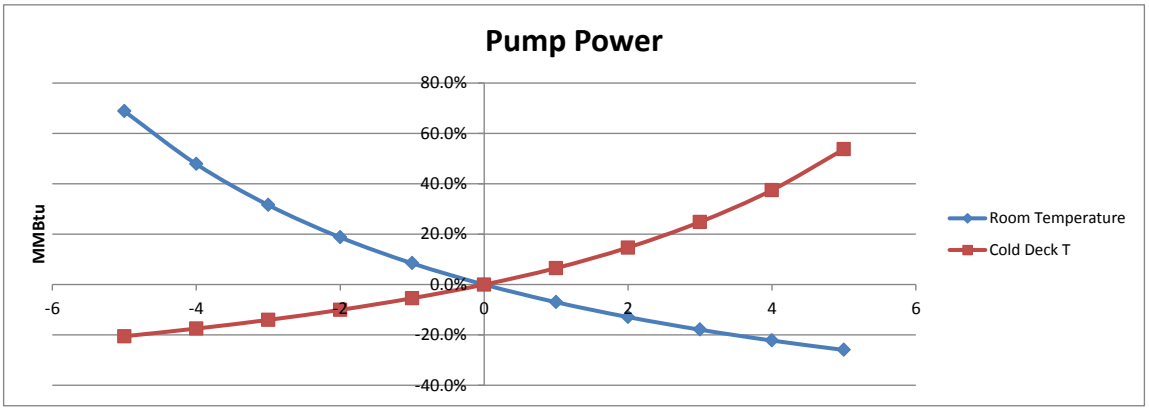
Pump Power
MMBtu
80.0%
60.0%
40.0%
20.0%
0.0%
-20.0%
-40.0%
-6
-4
-2
0
2
4
6
Room Temperature
Cold Deck T

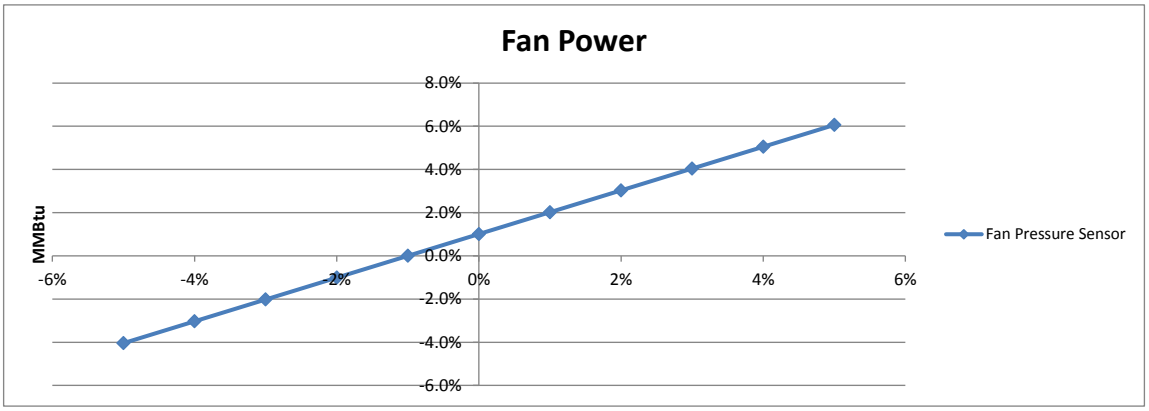
Fan Power
MMBtu
8.0%
6.0%
4.0%
2.0%
0.0%
-2.0%
-4.0%
-6.0%
-6%
-4%
-2%
0%
2%
4%
6%
Fan Pressure Sensor

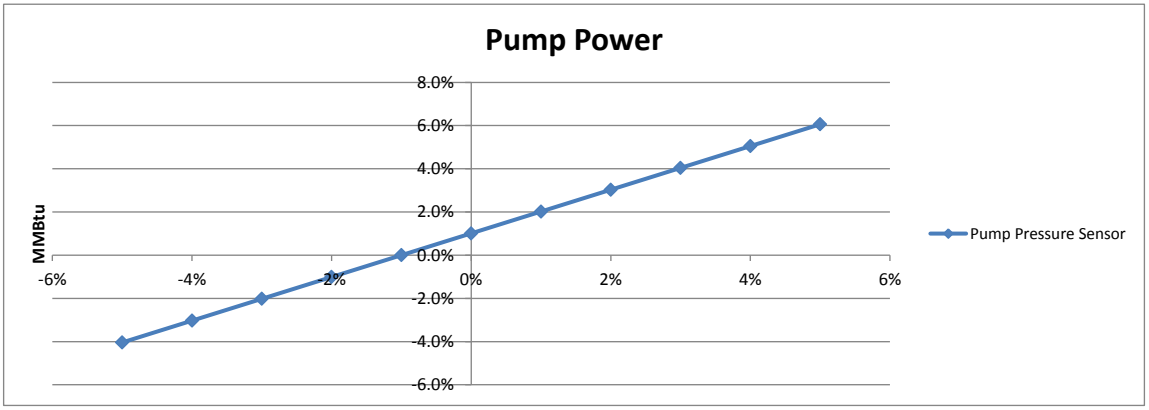
Pump Power
MMBtu
8.0%
6.0%
4.0%
2.0%
0.0%
-2.0%
-4.0%
-6.0%
-6%
-4%
-2%
0%
2%
4%
6%
Pump Pressure Sensor

SDVAV Interior Zone Load with 0% Minimum Air Flow and 20% outside air

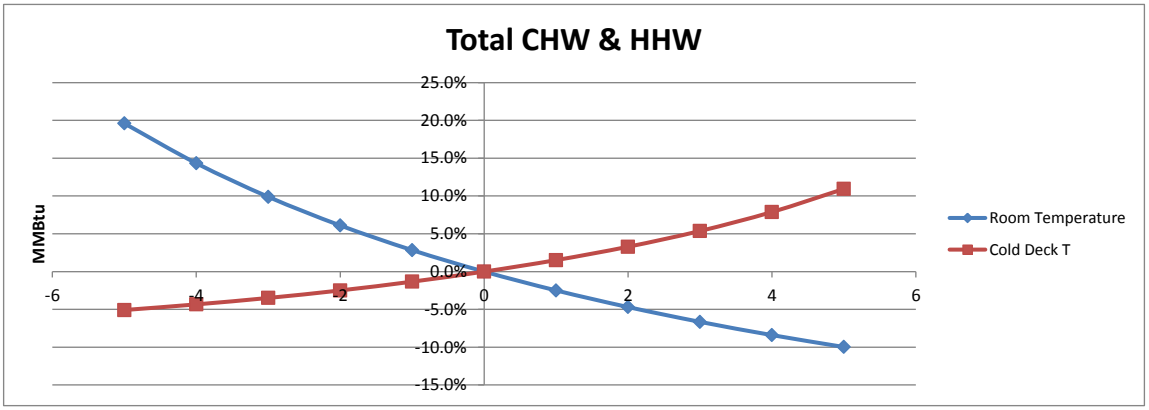

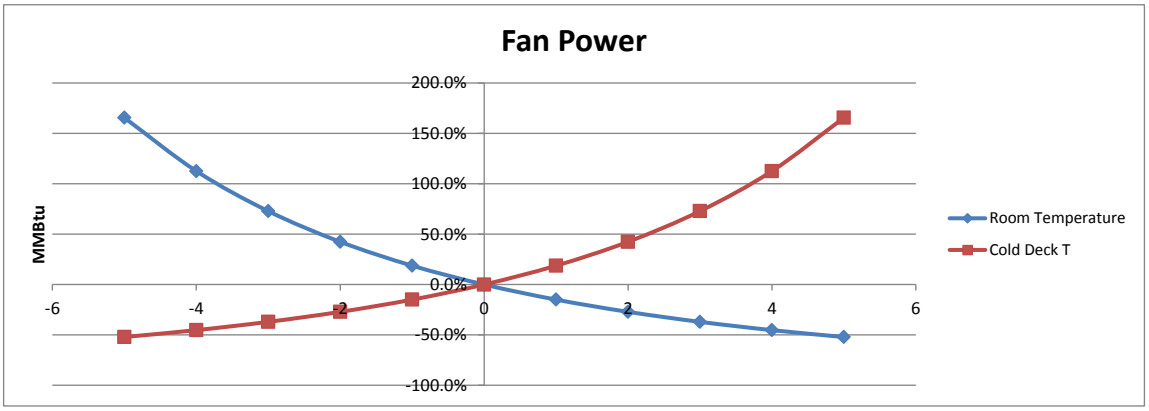

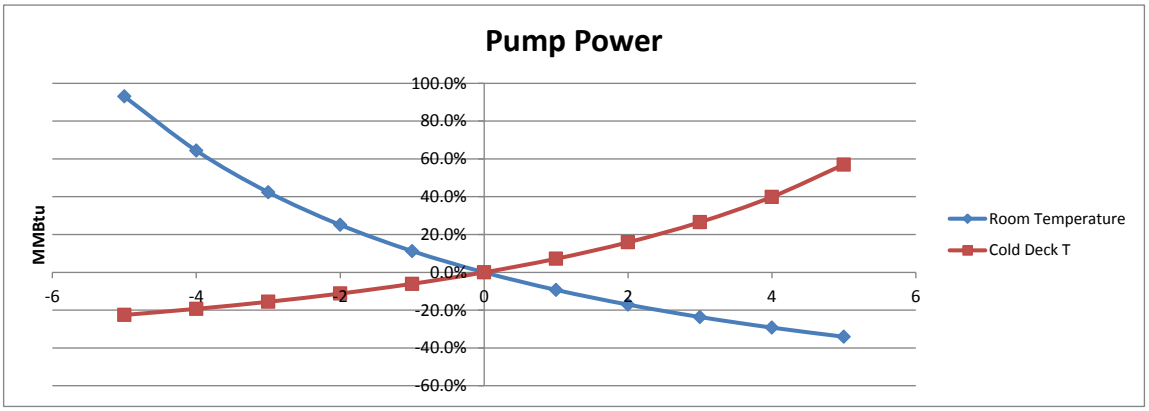

SDVAV Interior Zone Load with 0% Minimum Air Flow and 30% outside air

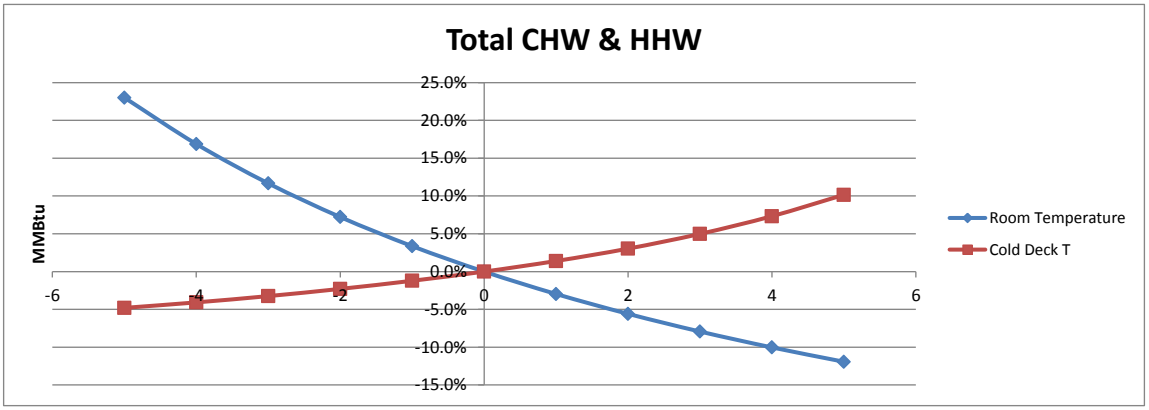

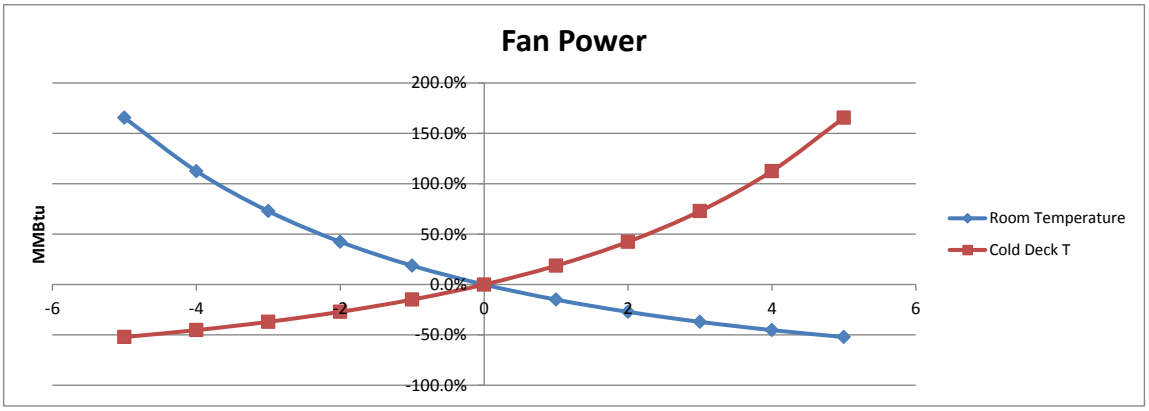

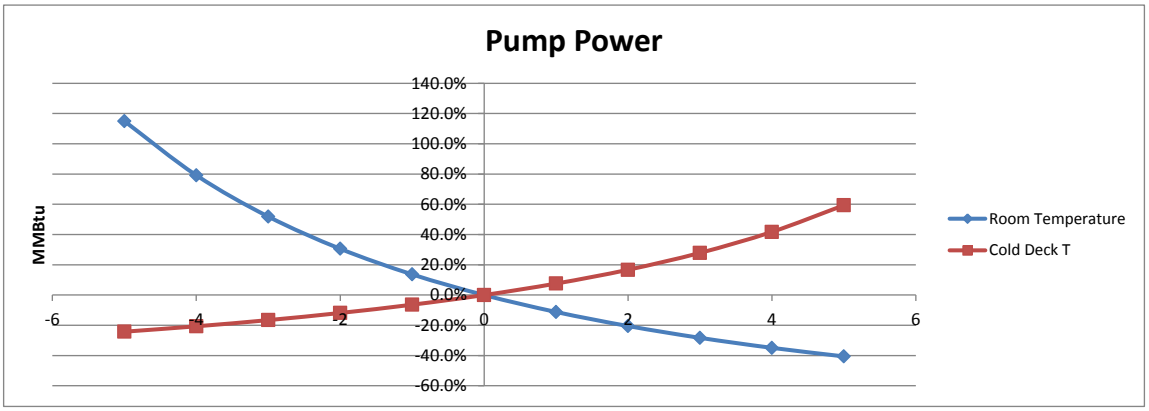

SDVAV Interior Zone Load with 50% Minimum Air Flow and 10% outside air

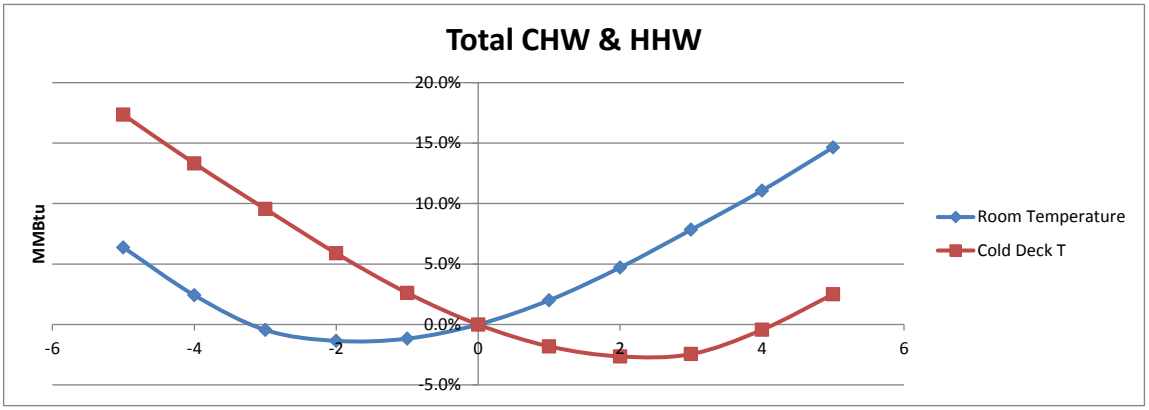

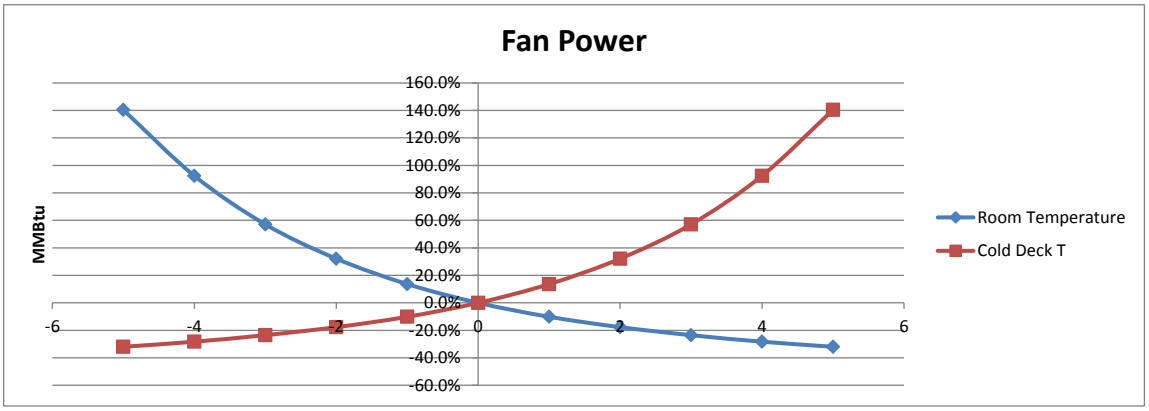

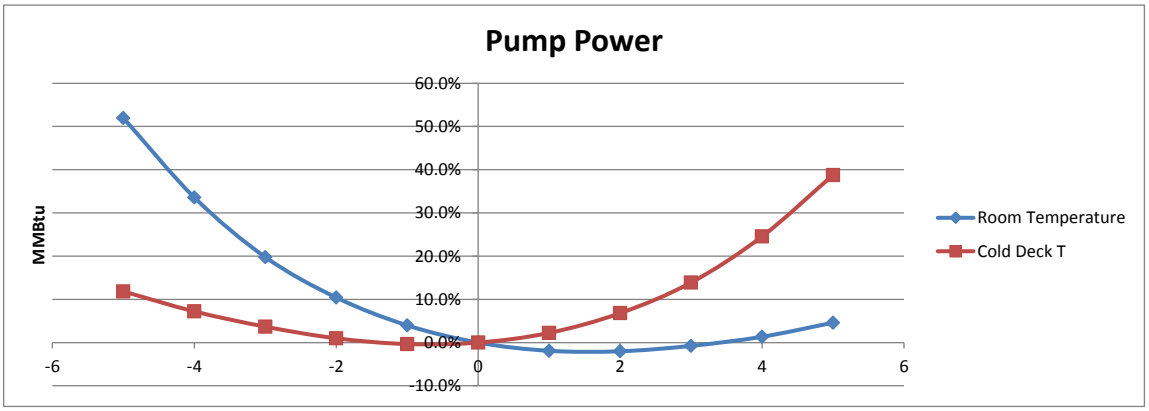

SDVAV Interior Zone Load with 50% Minimum Air Flow and 20% outside air

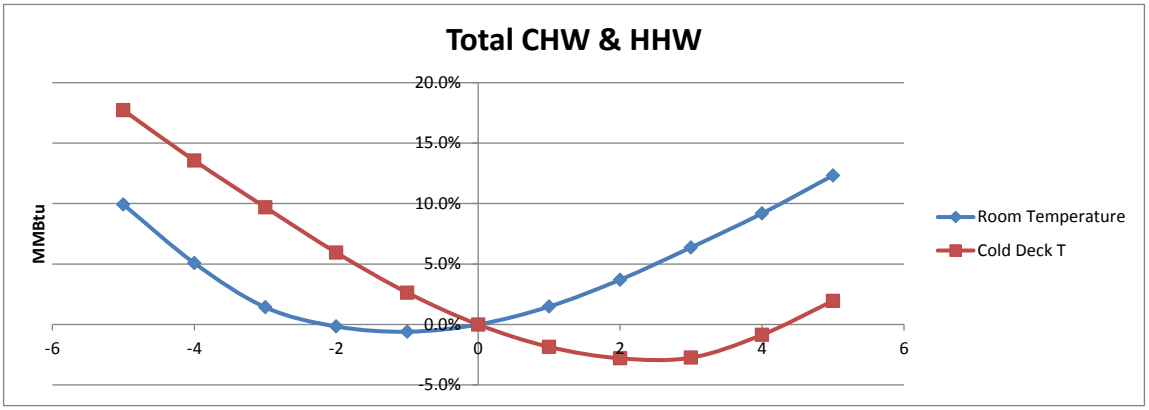

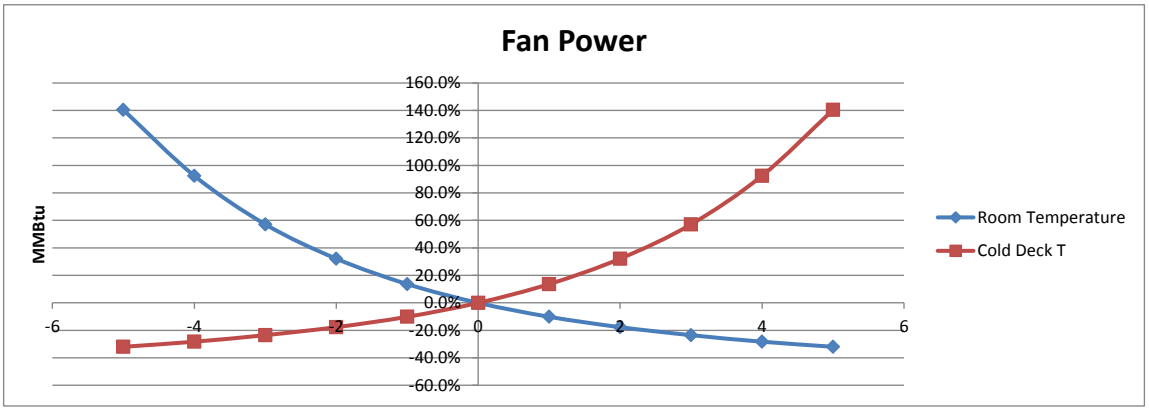

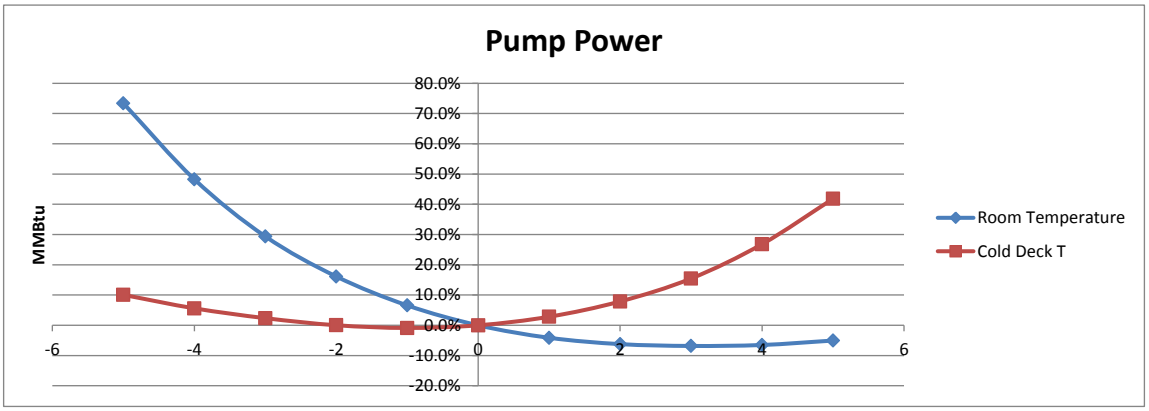

SDVAV Interior Zone Load with 50% Minimum Air Flow and 30% outside air

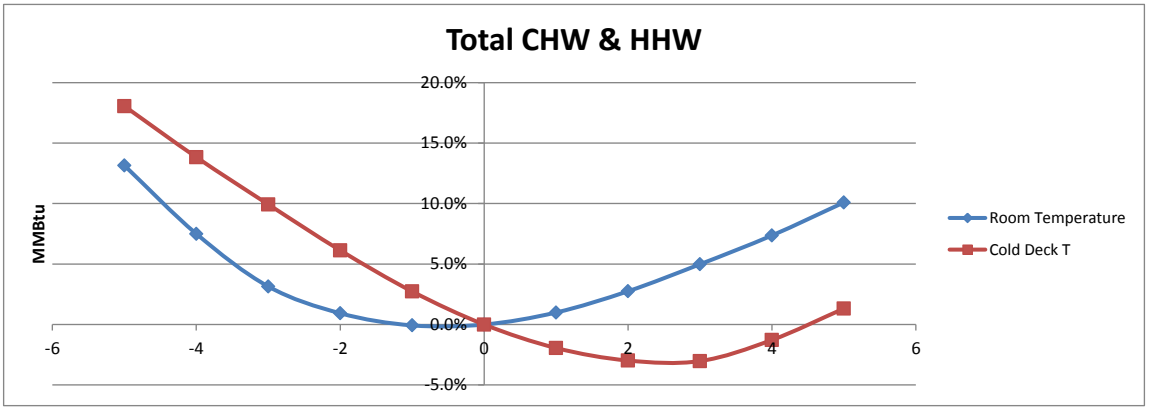

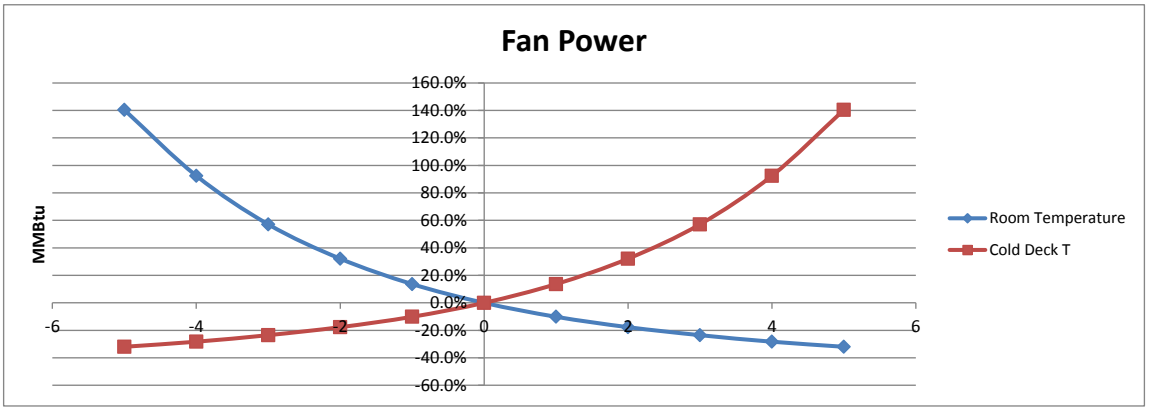

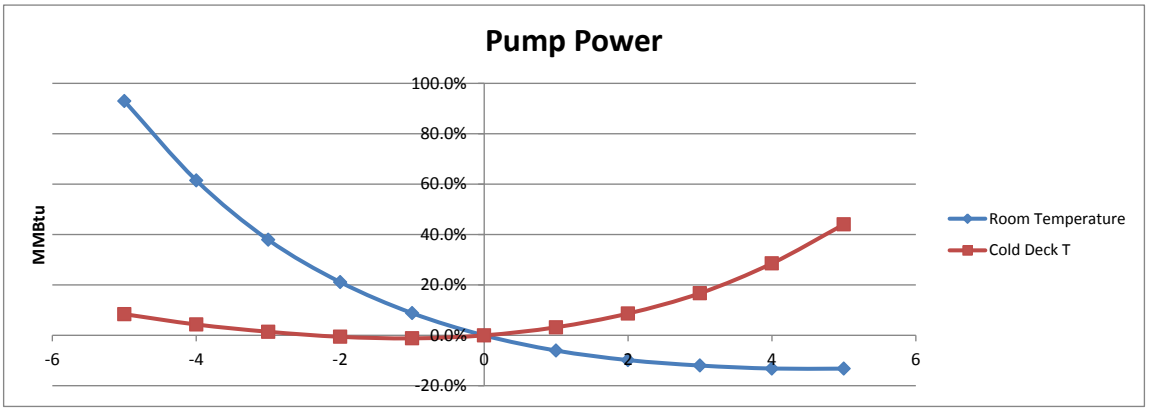

SDVAV Exterior and Interior Zone Load with 0% Minimum Air Flow and 10% outside air

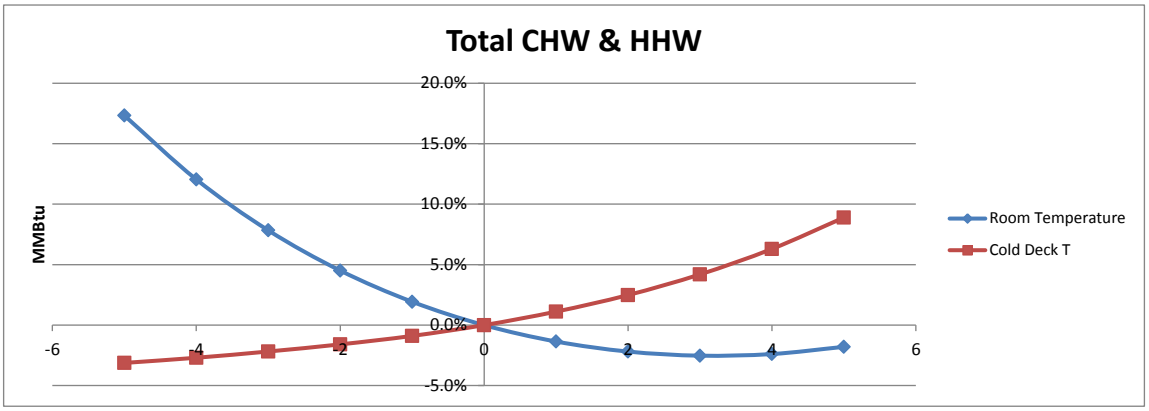

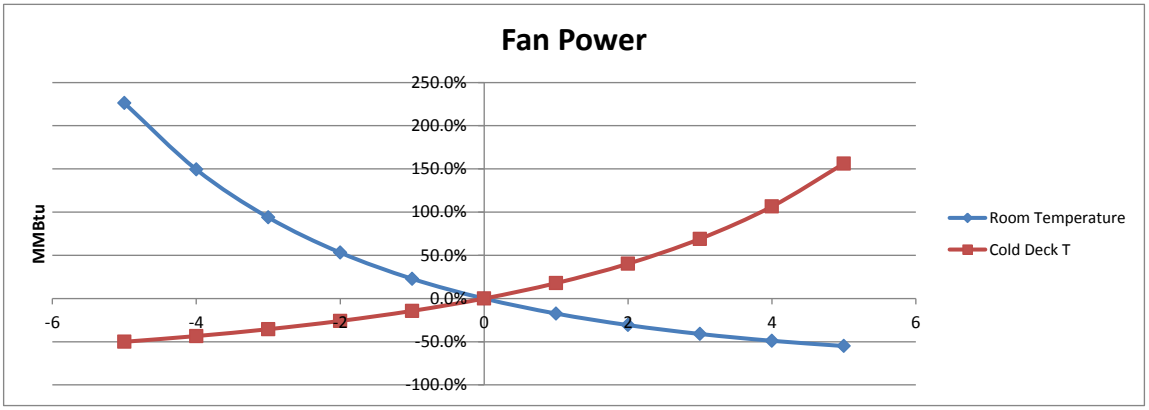

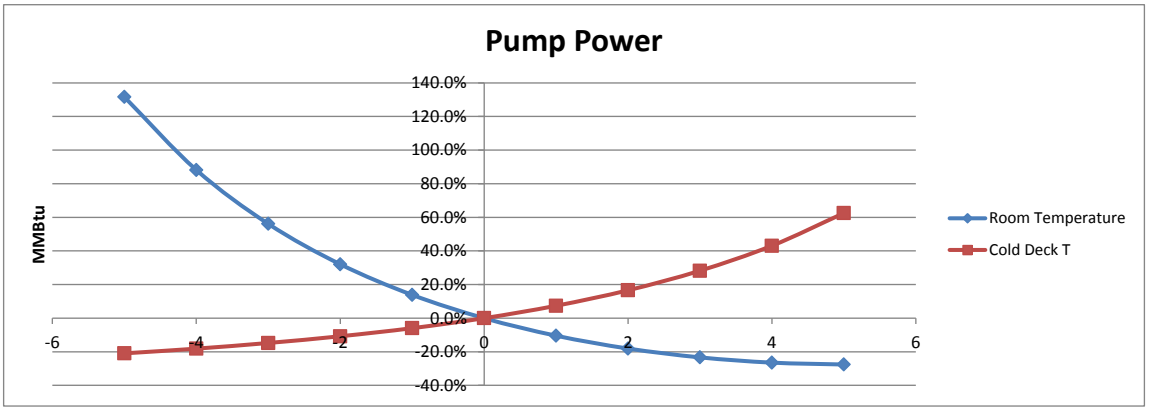

SDVAV Exterior and Interior Zone Load with 0% Minimum Air Flow and 20% outside air

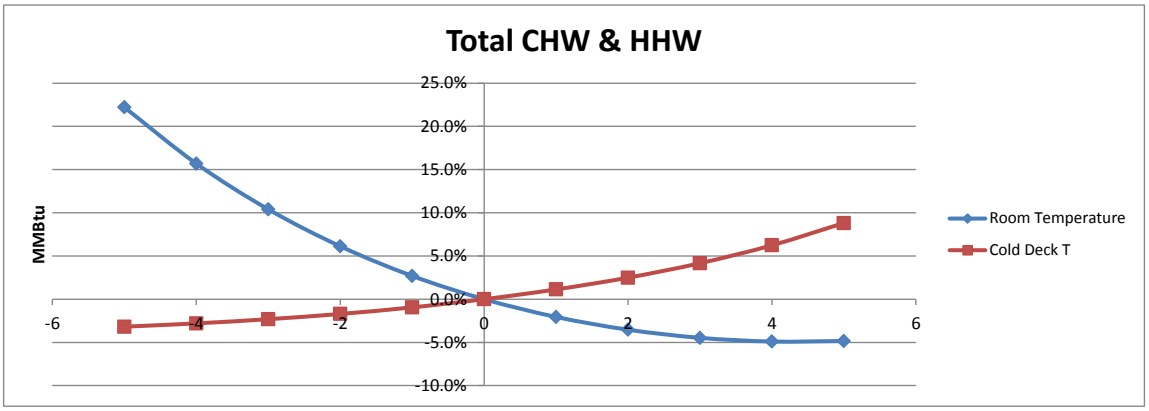

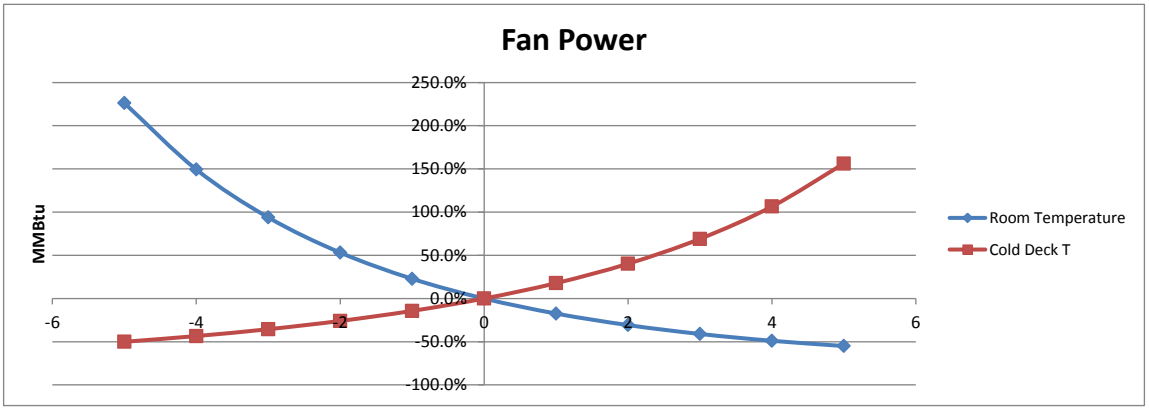

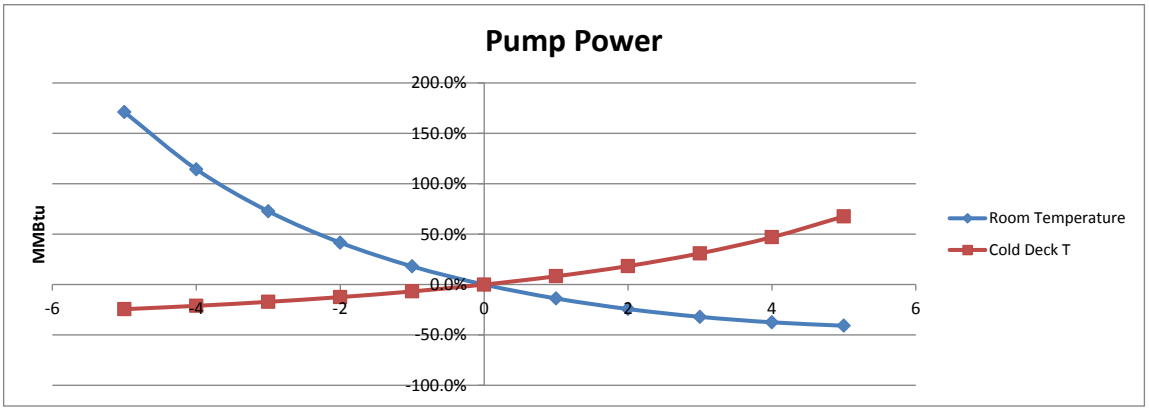

SDVAV Exterior and Interior Zone Load with 0% Minimum Air Flow and 30% outside air

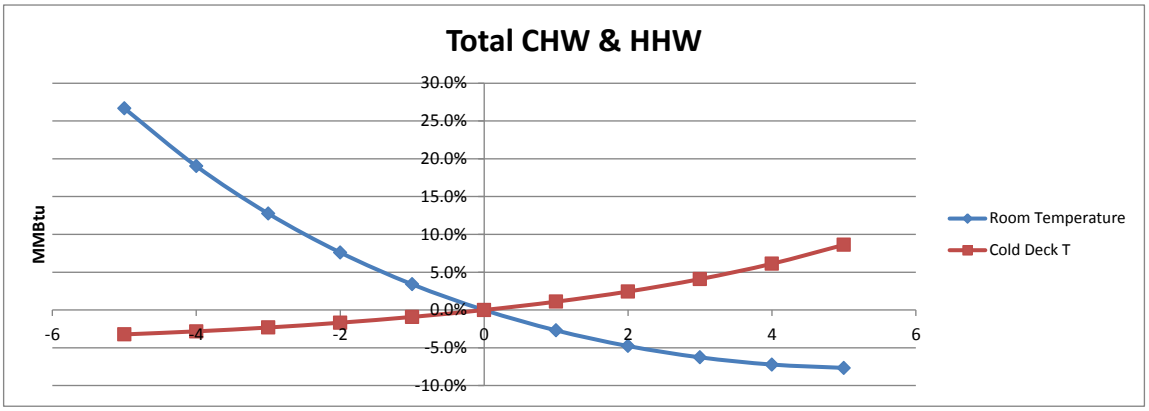

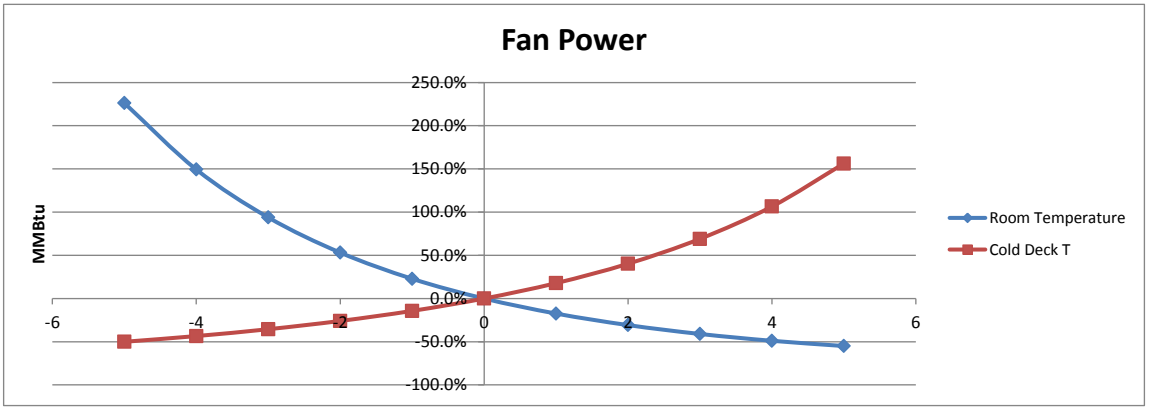

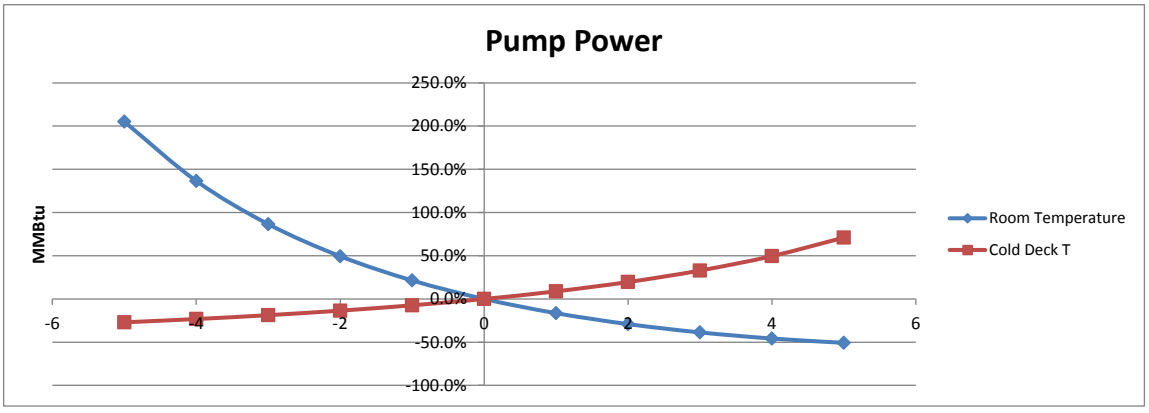

SDVAV Exterior and Interior Zone Load with 50% Minimum Air Flow and 10% outside air

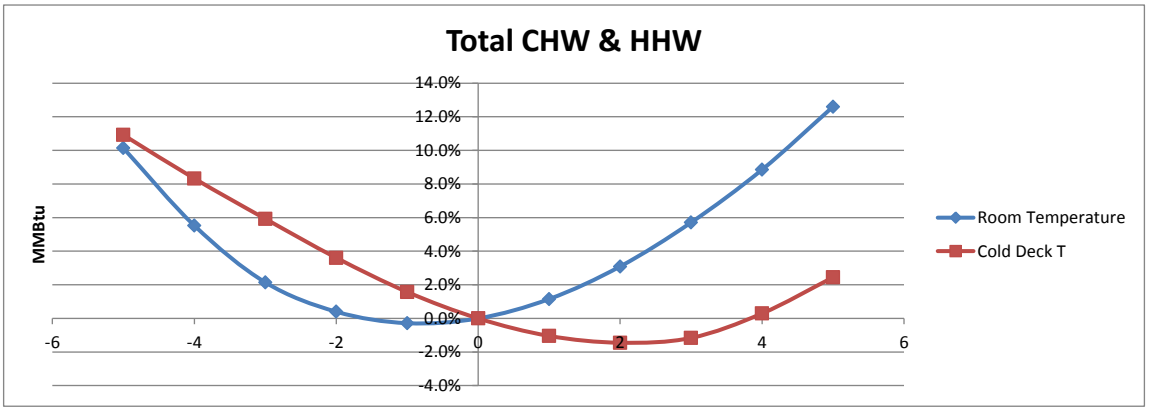

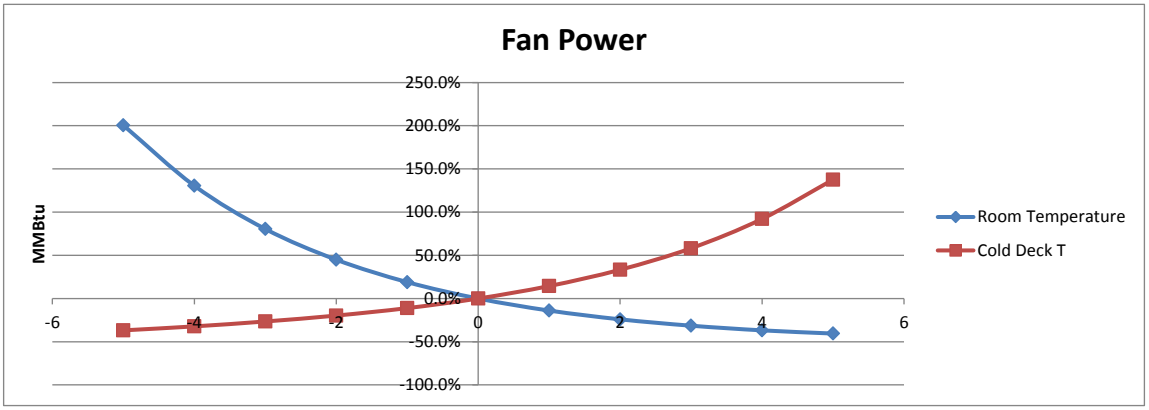

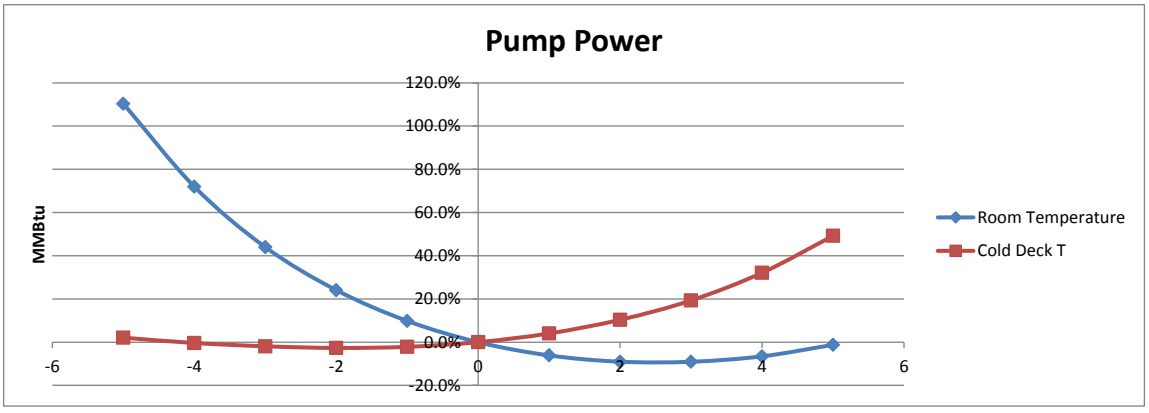

SDVAV Exterior and Interior Zone Load with 50% Minimum Air Flow and 20% outside air

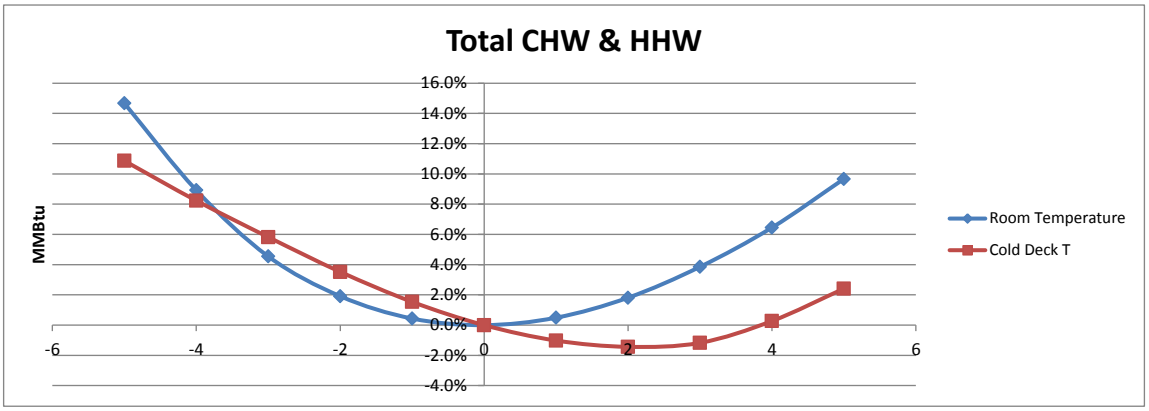

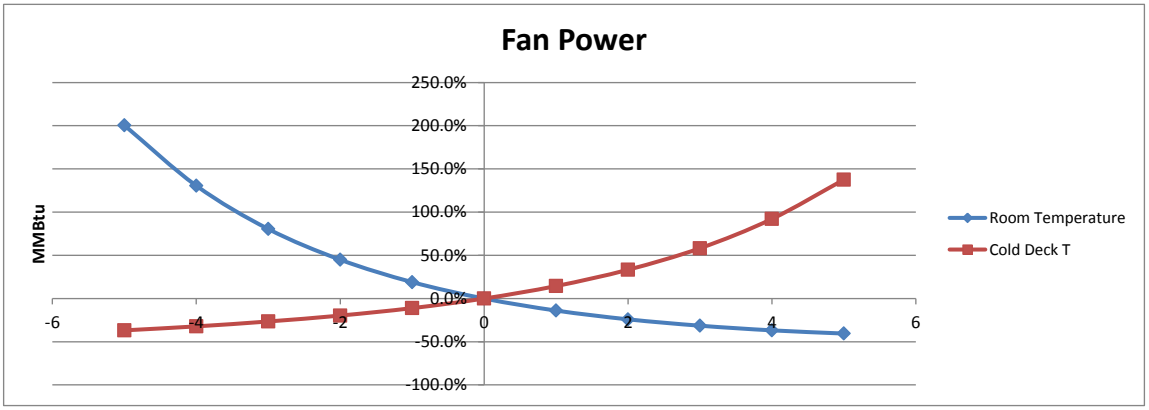

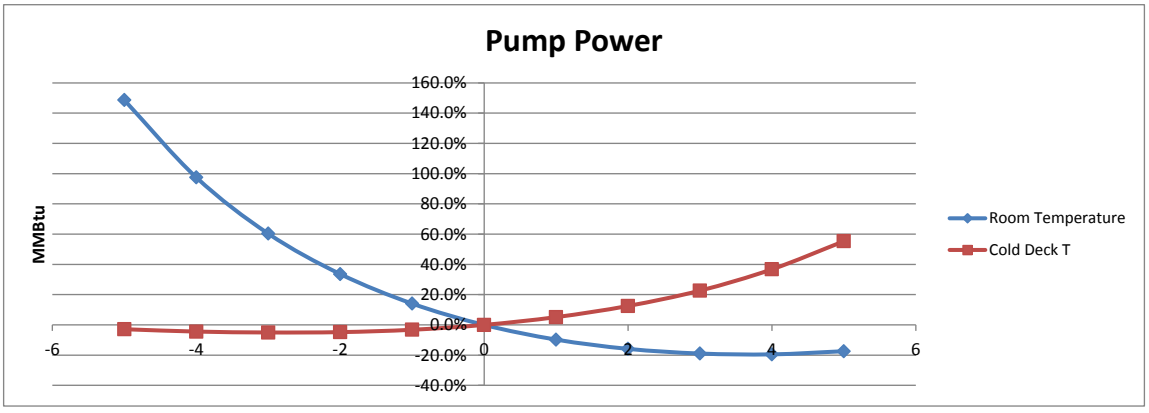

SDVAV Exterior and Interior Zone Load with 50% Minimum Air Flow and 30% outside air

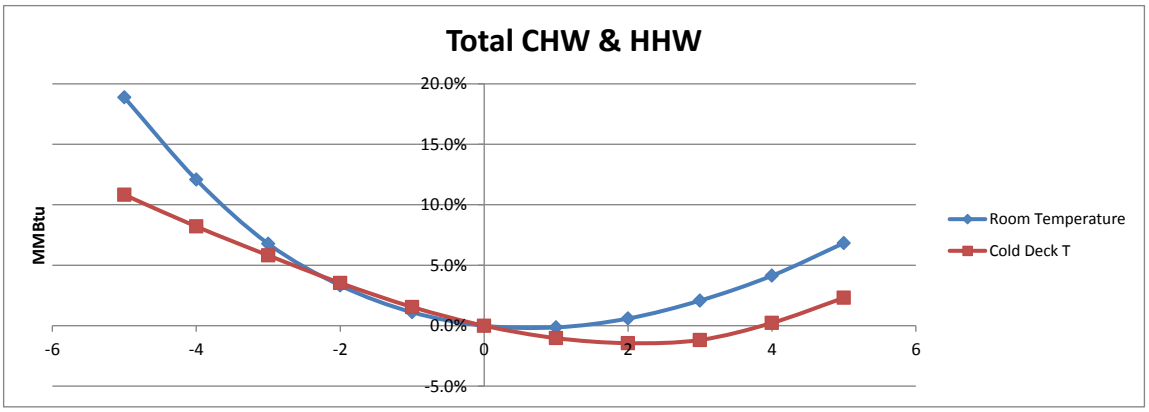

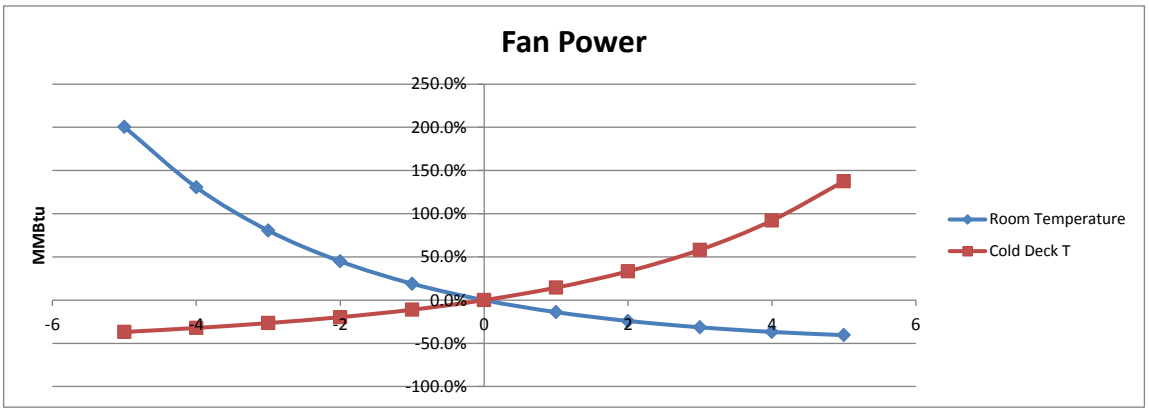

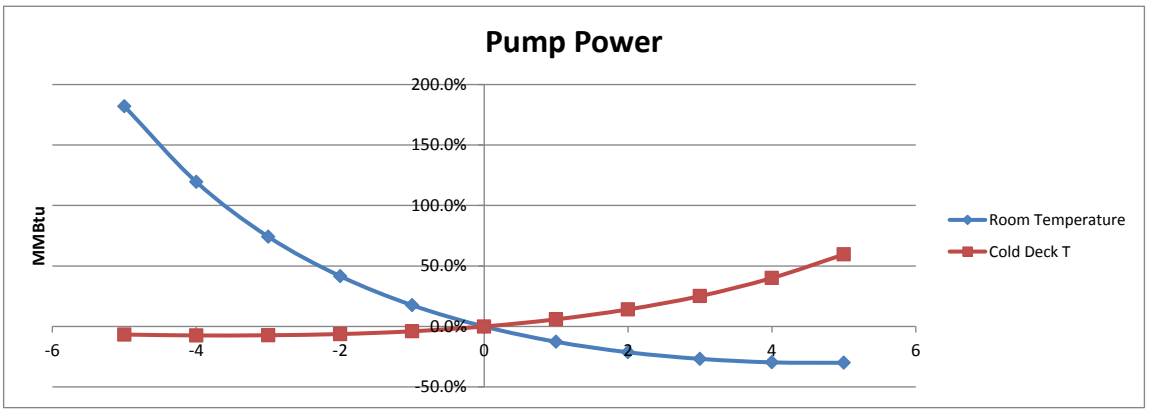

DDVAV Exterior and Interior Zone Load with 0% Minimum Air Flow and 10% outside air

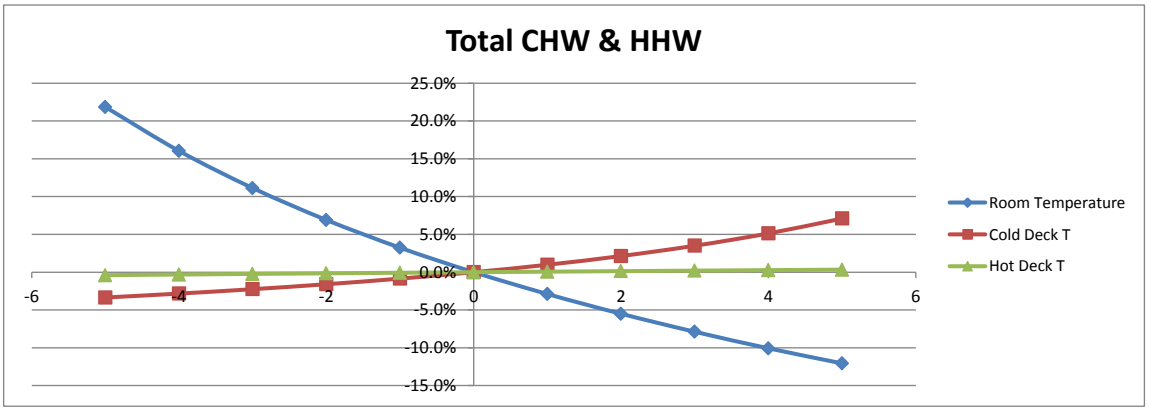

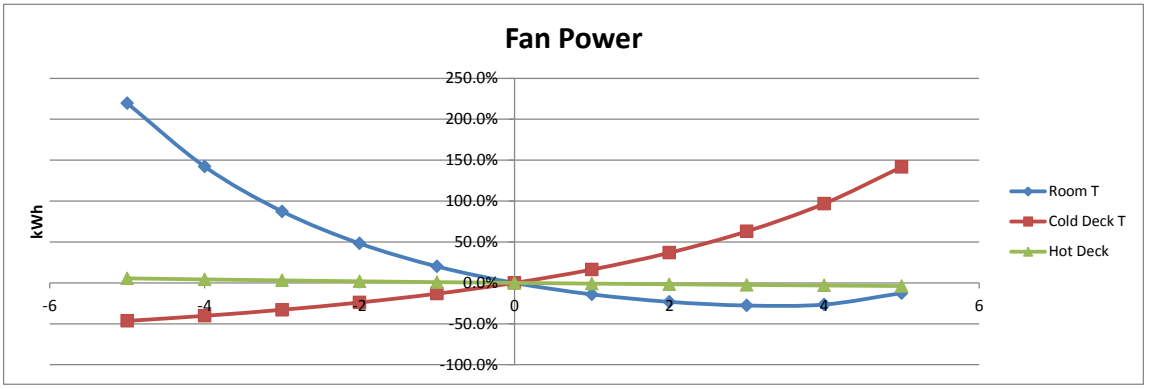

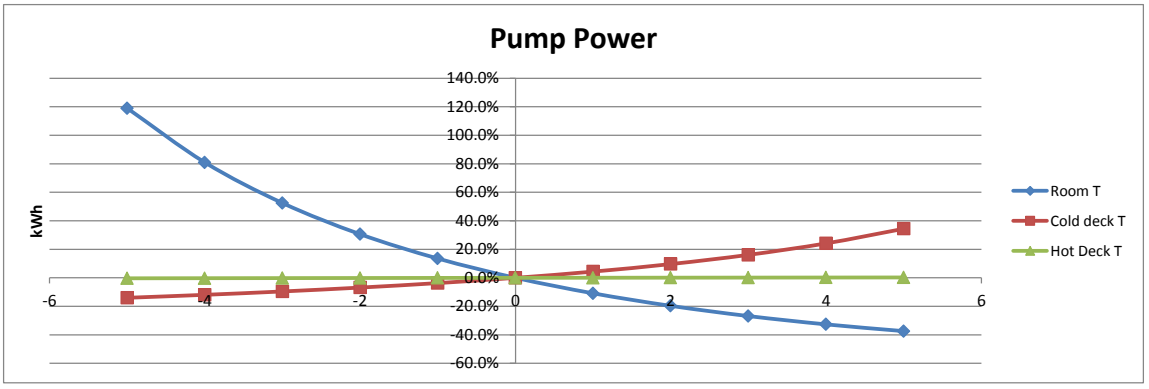

DDVAV Exterior and Interior Zone Load with 0% Minimum Air Flow and 20% outside air

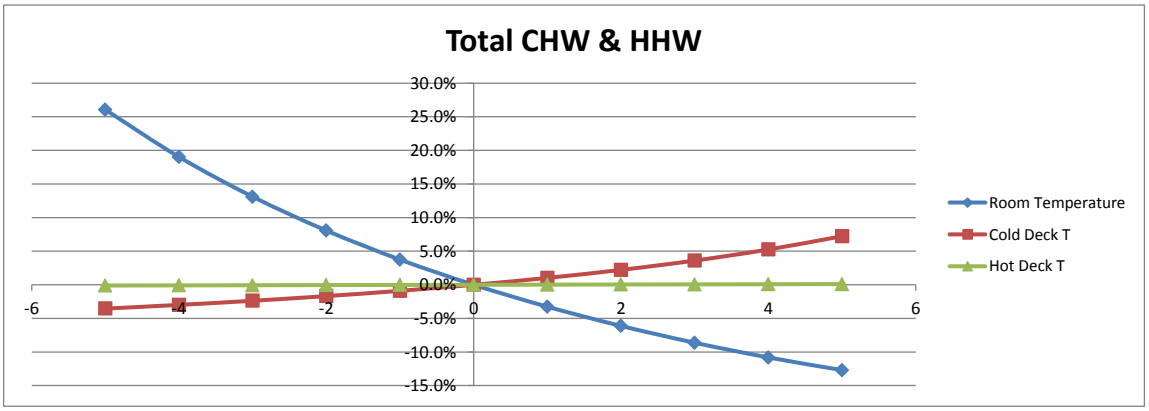

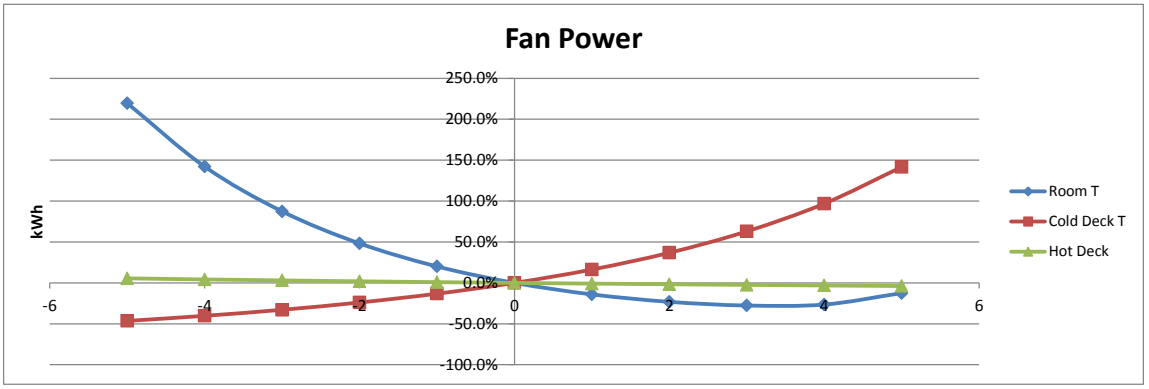

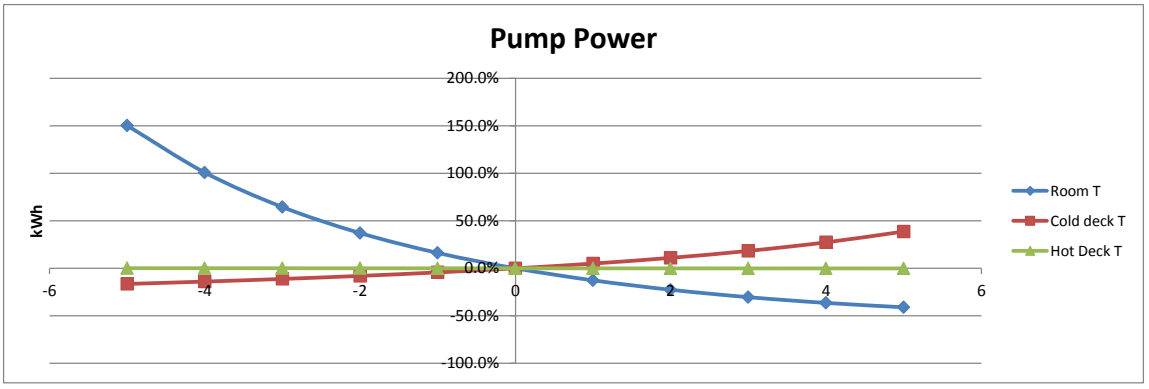

DDVAV Exterior and Interior Zone Load with 0% Minimum Air Flow and 30% outside air

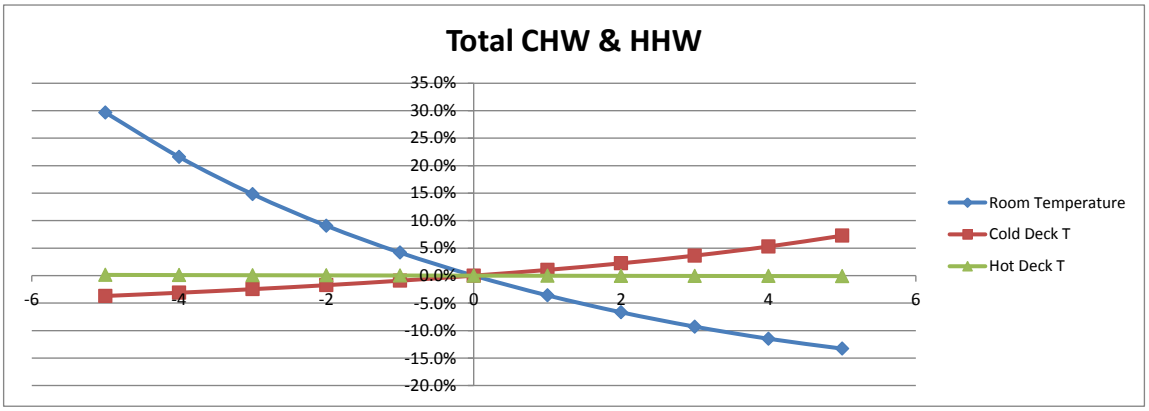

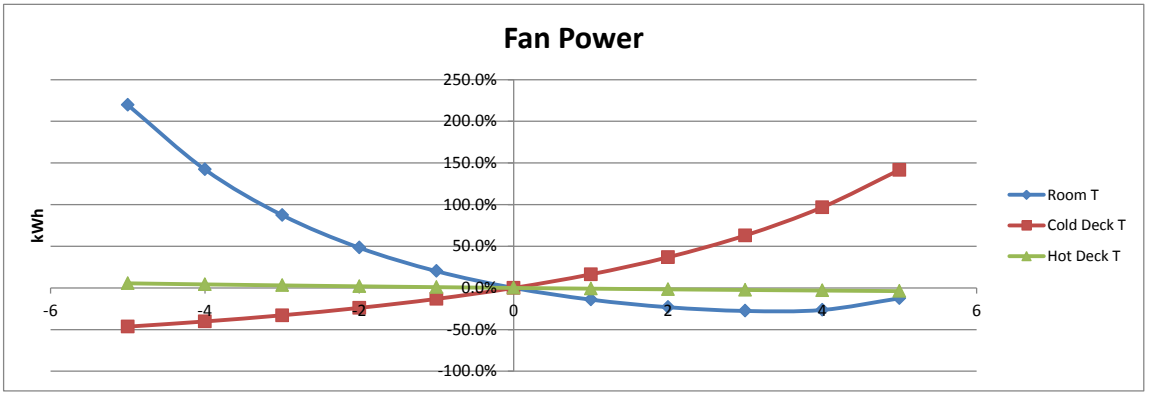

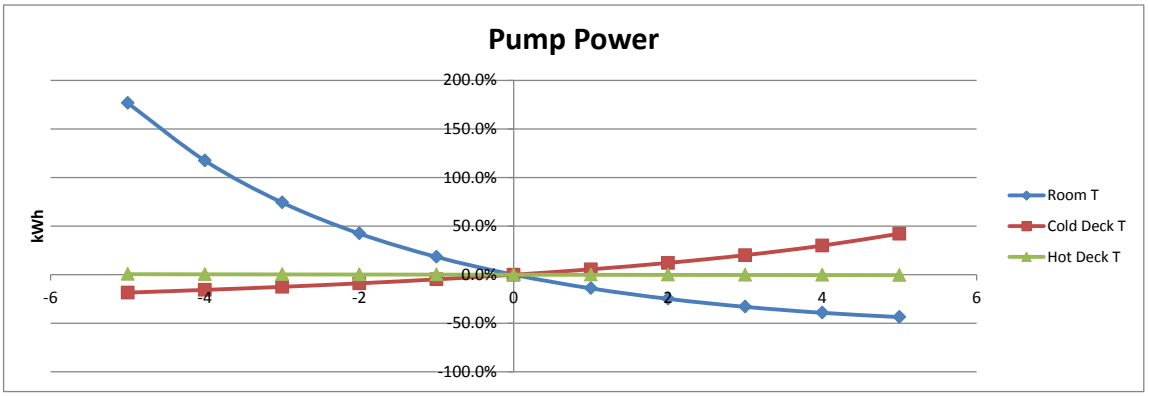

DDVAV Exterior and Interior Zone Load with 50% Minimum Air Flow and 10% outside air

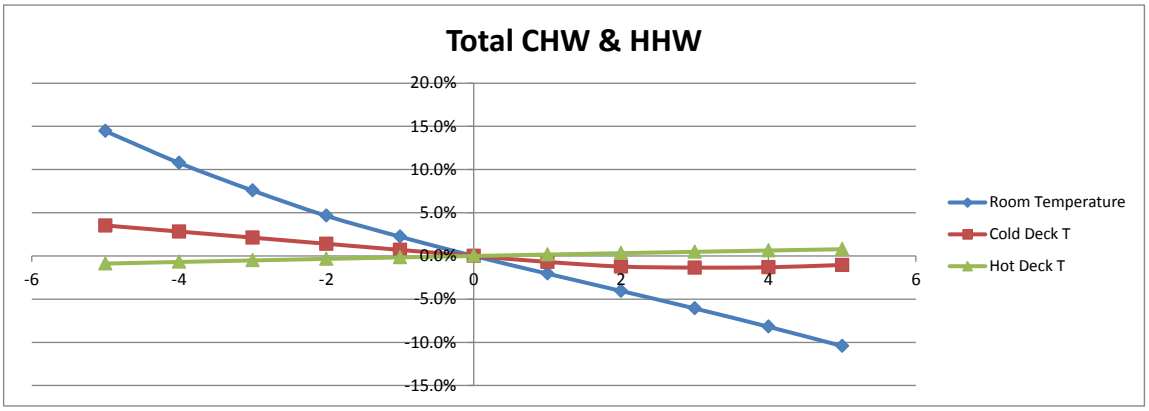

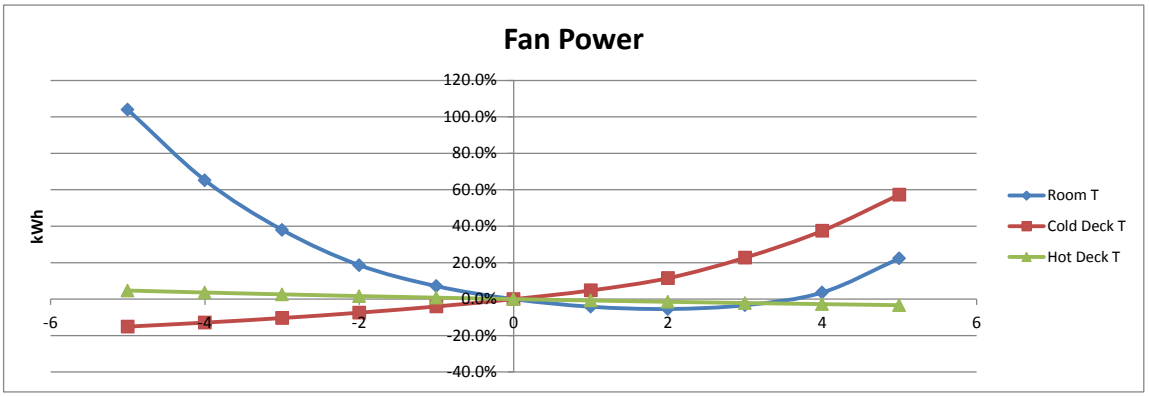

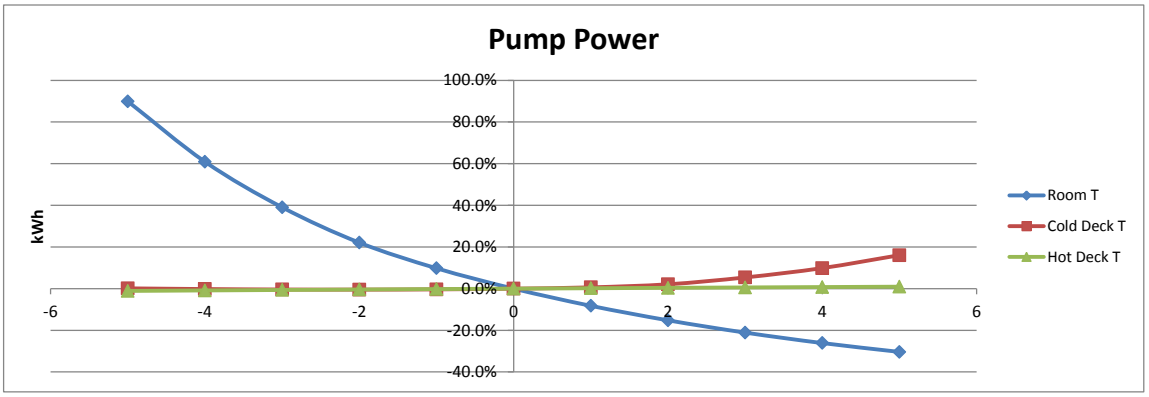

DDVAV Exterior and Interior Zone Load with 50% Minimum Air Flow and 20% outside air

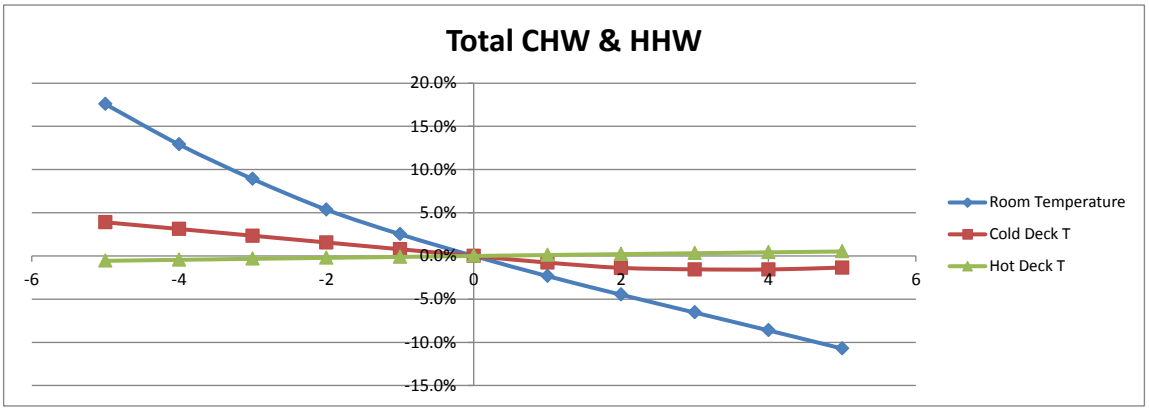

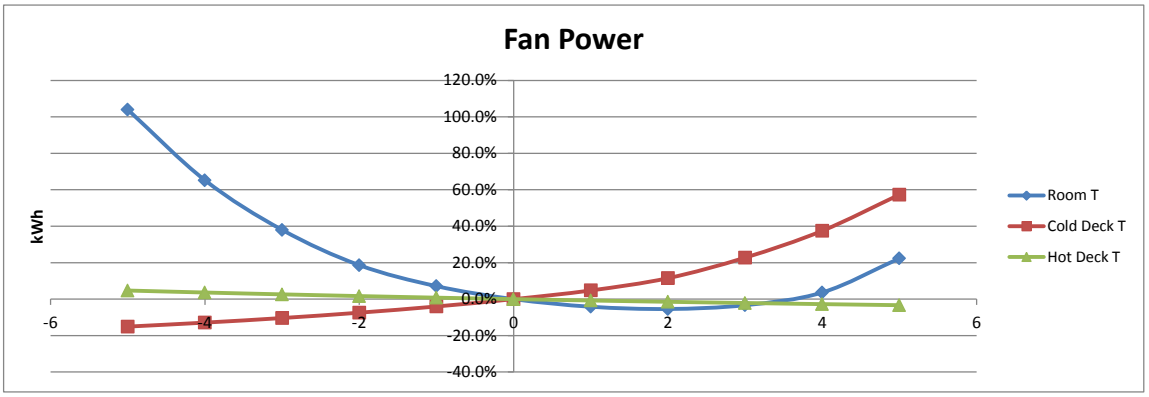

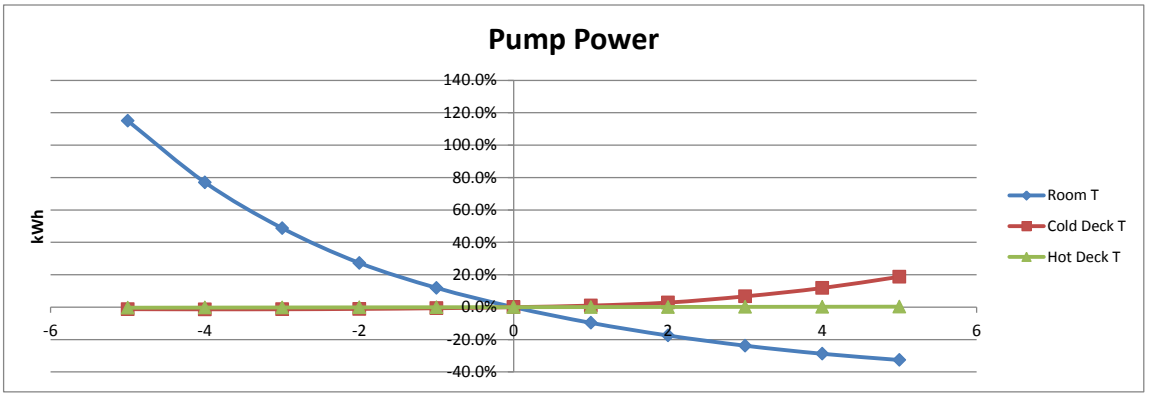

DDVAV Exterior and Interior Zone Load with 50% Minimum Air Flow and 30% outside air

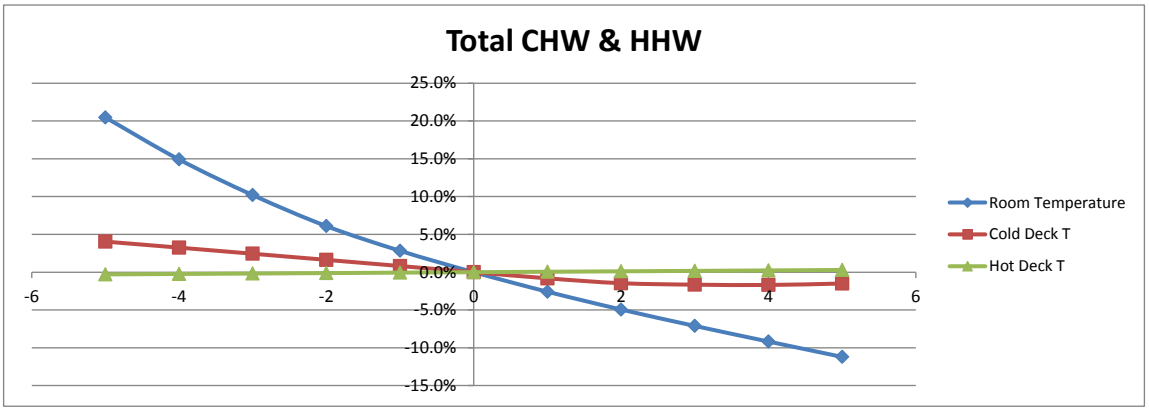

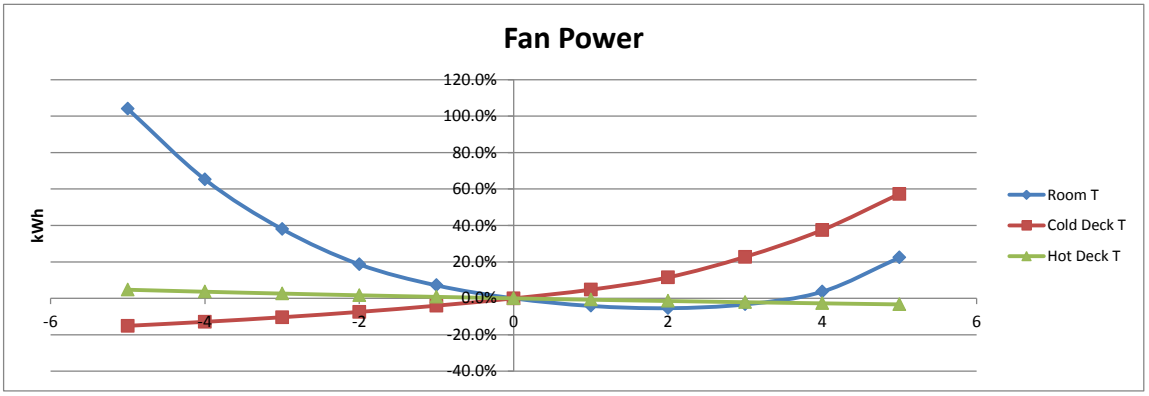

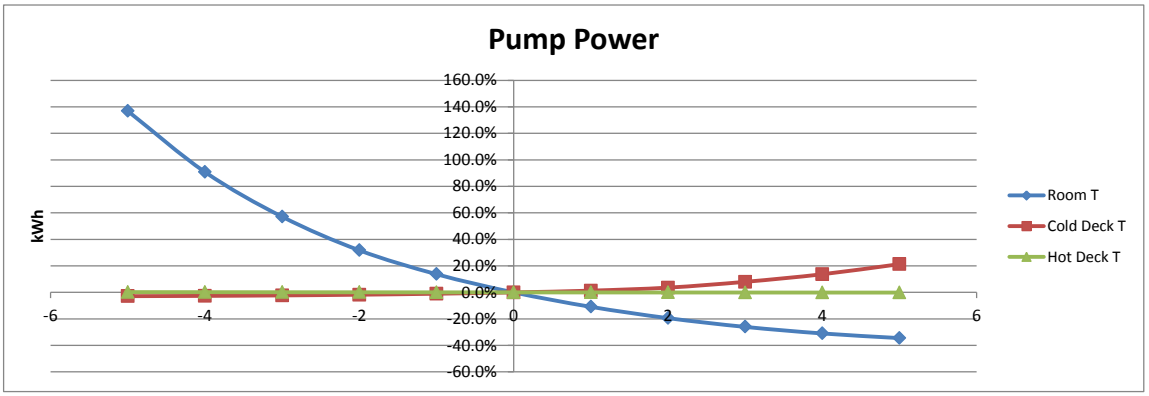

DDVAV Interior Zone Load with 0% Minimum Air Flow and 10% outside air

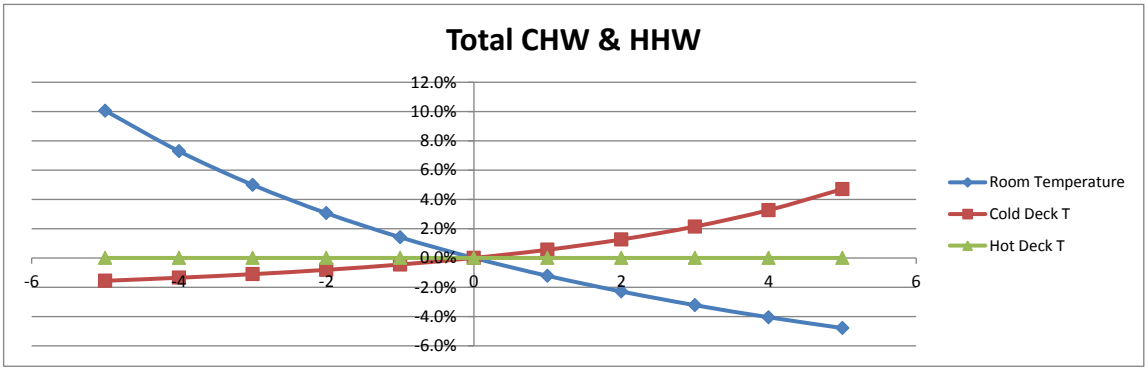

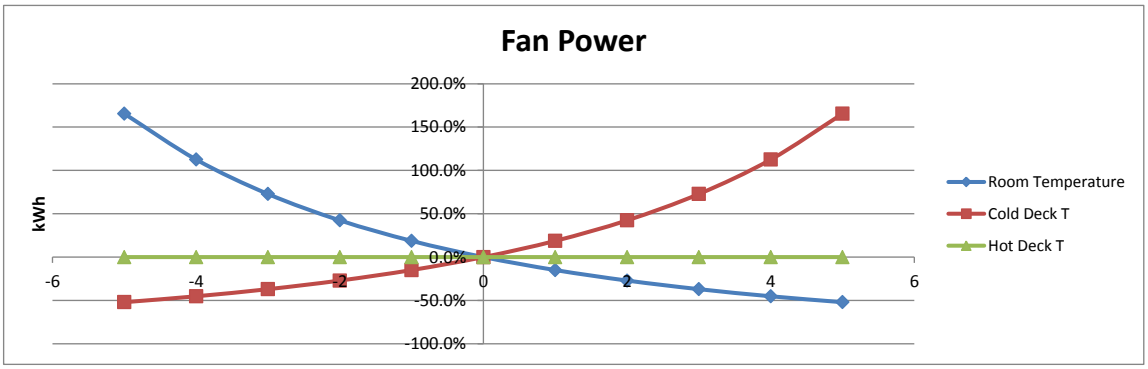

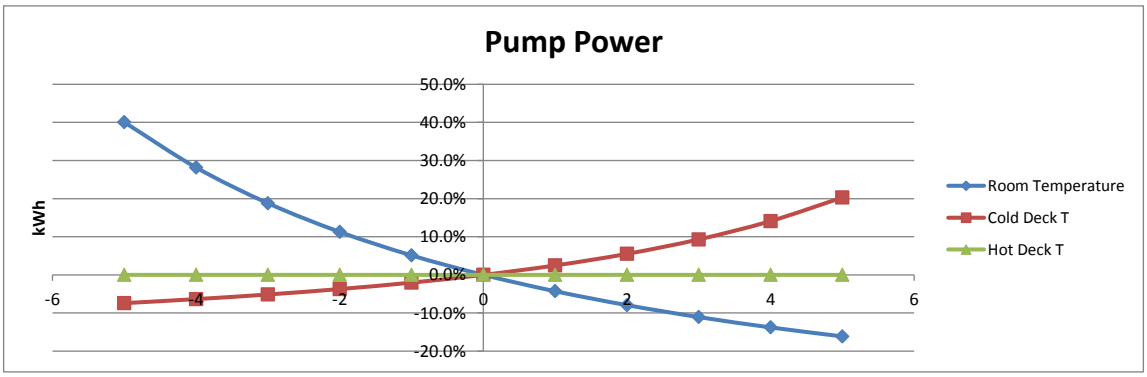

DDVAV Interior Zone Load with 0% Minimum Air Flow and 20% outside air

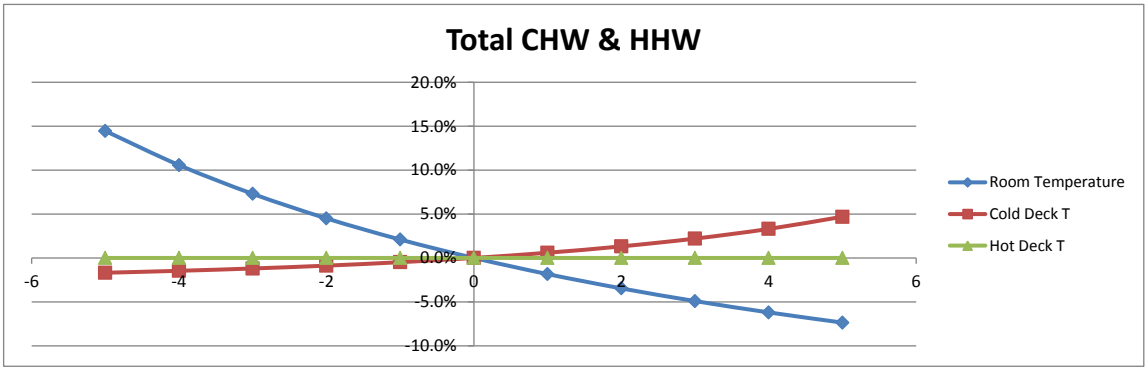

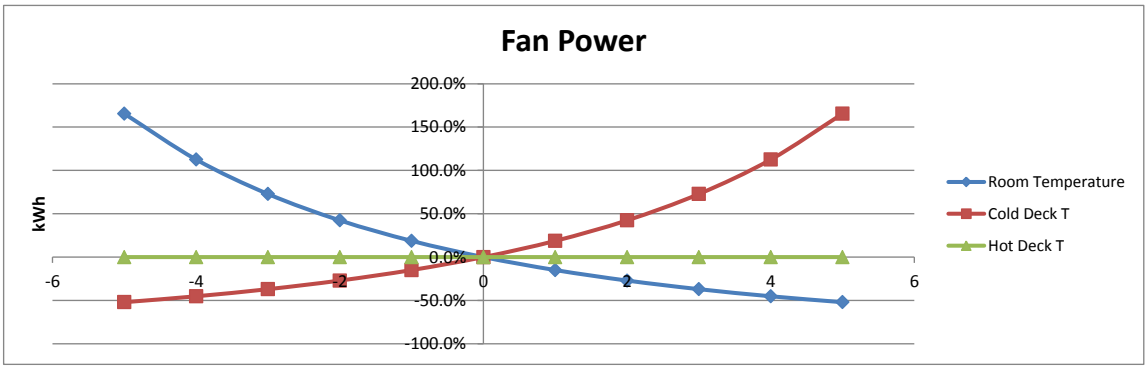

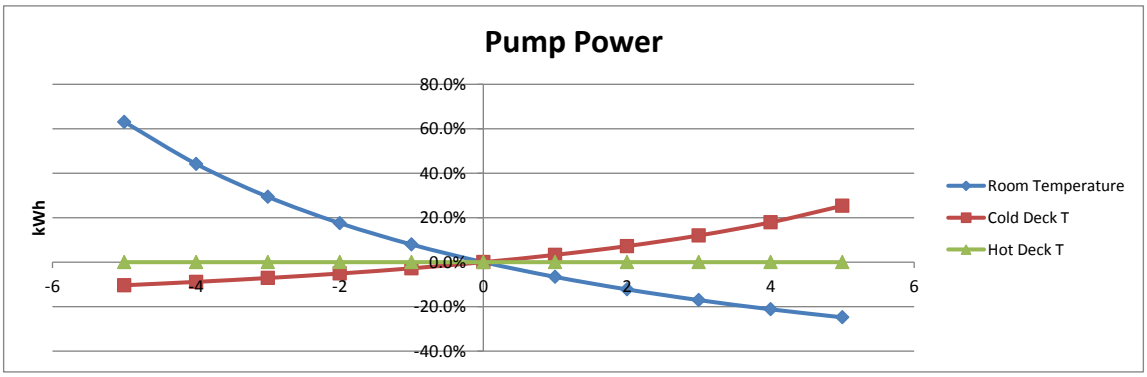

DDVAV Interior Zone Load with 0% Minimum Air Flow and 30% outside air

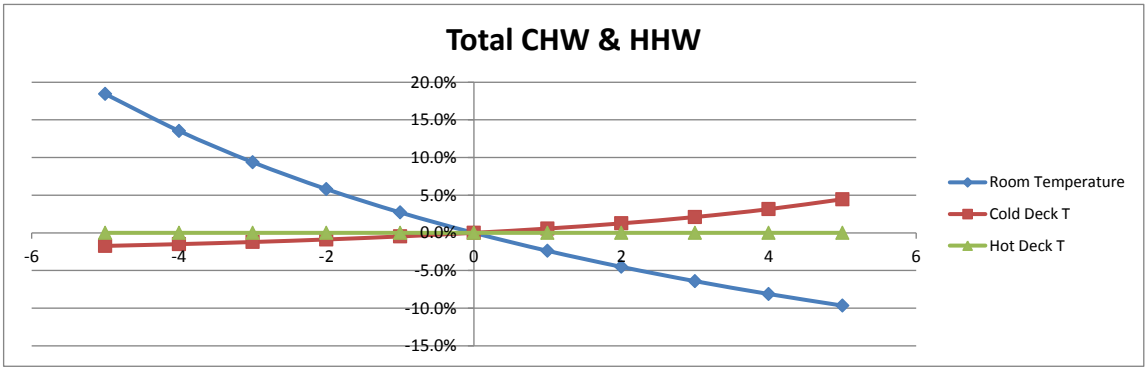

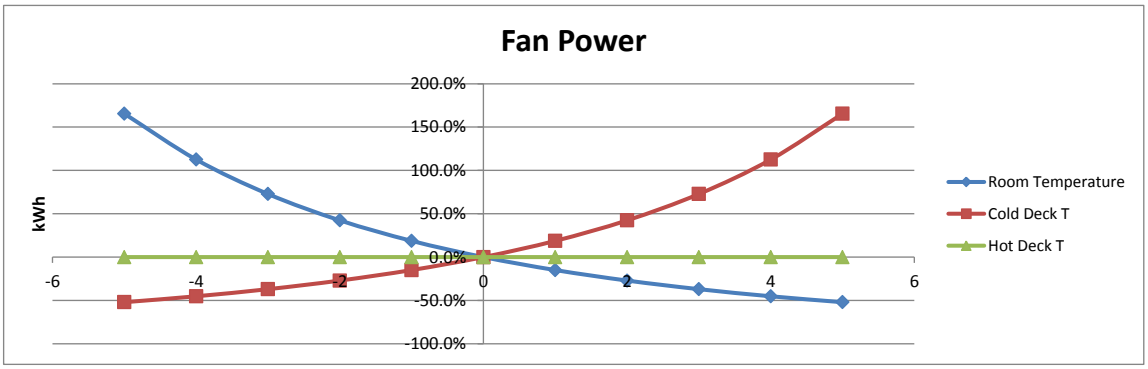

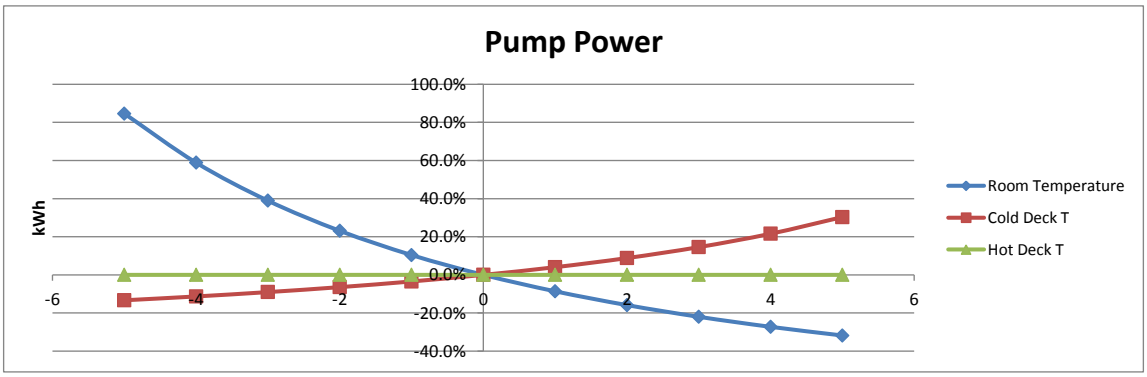

DDVAV Interior Zone Load with 50% Minimum Air Flow and 10% outside air

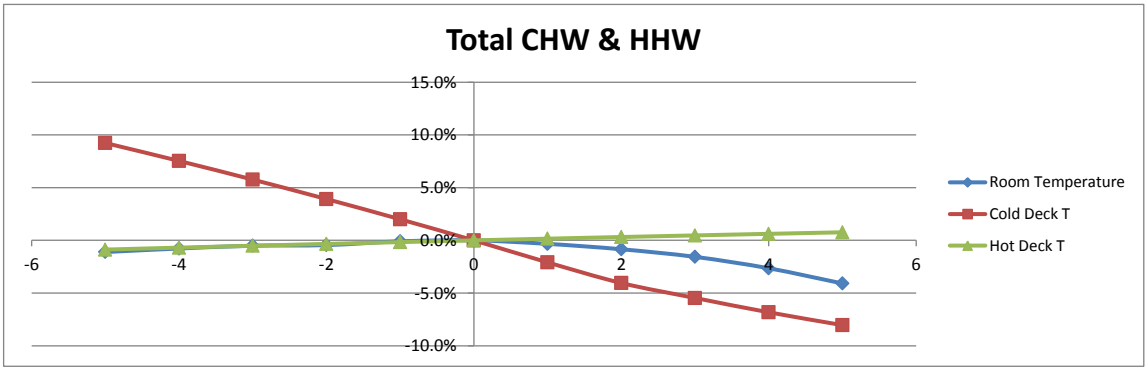

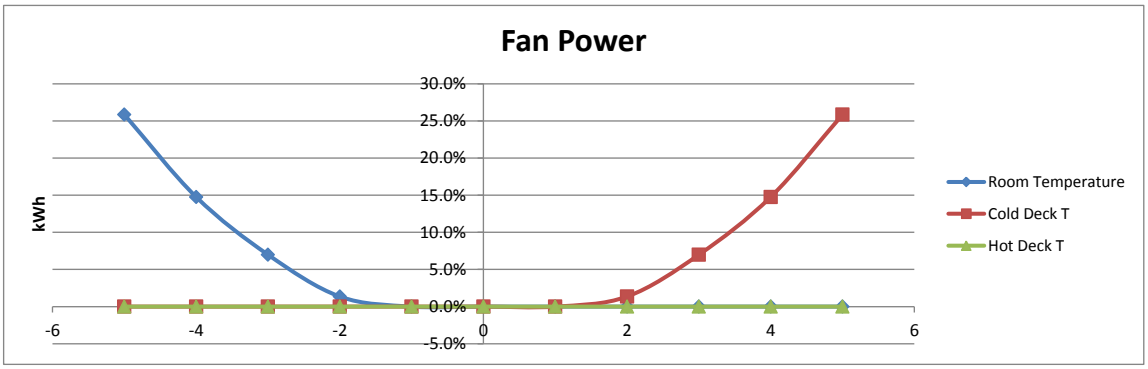

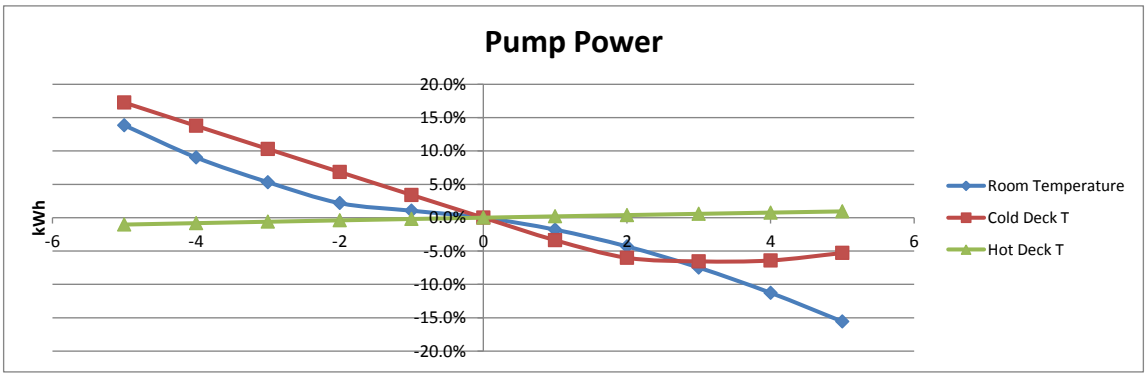

DDVAV Interior Zone Load with 50% Minimum Air Flow and 20% outside air

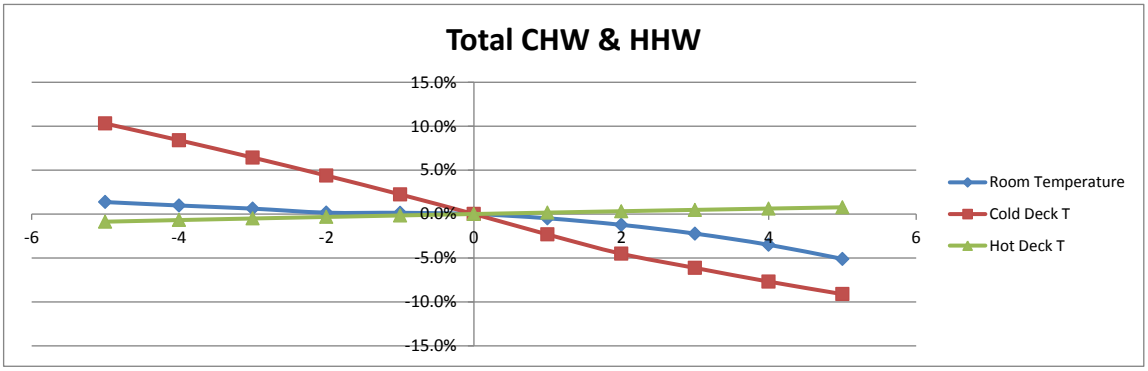

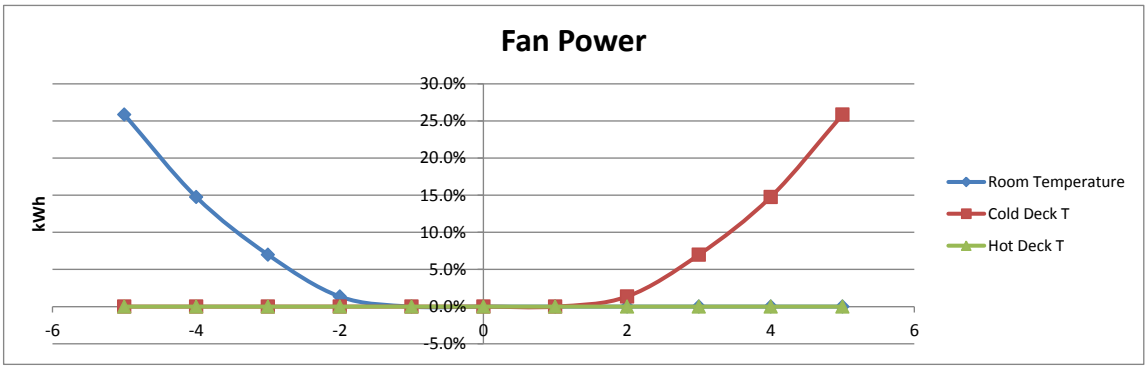

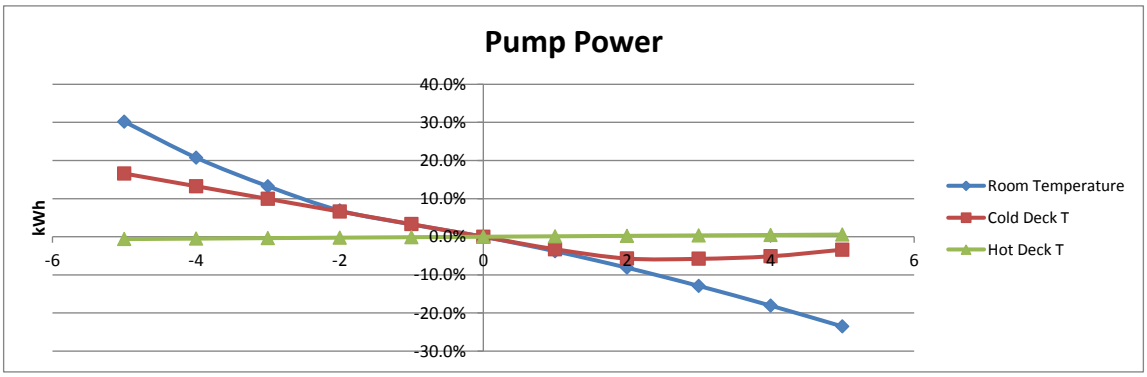

DDVAV Interior Zone Load with 50% Minimum Air Flow and 30% outside air

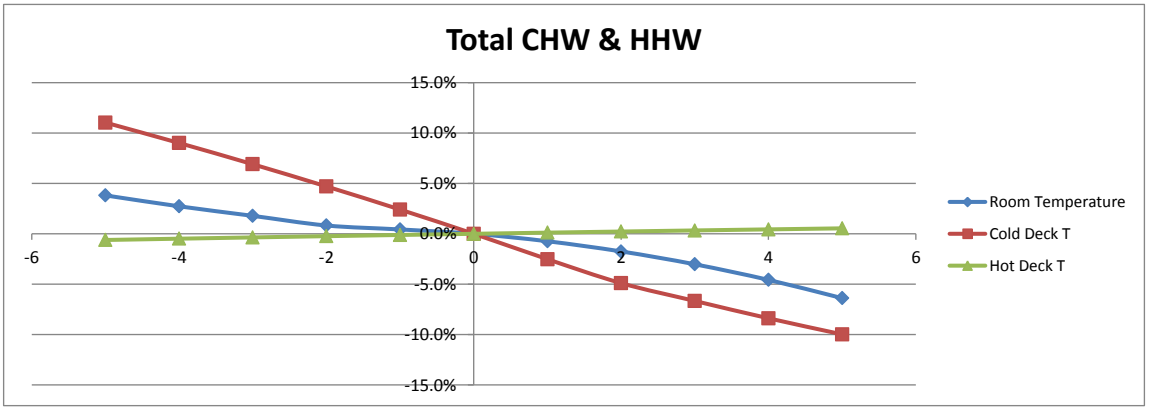

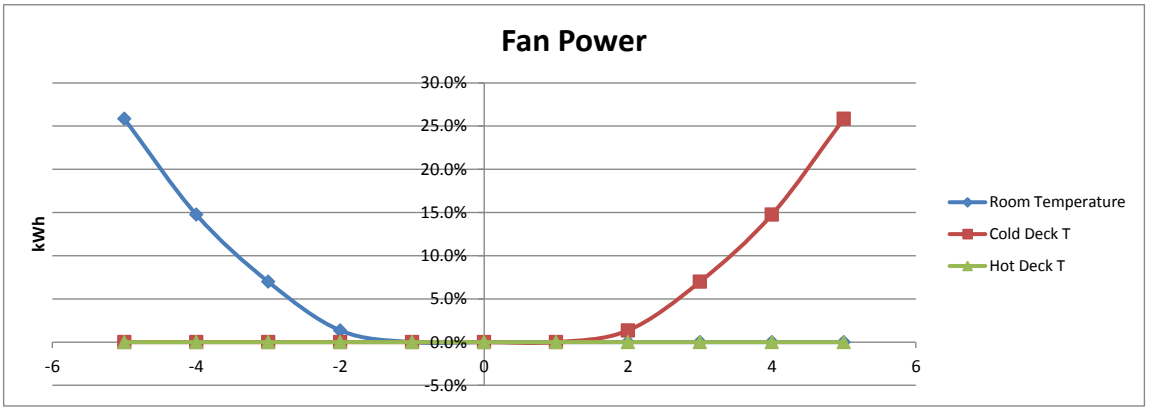

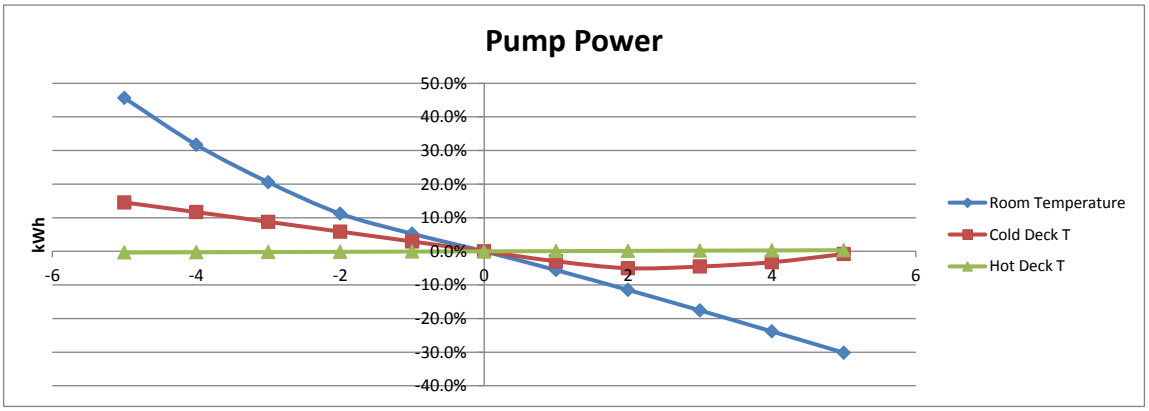

VITA

Name: Liang Ma

Address: Energy Systems Laboratory,

Texas A&M University

College Station, TX 77843

Email Address: tg05ahe@neo.tamu.edu

liangma0201@gmail.com

Education: B.En., Building Thermal Engineering, Harbin Institute of Technology, 2008

M.S, Mechanical Engineering, Texas A&M, 2011